Geochemical Interpretation of Water Quality in The Rajgir-Monghyr Hot Spring Belt, India

A Thesis Submitted in Partial Fulfilment of the
Requirments for the Degree of
DOCTOR OF PHILOSOPHY

by
GANESH SHANKER SHUKLA

to the
DEPARTMENT OF CIVIL ENGINEERING
Indian Institute of Technology
KANPUR-208 016
May 1981

- Hot Water Flow from Jointed Quartzite, Rameshwarkund, Monghyr. 25 October 1977, Photo: G.S. Shukla.

CERTIFICATE

This is to certify that this thesis entitled "Geochemical Interpretation of Water Quality in the Rajgir-Monghyr Hot Spring Belt, India" by Mr. G.S. Shukla, for the award of the Degree of Doctor of Philosophy, of the Indian Institute of Technology, Kanpur, is a record of bonafide research work carried out by him under my supervision and guidance. The results embodied in this thesis have not been submitted to any other University or Institute for the award of any degree or diploma.

B.C. Raymahashay

(B.C. Raymahashay)
Professor
Department of Civil Engineering
Indian Institute of Technology
Kanpur.

ACKNOWLEDGEMENTS

I acknowledge with a feeling of gratitude, the prompt and excellent guidance extended to me by my thesis supervisor, Professor B.C. Raymahashay. The sincerity of his approach has been a source of constant encouragement to me throughout the completion of this work.

I wish to express thanks to Dr. G.C. Pandey of Jawaharlal Nehru University, New Delhi for making available the results of his CSIR Project in the Rajgir-Monghyr area (Dr. B.C. Raymahashay, Joint Investigator).

To Dr. K.V.G.K. Gokhale and Dr. D.M. Rao, Engineering Geology Group, Department of Civil Engineering, I.I.T. Kanpur, I express my heartiest thanks for providing great help during this project.

I take this opportunity to express my sincere thanks to Dr. G.K. Mehta, Department of Physics, I.I.T. Kanpur for providing necessary facilities for working in the Nuclear Physics Laboratory, I.I.T. Kanpur.

The help and encouragement by my friends: Dr. K.L. Patel, Mr. N.K. Khosla and Mr. V.N. Bajpai are also gratefully acknowledged.

To the Institute employees, Mr. M.L. Srivastava and Shri Shivdutt (Engineering Geology), I record my sincere thanks for their friendly co-operation.

'G.S. Shukla

CONTENTS

LIST OF TABLES

LIST OF FIGURES

LIST OF FIELD PHOTOGRAPHS

NOTATIONS

The main symbols and their meanings are listed below. Some symbols inevitably are used for several different purposes at different places in the text. They are defined where they occur.

Symbol	Definition
a^o	Radius of hydrated ion
a_i	Individual ion activity
atm	Pressure in atmosphere
aq	Aqueous; refers to substances in solution
DTA	Differential Thermal Analysis
EDTA	Ethylene Diamine Tetra-acetic Acid
ΔG	Change in Gibbs-free energy for a chemical reaction
ΔG^o	ΔG when each product and reactant is in its standard state
gph	Gallon per hour (1 gallon = 4.5435 liter)
ΔH	Change in enthalpy
I	Ionic strength
K	Thermodynamic, or activity equilibrium constant
$K_{calcite}$	Solubility product of calcite
ln	Natural or base e logarithm (ln = 2.303 log)
log	Common or base 10 logarithm (log = 0.434 ln)
lph, lpm	Liter per hour, liter per minute
mA	Molar concentration of A

N	Normality (equivalents per liter)
nm	10^{-9} meter
P_{CO_2}	Partial pressure of carbon dioxide
pH	$-\log a_{H^+}$
p^k	$-\log K$
ppm	Parts per million (in dilute solutions; mg/liter)
R	Universal gas constant (1.99×10^{-3} kcal mole^{-1} deg^{-1})
S^o	Standard-state entropy
T	Temperature
TDS	Total Dissolved Solids (mg per liter)
TU	Tritium unit
Z	Valence charge of an ion
γ_i	Individual ion activity coefficient (a_i/m_i)

ABSTRACT

This thesis summarises the application of modern geochemical concepts in interpretation of the chemical compositions of hot springs in the Rajgir-Monghyr Belt. The main objectives of the work were (1) Systematic description of the thermal areas including geology and water chemistry; (2) Monitoring of seasonal fluctuations of water quality; (3) Development and testing of geochemical indicators of subsurface conditions; (4) Investigation of the influence of water-rock interaction on water composition and (5) Possible utilisation of the hot waters.

It was soon realised that the conventional SiO_2, Na-K and Na-K-Ca geothermometers do not work in this area because of large amount mixing of hot and cold waters. Using recently developed models for Mixed Waters, it is estimated that the fraction of hot component varies from 3.8 to 34.1 percent. The maximum subsurface temperature (Base Temperature) of the geothermal reservoir is estimated to be between 95°C and 240°C. Scattered information on the isotopic composition of waters strongly support the hot water fraction estimated from Mixing Models.

Construction of stability diagrams from available thermodynamic data shows that the water composition is such that a kaolinite type clay mineral will be stable in the hot spring environment. It is apparent that halloysite

present in soil profiles and altered rocks strongly influences water composition through mineral-water reactions.

The base temperature of the Rajgir-Monghyr geothermal reservoir is too low for power generation at the present time. However, utilisation of the hot waters for agro-industries, mineral water plants and for development of recreational facilities like spa, swimming pools etc. is considered feasible.

Chapter 1

INTRODUCTION

1.1. WATER QUALITY IN GEOTHERMAL AREAS

Natural hot waters have been used since earliest times for cooking, washing, bathing and curing or assuaging physical ailments, but only in the last 30 years has geothermal energy been harnessed to provide a significant proportion of the energy requirements of any country. The pioneering countries in this field are Italy, Iceland, Japan, Newzealand and U.S.A.. However, there are warm springs in most countries. At present water of these warm springs may be used for space heating and agricultural purposes, but in future, binary cycle system using heat transfer media of lower boiling point than water, such as 'freon' or other light hydrocarbon fluids may allow more extensive utilization of low temperature systems for electricity generation.

At present multidisciplinary geothermal exploration programmes, running in various countries, involving geological, geophysical and geochemical survey have thrown light on the localization of hot-springs, heat source and geochemistry of thermal fluids.

Detailed geochemical investigation of geothermal areas is felt essential, because majority of the problems

associated with development of any geothermal field are anyhow connected with the peculiar chemical composition of thermal fluids. The knowledge about the subsurface conditions can also be interpreted with the help of geochemical data. In this work full stress is given on the geochemical interpretation of water quality.

1.2. GEOTHERMAL PROVINCES OF INDIA

In this country attempts have been made recently towards this direction. Geological Survey of India recorded some 300 thermal springs, some of them are at boiling temperature. Few of these hot spring regions are located in structural environments similar to the regions now being explored in other countries. In India no recent volcanic activity is observed. Mild geyser activity is noticed in the hot springs of Manikaran (Himachal Pradesh), Puga (Ladakh) and few other places in the Himalayan region. The major thermal areas in India are (i) North-West Himalayan Belt, (ii) West Coast Region, (iii) Narmada-Sone Lineament, (iv) Bengal-Bihar Complex or The East Indian Archaean Geothermal Province. In the Himalayan belt about 72 centres of hot springs are known to occur and are mainly associated with major deep-seated faults and thrusts. Near the West Coast, about 23 hot springs are distributed along an approximate N-S direction over a distance of 300 km. between Bombay

and Ratnagiri. The alignment of springs is parallel to the major tectonic trend of this area. Neutral to mildly alkaline hot waters of Na-Ca-Cl-SO_4 type issue from shear and fracture zones at junction of two lava flows or contact of dolerite-dikes with basalts. The third region consists of the hot springs located along the lineament of the rivers Narbada and Sone. The East Indian Archaean Geothermal Province is situated in the Bihar and Bengal states where well known high temperature springs occur in two distinct geological settings. One group of springs is located in the Rajgir-Monghyr belt and others are distributed in the Palamau, Hazaribagh, Dhanbad and Santhal Paraganas district of Bihar and Birbhum district of West Bengal. Crustal movements have occurred in this region corresponding to the late phase of movements of the Himalayan Orogeny (Ghosh, 1954; Chaterji and Guha, 1968; Gupta et al., 1975; Krishnaswamy, 1975).

These springs are used for baths and also taken internally as medicinal or table water. Some of them are believed to be efficaceous in curing; skin-diseases, gout, rheumatism, metabolic disorders, paralysis, dyspepsia and diabetes. These springs show radio emanative properties, due to presence of radon. The reported radio activity varies from 0.224 to 9.270 mMc/liter of radon (CSIR, 1962).

1.3. OBJECTIVES OF THE PRESENT INVESTIGATION

With the above mentioned historical and geological background of the Rajgir-Monghyr springs, the objectives of the present work can be summarised as follows:

(1) Systematic description of the thermal areas including geology and water chemistry.

(2) Monitoring of seasonal fluctuations of water quality.

(3) Development and testing of geochemical indicators of subsurface conditions.

(4) Investigation of natural controls on water quality in terms of water-rock interaction.

(5) Evaluation of the thermal areas in terms of possible utilisation of hot waters.

Chapter 2

DESCRIPTION OF RAJGIR-MONGHYR HOT SPRING BELT

2.1. INTRODUCTION

The Rajgir-Monghyr hot spring belt is a NE-SW trending narrow zone situated between 85°E and 86°45'E longitude and 24°30'N and 25°30'N latitude. It is included in the Survey of India quarter inch toposheets No. 72G, 72H and 72K and corresponding one inch sheets. Table 2.1 summarises the location and physical characteristics of the major hot springs of this area. Figures 2.1 and 2.2 are location maps. It is convenient to describe the springs in three groups namely; (1) Rajgir Group, (2) Bhimbandh Group and (3) Sitakund Group from SW to NE.

2.2. RAJGIR GROUP

The hot springs of Rajgir are situated about 110 kilometers SSE of Patna and can be approached by road from Patna or by railway route via Baktiyarpur. Four representative springs of this area were studied. These are Makhdumkund, Surajkund, Brahamkund and Agnikund. Agnikund is situated about 19 kilometers SE of Rajgir, beyond the Rajgir-Jethian hill ranges also known as Baibhavgiri and Bipulagiri hills in the northern boundary of Gaya district.

TABLE 2.1. LOCATION, TEMPERATURE AND FLOW OF INDIVIDUAL SPRINGS IN THE RAJGIR-MONGHYR AREA.

Name of the Group of Springs	Co-ordinate	Temperature °C Observed		Flow
		Maximum	Minimum	lit/hr (lph)
Rajgir Group				
Brahamkund Surajkund Makhdumkund	25°01':85°30'	49°	32°	65,085
Agnikund	25°00':85°30'	49°	39°	40,860
Bhimbandh Group				
Bhimbandh	25°40':86°24'	65°	60°	45,400
Chormara	25°70':86°21'	65°	65°	31,780
Singhirishi	25°05':86°13'	32°	32°	59,020
Rishikund	25°14':86°32'	45°	39°	65,830
Rameshwarkund	25°08':86°29'	45°	45°	16,344
Sitakund Group				
Sitakund	24°15':85°19'	61°	33°	1,72,520

Source: Wealth of India, Vol. VI, p. 385, C.S.I.R., 1962.

2.3. BHIMBANDH GROUP

In this group are included a large number of hot springs spread over a wide area across the Kharagpur hills of Monghyr. The following description covers the occurrences at (1) Bhimbandh, (2) Chormara, (3) Rameshwarkund, (4) Rishikund and (5) Singhirishi.

2.3.1. BHIMBANDH

The hot springs at Bhimbandh can be approached by a diversion from Lachmipur, a village about 50 km SE of Monghyr town on the Jamui road. Observation were made at (1) a group of hot water flow· emerging from jointed quartzite near the Forest Rest House and (2) springs located on the bank of the Man river which flow through this area receiving the effluent of the hot springs.

2.3.2. CHORMARA

A group of seven springs is situated about 7 kilometers NW of Bhimbandh Forest Rest House and can be approached by the forest road. These springs are also known as 'Saptdhara', 'Satbhur' and 'Bhattikol'.

2.3.3. RAMESHWARKUND

This spring can be approached from Kharagpur, about 34 kilometers from Monghyr on the road to Jamui. One has to take a boat across the reservoir (lake) on Man river and reach the hot spring on the bank of Sindhwari Nadi which

is a tributary to Man river. A water fall about 50 meters high, further upstream on the Sindhwari Nadi and known as Panchkumari, was also sampled during this work.

2.3.4. RISHIKUND

Rishikund is about 12 kilometers south of Monghyr and can be approached by an unmetalled road via Ratanpur. There are two major group of springs located at the foot of quartzite ridge, denoted as "North" and "South" groups.

2.3.5. SINGHIRISHI

This group of springs, situated 50 kilometers SSW from Monghyr, can be approached in several parts. Monghyr to Rampur part can be covered by road transport; Rampur to village Sahur, 8 kilometers distance, can be approached by forest road; Sahur to Mombe Dam, that is located 8 kilometers SE of Sahur, has to be followed by a jungle path. From this dam to Singhirishi temple one has to walk 5 kilometers in southerly direction.

2.4. SITAKUND GROUP

Sitakund is located about 8 kilometers east of Monghyr town on the flood plain of the Ganges river and can be approached by road. In its situation near a populated area and away from densely forested hills, it is distinct from other springs described so far. Five enclosed tanks named Sita, Ram, Bharat, Shatrughan, Lakshman kund and

a dug well occur within an area of 500 square meters. Out of these only Sitakund is a hot spring. The combined out-flow is used for irrigation in the nearby fields.

2.5. REGIONAL GEOLOGY OF RAJGIR-MONGHYR HOT SPRING BELT

In the Precambrian Peninsular shield of Bihar, two hot spring belts are found. One extends in a NE-SW direction from Ambikapur (M.P.) to Monghyr (Bihar) including the Rajgir and Bhimbandh hot spring group. The other belt shows an E-W trend and extends from Daltonganj to Suri (West Bengal) area (Figure 2.3).

The first belt of hot springs is situated along a deep-seated major thrust descending to great depth (ONGC, 1968; Figure 2.3). The Rajgir-Monghyr springs are located in rocks of the Dharwar System.

2.6. LOCAL GEOLOGICAL SETTING

The Rajgir hills are situated in the south-western portion of the submetamorphic belt of Bihar. The regional trend of Rajgir hills is NE-SW. The alternate bands of quartzite and phyllite are characterised by elevated ridges and deep eroded valley floors respectively.

The quartzite formations of this area are characterised by excellent primary non-diastrophic structures like cross-bedding and stratification marked by prominent red ferruginous bands.

The formations of the area may be classified into following groups as adapted from Das (1967), Srivastava and Sengupta (1968), Guha (1970) and Wadia (1975).

		Recent Alluviam Laterite and Conglomerate	
Archean Group	Dharwar System 2400-1800 million years	Younger Phyllites :	Grey phyllites and Banded ferruginous red phyllites.
		Quartzites :	Grey quartzites, white quartzites, Banded ferruginous quartzites with jasper bands.
		Older Phyllites :	Compact grey phyllites with laminations of ferruginous material
		(Basement not seen)	

The basement is not exposed around Rajgir area, but has been described as 'Unclassified Crystalline Rocks' or Granitic rocks with mica-schist, amphibolites and migmatites (Das, 1967).

The rocks of this area appear to have been tightly folded (superimposed folding) into isoclines and strongly affected by two parallel strike faults at northern and southern limbs. The folds plunge in NE direction and the general strike of the fold axis is ENE-WSW. Several faults have been located in this region with trends more or less parallel to cross-fold directions such as NE-SW, NW-SE and E-W.

The quartzites are highly jointed and fractured. These deep seated joints provide the possible changes for hot water flow in the springs. The joint surface is highly weathered and coated with leached iron and at some places perfect haemetite crystals are also deposited.

DESCRIPTION OF FIGURES

Figure 2.1 Location Map, Rajgir

Figure 2.2. Location Map, Monghyr

Figure 2.3. Geological and Tectonic Map (ONGC, 1968)

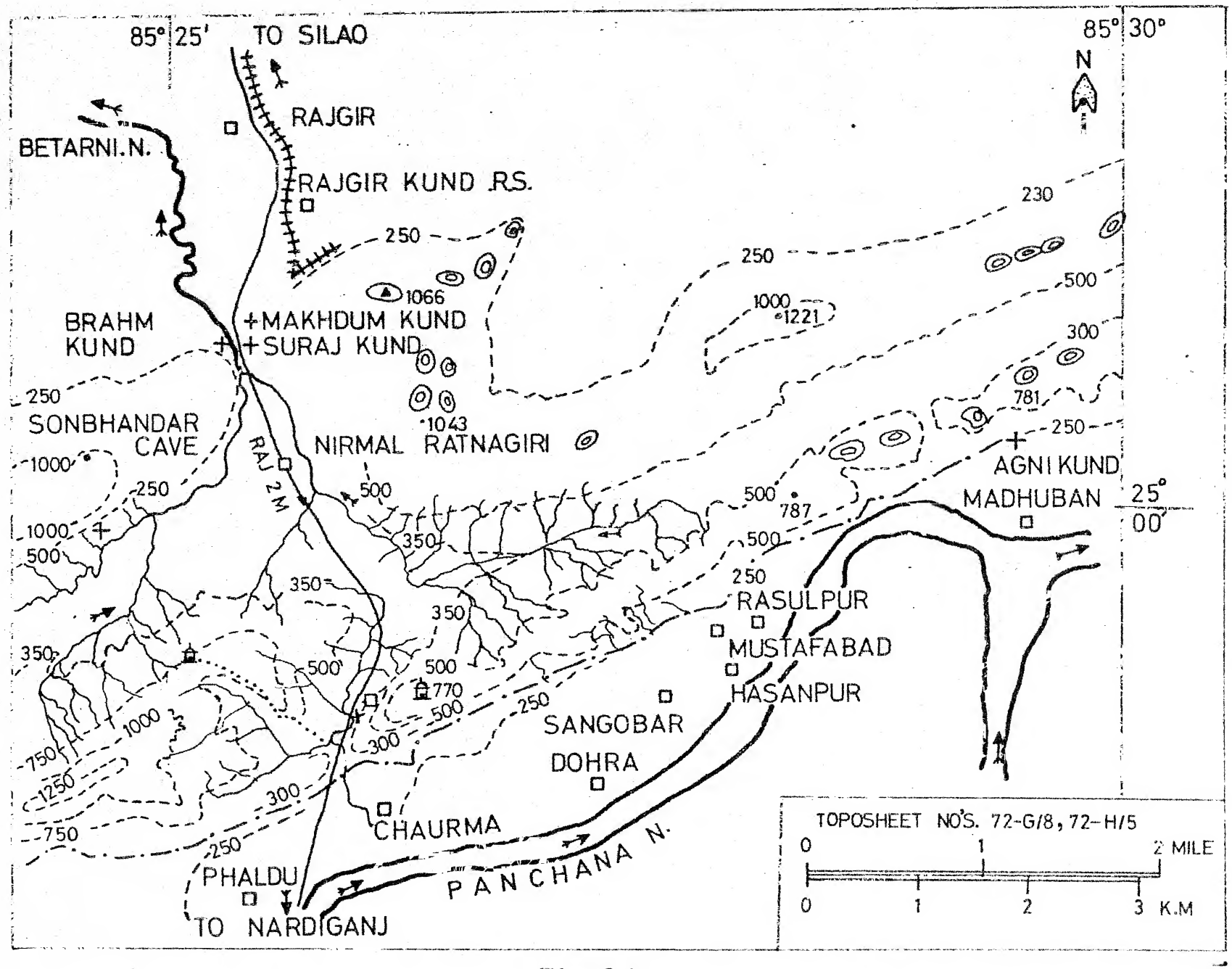
85° 25'
TO SILAO
85° 30'
N
RAJGIR
BETARNI.N.
RAJGIR KUND R.S.
250
230
1066
BRAHM KUND
MAKHDUM KUND
SURAJ KUND
1000
1221
500
300
250
781
SONBHANDAR CAVE
1043
NIRMAL RATNAGIRI
RAJ 2M
AGNI KUND
MADHUBAN
25° 00'
1000
500
350
787
RASULPUR
MUSTAFABAD
HASANPUR
770
SANGOBAR
DOHRA
750
1250
CHAURMA
PHALDU
PANCHANA N.
TO NARDIGANJ
TOPOSHEET NO'S. 72-G/8, 72-H/5
0 1 2 MILE
0 1 2 3 K.M

Fig. 2.1

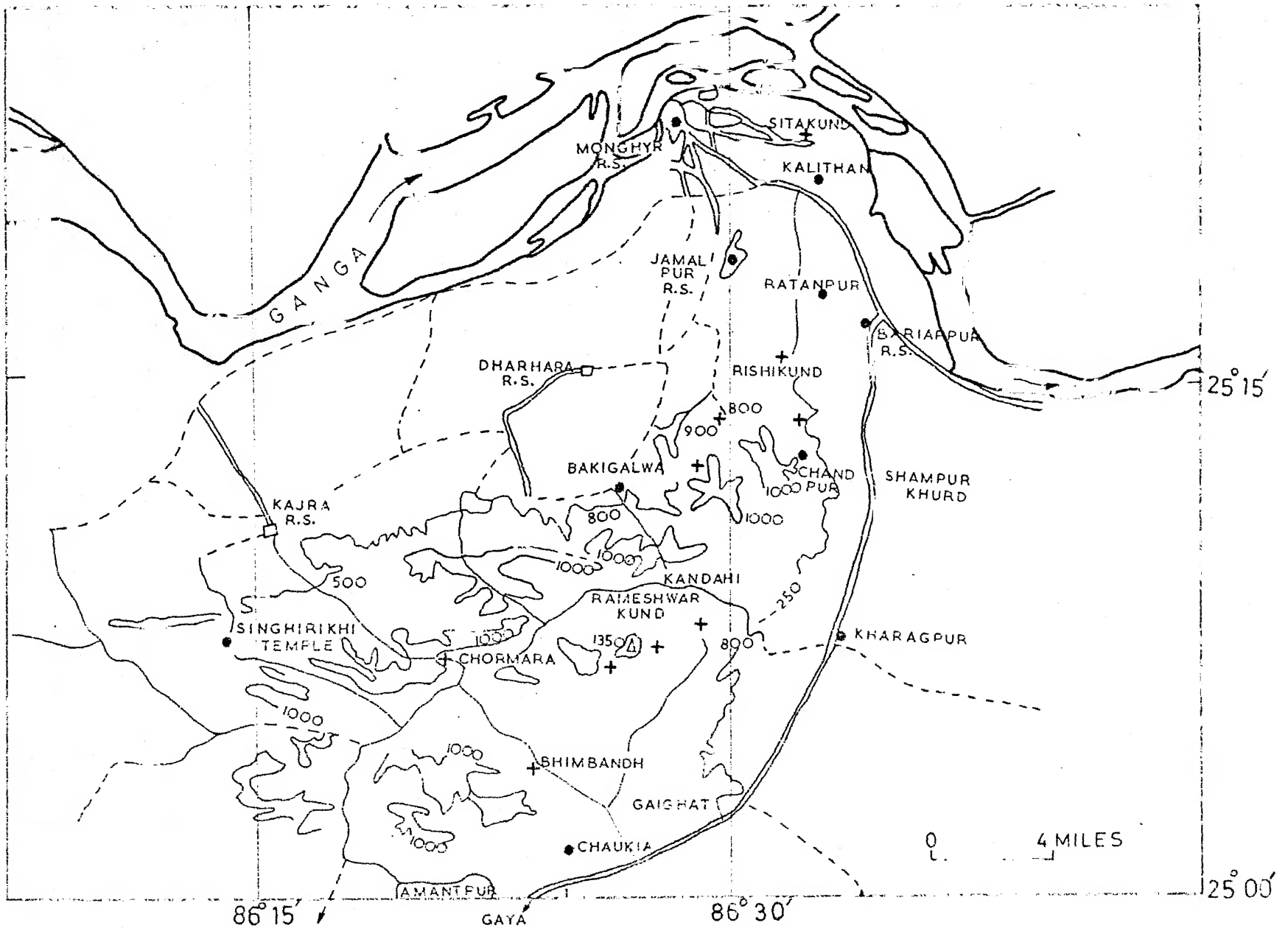
GANGA
MONGHYR R.S.
SITAKUND
KALITHAN
JAMALPUR R.S.
RATANPUR
BARIARPUR R.S.
DHARHARA R.S.
RISHIKUND
800
900
BAKIGALWA
CHANDPUR
1000
SHAMPUR KHURD
KAJRA R.S.
800
1000
1000
500
KANDAHI
RAMESHWAR KUND
250
SINGHIRIKHI TEMPLE
1000
CHORMARA
1350
800
KHARAGPUR
1000
BHIMBANDH
1000
GAIGHAT
1000
CHAUKIA
AMANTPUR
GAYA
0
4 MILES
25° 15′
25° 00′
86° 15′
86° 30′

Fig. 2.2

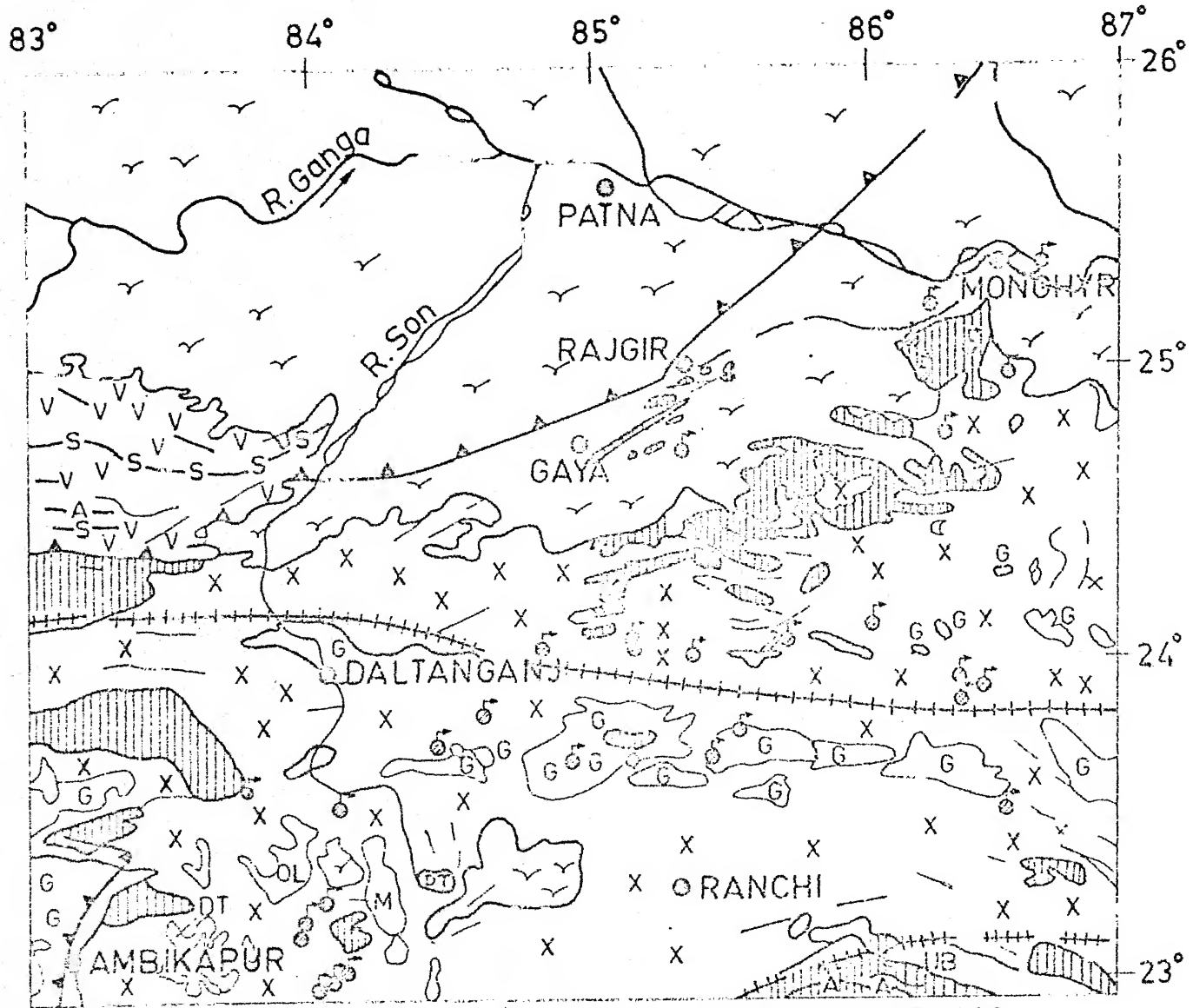

LEGEND

- Principal deep seated fault
- Thrust (separating platforms and geosynclines)
- Thrust
- Anticline
- Syncline
- General trends in folded areas

FORMATIONS

- Oligocene
- Miocene
- Alluvium
- Ultrabasics
- Dharwars
- Unclassified crystalline rocks
- Gondwana
- Deccan trap
- Vindhyans

Fig. 2.3

Chapter 3

METHOD OF WORK

3.1. INTRODUCTION

In this chapter, is described the method of observations in the field, collection of rock and water samples and analytical techniques for the study of these samples. The details are grouped under (i) field-work, (ii) laboratory methods.

3.2. FIELD WORK

A review of existing literature on the Rajgir-Monghyr hot spring belt and consultation of available toposheets (72-G, H and K) and geologic maps indicated that the springs can be grouped into three locations: (i) Rajgir group, (ii) Bhimbandh group and (iii) Sitakund group. Field work was carried out to measure temperature, pH, alkalinity and flow of the springs under natural conditions. Representative samples of fresh country rock including various lithologic types, weathered soil profiles and rocks and sediments in contact with the spring waters were collected for later laboratory studies.

Table 2.1 and Figure 2.1 summarise the location and physico-chemical characteristics of the major springs.

3.2.1. TEMPERATURE

Temperature was measured by a 110°C thermometer with an accuracy of ±0.1°C. Efforts were made to record the maximum temperature at the spring.

3.2.2. pH

Field pH was measured at the same spot where temperature was recorded by means of B.D.H. pH indicator papers and cross-checked by a portable battery operated Philips pH meter at the Rajgir springs. Field pH data were considered important because of the high temperature of some of the springs and occurrence of gas bubbles at their outlets. This was confirmed by comparison with laboratory pH values recorded as early as possible after field work.

3.2.3. CO_2

At many springs, where the effluent gases could be channelised through a tubing, presence of carbon dioxide was confirmed by lime-water test. A suction pump with carbon dioxide detector tube manufactured by MINES SAFETY EQUIPMENT COMPANY, PITTSBURGH,U.S.A., was successfully used at the Agnikund spring, Rajgir.

3.2.4. ALKALINITY

Alkalinity was determined in the field by quickly titrating the hot water against the standard (0.02 N) HCl using Phenolphthalein and Methyl Orange indicators. None

of the waters showed the characteristic pink color after addition of Phenolphthalein indicating the absence of carbonate alkalinity. The readings upto the Methyl Orange end-point were therefore utilised to calculate bicarbonate concentrations. For convenience of titration under field conditions, polythene beakers and a Doctor's syringe were used.

3.2.5. FLOW

Flow of the springs was measured by channelising the water into a graduated polythene cylinder and measuring the time with a stop-watch having a least count of one second.

3.2.6. COLLECTION OF WATER SAMPLES

About 500 ml of clear water sample was collected in double stoppered polythene bottles taking care not to entrap any air bubble. Samples were collected from all the major hot springs as well as local wells and rivers as reference cold water sources. In order to verify seasonal variations, if any, the field measurements and analysis were repeated during the three main seasons of summer (May), winter (February) and monsoon (June to October). None of the samples showed any precipitation in the bottles during storage.

3.2.7. COLLECTION OF GEOLOGIC DATA

The country rock around the springs was studied in detail with respect to rock type, structural features, weathering and hydrothermal alterations. Dip and strike of bedding-planes and orientation of all major joint-planes were recorded by means of clinometer compass. Observations were made regarding control of flow of the springs through joints. Representative samples were collected for later petrographic, X-ray diffraction, D.T.A. and Electron Microscopic investigations.

3.3. LABORATORY METHODS

The following major constituents of hot springs and cold water samples were quantitatively determined: Na^{+}, K^{+}, Ca^{++}, Mg^{++}, SiO_2, Cl^{-}, HCO_3^{-}, $SO_4^{=}$ and T.D.S.. Temperature and pH were also measured in the laboratory. Method of analysis was adopted from Standard Methods (12th edition, 1965). Rocks and soil samples were finely grounded for X-ray diffraction, D.T.A. and electron-microscope studies. Limited number of thin section of rocks were prepared for mineral identification and textural studies under petrographic microscope.

3.3.1. SODIUM AND POTASSIUM

Na^{+} and K^{+} were determined by a SYSTRONICS M K-1 Flame photometer having a moving spot galvanometer calibrated

with standard NaCl and KCl solutions giving full scale reflection for 25 mg per liter. The zero of the scale was set with the distilled water and the lowest detection limit was 0.25 mg per liter.

3.3.2. CALCIUM AND MAGNESIUM

The complexometric titration method using standard (0.01 M) E.D.T.A. was used to determine total hardness equivalents of $Ca^{++} + Mg^{++}$. A buffer solution (NH_4Cl, NH_4OH at pH 10) and Erichrome Black T dye indicator were used for this purpose. Calcium hardness was determined separately by E.D.T.A. titration using 1 N NaOH and Murexide dye indicator. Magnesium was calculated by difference between the first and the second titrations. Accuracy of E.D.T.A. titration method is about $\pm$10 percent.

3.3.3. SILICA

Dissolved silica in the monomeric form (H_4SiO_4) was determined by the colorimetric ammonium molybdate yellow method. Intensity of the yellow color was measured by a SYSTRONICS 103 SPECTRO COLORIMETER at 410 nm with an accuracy of $\pm$1.0 percent. A calibration curve with distilled water blank and standard silica solution (1 to 20 mg per liter) was used for the determination of silica in the sample.

3.3.4. CHLORIDE

Chloride was determined by the Mohr method which involves titration with standard $AgNO_3$ (0.01 N) solution using K_2CrO_4 indicator. Reagent blank with distilled water was used. Relatively high chloride samples were diluted for accurate titration. Accuracy of the titration is $\pm$5.0 percent.

3.3.5. BICARBONATE

Bicarbonate was determined by titration with 0.02 N HCl upto Methyl Orange end-point. Accuracy of the method is $\pm$10.0 percent.

3.3.6. SULPHATE

Sulphate was determined by turbiditimetric method in which $BaSO_4$ is precipitated on addition of $BaCl_2$ in presence of a conditioning solution containing glycerol, HCl, ethyl alcohol and NaCl. The turbidity was measured in a SYSTRONICS 103 SPECTRO COLORIMETER at 425 nm within 3 to 10 minutes. A calibration curve was prepared using distilled water blank and standard solutions in the range of 1 to 20 mg per liter. Samples were diluted within the range of the standards whenever needed. Accuracy of the method is $\pm$10 percent.

3.3.7. TOTAL DISSOLVED SOLIDS

Total dissolved solid was calculated from measurement of specific conductivity using the statistical relationship:

T.D.S. (in mg/liter) = 0.65 x Specific conductivity (in micromhos/cm at 25°C)

A German make Meterohm conductivity meter having an accuracy of $\pm$0.5 percent was used for this purpose.

3.3.8. TEMPERATURE AND pH

For each of the samples pH was redetermined at laboratory temperature using a PHILIPS PRECISION pH METER, standard buffer solutions and a 110°C thermometer.

3.3.9. ANALYSIS OF ROCK, SEDIMENT AND DEPOSIT FROM SPRING WATER

(a) Petrographic studies of fresh and weathered rock samples were carried out using MEOPTA-CZECHOSLOVAKIA make microscope. Results are summarised in Table 6.1.

(b) The weathered portions of the rocks were separated and after grinding upto 200 mesh size subjected to X-ray diffraction studies to find out mineralogical composition.

(c) The clay fraction was separated, from the bulk powder by decanting from water suspension, after treating with HCl and H_2O_2 (20%) solution to decompose organic matter. Slides were prepared for X-ray

diffraction studies using FeK_{α} radiations on GENERAL ELECTRIC XRD-5 X-RAY DIFFRACTOMETER. Wherever needed samples were studied after glycolation also. Diffractograms are given in Chapter 6.

(d) To supplement the findings of X-ray investigations a few samples were prepared for D.T.A. using DERIVATOGRAPH MOM THERMAL ANALYSER. D.T.A. curves are shown in Figure 6.11.

(e) To confirm the type of clay minerals selected samples were studied under PHILIPS E.M. 301 TRANSMISSION ELECTRON MICROSCOPE. Results are given in Chapter 6.

(f) Semi-quantitative elemental analysis of the deposit from the spring water was carried out using the VEERLAND DIRECT READING SPECTROSCOPE, U.S.A. Model-6.

Chapter 4

THERMAL WATER COMPOSITION

4.1. INTRODUCTION

Natural waters occurring in geothermal reservoirs is collectively known as Geothermal Waters or Thermal Waters. This includes waters issuing from hot springs and steam vents as well as discharges from deep wells. The chemical nature of thermal water is of utmost importance both for academic and practical utilisation purposes. In fact, most of the problems associated with exploration and utilisation of geothermal systems are related to the peculiar chemistry of thermal waters.

Depending on the nature of discharge, geothermal reservoirs can be broadly classified into two groups, namely: (i) vapour-dominated and (ii) hot water systems. White (1970) observed certain chemical characteristics which distinguish these two types. For example, relatively high chloride content (more than 50 ppm) is a characteristic feature of hot water systems. Experience to date suggests that hot water systems are much more abundant than vapour-dominated systems perhaps by a ratio of 20 to 1.

Considering the hot water reservoirs alone, a commonly adopted classification is based on measured or estimated subsurface water temperature. Reservoirs with

temperature above 100°C belong to 'High Temperature' type. In these geothermal areas, deposition of siliceous sinter and geyser activity are common features. It is obvious that the high temperature reservoirs have greater potential for generation of geothermal energy. According to Ellis and Mahon (1977) appreciable quantities of electricity has been produced in areas where there is water and steam at temperatures in excess of about 180°C within one to two kilometers of the surface. These geothermal waters occur in zones of unusually high temperature gradient, for example, in recent volcanic areas. As a corollary, 'Low Temperature' thermal waters occur in many parts of the world in areas of recent tectonic activity, active metamorphism and unusually deep ground water circulation. A common precipitate from low temperature waters is $CaCO_3$ or travertine. Although not attractive from power generation point of view, their wide occurrence make the low temperature or warm water systems more economical for small scale utilisation like community heating. The Rajgir-Monghyr hot spring belt falls in this latter category.

The most remarkable feature of hot spring waters is their wide range of compositions (White, 1957; Uzumasa, 1965). At the same time, there is enough distinction in concentration levels to call for a classification based on chemical composition. The classification scheme originally proposed by White (1957) for thermal waters of

volcanic origin has been adopted by Ellis and Mahon (1977) for non-volcanic areas also. Four major groups are readily recognised namely, (i) Alkali-Chloride-Waters, (ii) Acid-Sulphate-Waters, (iii) Acid-Sulphate-Chloride Waters and (iv) Bicarbonate-Waters. The major chemical features are summarised in Table 4.1.

This scheme of classification is based on pH value and relative proportion of chloride, sulphate and bicarbonate. The alkali-chloride-waters are rich in sodium, potassium, chloride and silica and very commonly erupt as geysers with high discharge. The alkali-sulphate-waters, on the other hand, are mostly near surface mud pots with relatively small discharge. The acidity is traced to surface oxidation of effluent hydrogen sulphide gas. The acid-sulphate-chloride type is usually a mixture of above two types. The bicarbonate-waters represent carbon dioxide rich systems.

The Geological Survey of India has recorded about 300 hot springs throughout the country. Indian spring waters can be classified into four main types on the basis of their chemical composition (CSIR, 1962). These are:

(i) "Simple" or "Indifferent", characterised by low mineral content;

(ii) Alkaline; containing high sodium and bicarbonate,

(iii) Sulphur waters; characterised by the presence of hydrogen sulphide gas and often sulphate radical and

TABLE 4.1. CLASSIFICATION OF THERMAL WATERS. (Ellis and Mahon, 1977).

Type	Alkali Chloride Waters	Alkali Sulphate Waters	Acid Sulphate Chloride Waters	Bicarbonate Water
Location	Geyser 238 El Tatio Chile	Waiotapu Newzealand	Waiotapu Newzealand	Well 5 Wairakei Newzealand
pH	7.32	2.8	2.8	8.6
Na^+	4340	43	405	230
K^+	520	11	74	17
Ca^{++}	272	27	40	12
Mg^{++}	0.5	3.5	7.5	1.7
Cl^-	7922	32	612	2.7
$SO_4^{=}$	30	347	666	11
HCO_3^-	46	0	0	680
SiO_2	260	280	370	191

Note: Concentrations in milligrams per kilogram.

(iv) Saline waters contain high chloride level.

Characteristic features are summarised in Table 4.2.

The 'simple' or 'indifferent' waters are characterised by mineral content as low as 40 ppm and rarely 500 ppm. The Rajgir Waters have been included in this type.

4.2. THERMAL WATER COMPOSITION IN RAJGIR-MONGHYR AREA

Table 4.3 summarises the analysis of thermal waters collected from major hot springs around Rajgir, Bhimbandh and Monghyr. Seasonal variation in the composition was covered by collecting samples in the months of May (as summer), June to October (as monsoon period), and February (as winter). Details of the sample collection and analytical method have been described in Chapter 3.

4.2.1. CATION-ANION BALANCE

If a water analysis covers all the major dissolved constituents, the total cations should be equal to the total anions on equivalent basis. However, in reality, there is usually a small discrepancy because of various factors like analytical errors, presence of constituents not analysed etc. The cation anion balance of the Rajgir-Monghyr water was verified by the following method.

The parts per million (ppm) values of positive and negative ions, were converted to milliequivalent per liter unit by the following relationships.

TABLE 4.2. CHARACTERISTICS OF TYPICAL THERMAL WATERS OF INDIA, ANALYSES IN ppm (CSIR, 1962).

Type	Simple or Indifferent (Brahamkund, Rajgir, Bihar)	Alkali-bicarbonate (Sohna, Gurgaon, Haryana)	Sulphate-water (Surajkund, Hazaribagh, Bihar)	Chloride (Vajreshwari, Maharashtra)
Sodium	2.0	123.0	146.0	710.0
Potassium	Nil	-	-	-
Magnesium	Trace	3.6	Trace	-
Calcium	11.4	11.4	2.9	153.7
Iron	Nil	Nil	Nil	-
Aluminium	Nil	46.7	Nil	-
Bicarbonate	24.0	270.0	123.0 ($CO_3^{=}+HCO_3^{-}$)	9.2 ($CO_3^{=}$)
Sulphate	Trace	11.0	65.0	155.5
Chloride	4.0	199.0	92.0	1241.0
Fluoride	-	Nil	21.0	-
Silica	25.6 ($HSiO_3$)	44.0 (SiO_2)	164.26 ($HSiO_2$)	6.42 ($HSiO_3$)
Temperature (°C)	42.5	46.0	87.0	44.0
Radon (mMc/lit)	6.87	2.93	1.41	Nil
Flow (gph)	8000	580	3000	60

TABLE 4.3. CHEMICAL ANALYSIS OF SPRING WATERS FROM RAJGIR-MONGHYR-BELT (parts per million).

Spring	Sitakund Hot			Rishikund South		
Date	23.10.77	25.2.78*	21.5.78	24.10.77*	26.2.78	22.5.78
Temp.°C	61°	45°	47°	42°	40°	39°
pH	6.5	6.5	7.0	4.85	5.0	5.5
Na^+	24.50	26.00	23.80	3.50	3.90	3.40
K^+	3.90	4.10	1.50	1.20	1.50	1.20
Ca^{++}	36.80	35.10	28.07	3.12	3.40	2.90
Mg^{++}	10.53	8.70	7.20	0.63	0.91	0.60
HCO_3^-	141.20	151.90	143.80	12.84	11.27	13.80
Cl^-	34.08	38.10	24.50	4.97	5.00	5.49
$SO_4^=$	3.00	3.00	5.60	1.20	1.10	1.10
SiO_2	53	49	62	35	37	32
T.D.S.	169.60	208.00	170.20	19.17	18.20	20.15

Spring	Rishikund North			Bhimbandh Road Side		
Date	24.10.77*	26.2.78	22.5.78	24.10.77	26.2.78*	24.5.78
Temp.°C	45°	41°	44°	60°	65°	59°
pH	5.8	5.0	5.5	5.5	6.0	5.0
Na^+	3.10	3.60	3.30	3.50	4.10	4.90
K^+	1.10	1.41	1.20	0.63	1.60	1.60
Ca^{++}	2.70	3.70	2.90	2.40	2.20	1.96
Mg^{++}	0.42	0.89	0.39	0.29	1.10	0.91
HCO_3^-	11.56	12.12	16.89	11.50	14.20	13.50
Cl^-	5.68	5.50	5.49	4.02	7.40	7.38
$SO_4^=$	1.20	1.20	1.20	2.00	1.50	2.10
SiO_2	37	38	38	57	51	54
T.D.S.	17.80	18.20	18.20	16.90	14.30	14.30

Contd...

TABLE 4.3 (continued)

Spring	Bhimbandh Pool			Chormara	Rameshwar Kund
Date	24.10.77	26.2.78	24.5.78*	23.5.78	25.10.77
Temp.°C	63°	65°	60°	65°	45°
pH	5.5	6.5	5.5	5.5	5.5
Na^+	4.50	4.60	4.80	5.06	2.00
K^+	1.45	1.50	1.96	0.50	0.21
Ca^{++}	2.08	2.10	1.96	3.52	1.60
Mg^{++}	0.84	1.10	0.75	1.44	0.77
HCO_3^-	11.60	14.20	13.50	25.70	12.80
Cl^-	7.81	7.50	7.38	4.99	3.35
$SO_4^=$	1.90	1.80	1.70	2.00	2.00
SiO_2	45	45	39	88	41.50
T.D.S.	14.30	14.30	14.95	20.78	17.60

Spring	Agnikund			Near Agnikund	Singhirishi
Date	30.10.77*	18.2.77	30.5.78	30.10.77	28.10.77
Temp.°C	49°	39°	41°	35°	32°
pH	6.0	6.0	6.0	6.0	5.5
Na^+	7.00	13.75	4.56	6.25	4.00
K^+	0.84	6.20	0.50	0.42	0.42
Ca^{++}	4.80	19.24	3.84	4.16	1.92
Mg^{++}	1.16	27.20	0.76	0.58	0.77
HCO_3^-	24.40	35.00	25.70	9.60	7.70
Cl^-	3.57	31.95	4.49	2.90	3.79
$SO_4^=$	3.90	4.00	10.67	4.30	4.10
SiO_2	41.50	45.00	60.00	34.00	20.50
T.D.S.	38.00	95.60	23.95	34.00	16.20

Contd...

TABLE 4.3 (continued)

Spring	Surajkund			Brahamkund		
Date	31.10.77*	19.2.77	29.5.78	31.10.77	19.2.77	29.5.78*
Temp.°C	41°	41°	41°	41°	38°	45°
pH	6.0	5.5	6.1	6.0	6.0	6.1
Na^+	2.80	7.25	3.00	3.40	6.00	3.60
K^+	1.20	7.50	1.20	1.20	5.00	1.50
Ca^{++}	4.50	24.05	4.21	5.20	16.00	5.90
Mg^{++}	1.05	13.59	1.01	1.68	17.50	1.12
HCO_3^-	17.98	12.38	18.50	17.98	20.10	23.70
Cl^-	5.96	24.80	5.68	5.96	17.50	5.82
$SO_4^=$	2.10	4.00	2.00	2.00	5.00	2.10
SiO_2	27.00	22.00	28.00	26.00	26.80	25.00
T.D.S.	22.40	55.20	24.05	27.30	56.80	31.20

Spring	Makhdumkund		
Date	31.10.77*	19.2.77	29.5.78
Temp.°C	35°	38°	32°
pH	6.0	6.0	6.1
Na^+	2.90	7.50	3.00
K^+	1.10	5.00	1.20
Ca^{++}	4.16	12.80	4.20
Mg^{++}	0.84	9.73	0.729
HCO_3^-	15.40	16.00	16.59
Cl^-	5.68	23.00	5.68
$SO_4^=$	2.20	5.00	2.10
SiO_2	28.00	23.00	28.00
T.D.S.	20.80	42.20	22.78

(i) $\frac{\text{ppm}}{\text{Molecular or Atomic weight}} \times 10^{-3} = \frac{\text{moles}}{\text{liter}}$ (4.1)

e.g., Sodium in Sitakund hot water in February 1978 amounts to 26 ppm (Table 4.3).

So, Na^+ in moles per liter $= \frac{26}{23} \times 10^{-3}$

$= 1.1304 \times 10^{-3}$

or, $Na^+ = 1.1304$ millimoles per liter.

(ii) $\frac{\text{ppm}}{\text{Equivalent weight}} \times 10^{-3} =$ Equivalent per liter (4.2)

where equivalent weight is equal to:

$$\frac{\text{Atomic or molecular weight}}{\text{Valency}},$$

e.g., Calcium in Sitakund hot water in February 1978 is equal to 35 ppm. Therefore,

Ca^{++} in equivalent per liter $= \frac{35}{40.08 \times 2} \times 10^{-3}$ —

$= 1.752 \times 10^{-3} \frac{\text{equivalent}}{\text{liter}}$

or, $Ca^{++} = 1.752$ milliequivalent per liter

The discrepancy in cation-anion balance has then calculated using the following relationship (Water Well Hand Book, 1967).

The percentage discrepancy =

$$\frac{\text{Sum of cations} - \text{Sum of anions}}{\text{Sum of cations} + \text{Sum of anions}} \times 100$$

where cation and anion concentrations are expressed in equivalent per liter. The calculation for Sitakund hot spring, February 1978 is illustrated below.

Cations (milliequivalent per liter)		Anions (milliequivalent per liter)	
Na^+	1.130	$SO_4^=$	0.062
K^+	0.105	Cl^-	1.074
Ca^{++}	1.752	HCO_3^-	2.490
Mg^{++}	0.715		
Sum (cations)	3.702	Sum (anions)	3.626

$$\text{Percentage Discrepancy} = \frac{3.702 - 3.626}{3.702 + 3.626} \times 100$$

$$= 1.03 \text{ percent}$$

The discrepancy in cation-anion balance calculated by this method widely varied from sample to sample, although they are generally less than five percent. For the purpose of further interpretation of water analysis of a particular spring, the set which has minimum discrepancy was selected and is identified with an asterisk in

Table 4.3. The accepted analysis of the twelve samples is again summarised in Table 4.4.

4.2.2. CONCENTRATION LEVELS

It may be pointed out that the concentrations of chemical species in Rajgir-Monghyr waters is very low. The total dissolved solids in most of the spring water is around 20 ppm. There are a few exceptions e.g., Sitakund hot (T.D.S. about 200 ppm) and Rajgir group of springs (T.D.S. about 50 ppm). Because of their remarkably low mineral content, the Rajgir-Monghyr springs have been classified as 'simple' or 'indifferent' waters (CSIR, 1962). Gupta and others (1975) also comment that from geochemical point of view, the mildly acidic, low T.D.S. waters of the Rajgir-Monghyr belt are rather unique in the world. These waters are also known to be radioactive and contain from 1 to 6.9 mMc per liter of radon (CSIR, 1962). The effluent gases contain 15 to 20% CO_2, 1% CH_4, 6-9% O_2 and 70-80% Nitrogen (Gupta and others, 1975). These authors have classified these springs as "Calcium-Magnesium-Bicarbonate" type. However, in this analysis it is found that sodium and chloride are equally important compared to calcium and bicarbonate whereas magnesium is relatively negligible. The waters can, therefore, classified as Na-Ca-Cl-HCO_3 type.

The pH of waters in Rajgir area was found to vary from 5.5 at 41°C to 6.1 at 40°C. Bhimbandh group of

TABLE 4.4. CHEMICAL ANALYSIS OF SPRING WATERS FROM RAJGIR-MONGHYR BELT SELECTED FOR FURTHER INTERPRETATION (millimoles per liter).

Spring	Sitakund Hot	Rishikund South	Rishikund North
Date	25.2.78	24.10.77	24.10.77
Temp. °C	45°	42°	45°
pH	6.50	4.85	5.80
Na^+	1.130	0.152	0.135
K^+	0.105	0.030	0.028
Ca^{++}	0.878	0.078	0.068
Mg^{++}	0.358	0.026	0.017
HCO_3^-	2.490	0.210	0.189
Cl^-	1.074	0.140	0.160
$SO_4^=$	0.031	0.012	0.012
SiO_2	0.804	0.574	0.607

Spring	Bhimbandh Road Side	Bhimbandh Pool	Chormara
Date	26.2.78	24.5.78	23.5.78
Temp. °C	65°	60°	65°
pH	6.0	5.5	5.5
Na^+	0.178	0.210	0.220
K^+	0.041	0.050	0.013
Ca^{++}	0.055	0.049	0.088
Mg^{++}	0.045	0.031	0.059
HCO_3^-	0.230	0.220	0.421
Cl^-	0.209	0.208	0.141
$SO_4^=$	0.016	0.018	0.021
SiO_2	0.836	0.640	1.443

Contd...

TABLE 4.4 (continued)

Spring	Rameshwarkund	Singhirishi	Agnikund
Date	25.10.77	28.10.77	30.10.77
Temp. °C	45°	32°	49°
pH	5.5	5.5	6.0
Na^{+}	0.087	0.174	0.304
K^{+}	0.005	0.011	0.021
Ca^{++}	0.040	0.048	0.120
Mg^{++}	0.032	0.032	0.048
HCO_3^{-}	0.210	0.126	0.399
Cl^{-}	0.094	0.107	0.101
$SO_4^{=}$	0.021	0.043	0.041
SiO_2	0.681	0.336	0.681

Spring	Surajkund	Brahamkund	Makhdumkund
Date	31.10.77	29.5.78	31.10.77
Temp. °C	41°	45°	35°
pH	6.0	6.1	6.0
Na^{+}	0.122	0.157	0.126
K^{+}	0.031	0.038	0.028
Ca^{++}	0.113	0.148	0.104
Mg^{++}	0.043	0.046	0.033
HCO_3^{-}	0.290	0.390	0.250
Cl^{-}	0.168	0.164	0.160
$SO_4^{=}$	0.022	0.022	0.023
SiO_2	0.443	0.410	0.459

springs have pH varying from 4.85 at 42°C to 6.0 at 65°C. The Sitakund hot spring has pH between 6.5 at 45°C and 7.0 at 47°C. The neutral pH of the water is around 6.8 at 40°C and decreases to about 6.5 at 60°C (Ellis and Mahon, 1977). The Rajgir-Monghyr springs can, therefore, be classified as acidic whereas the Sitakund spring is near-neutral or slightly alkaline at the vent temperature.

The cations viz., sodium, potassium, calcium, magnesium in all these thermal waters have been found to be lower than the corresponding cation concentrations in the local meteoric water (Table 4.5). It may be mentioned that among all the hot springs, Sitakund hot spring has extraordinarily high cation concentrations. For example, sodium ion concentration in Sitakund hot spring and Sitakund cold water is 25 ppm and 36 ppm respectively. The corresponding value for other springs is around 5 ppm.

The bicarbonate concentrations at Sitakund Hot, Chormara and Rajgir springs are 140, 25 and 20 ppm respectively. The corresponding value for other springs is around 12 ppm only.

It is interesting to note that the bicarbonate content of these thermal waters is remarkably lower than the bicarbonate concentration in meteoric (non-thermal) waters, which is around 200 ppm (Table 4.5).

The sulphate content in meteoric water, Sitakund hot spring and rest of the other hot springs is respectively

TABLE 4.5. CHEMICAL ANALYSIS OF METEORIC (NON-THERMAL) WATERS FROM RAJGIR-MONGHYR-AREA (parts per million).

Source	Sitakund Cold			Man River		
Date	23.10.77	25.2.78	21.5.78	24.10.77	26.2.78	25.5.78
Temp.°C	34°	24°	33°	28°	24°	33°
pH	7.3	7.1	7.0	5.5	5.5	5.5
Na^{+}	62.0	36.0	36.0	4.8	5.4	4.9
K^{+}	9.60	7.50	9.00	1.60	2.40	1.70
Ca^{++}	57.60	70.10	58.00	2.77	1.30	2.40
Mg^{++}	1.45	12.50	12.13	0.42	0.80	0.69
HCO_3^{-}	196.4	199.9	250.1	19.2	15.0	20.1
Cl^{-}	29.04	21.10	23.40	5.39	6.70	5.68
$SO_4^{=}$	10.0	3.0	4.0	1.2	1.1	1.7
SiO_2	36	61	68	30	31	32
T.D.S.	209.00	266.50	273.60	17.50	15.60	18.20

Source	Tube Well (Bhimbandh)
Date	23.5.78
Temp.°C	27°
pH	5.7
Na^{+}	3.8
K^{+}	0.25
Ca^{++}	4.01
Mg^{++}	3.07
HCO_3^{-}	47.5
Cl^{-}	6.24
$SO_4^{=}$	3.0
SiO_2	18
T.D.S.	33.21

5, 4 and less than 2 ppm, chloride in the corresponding waters is 65, 34 and less than 6 ppm respectively.

The silica content of these springs varies from 18 ppm to 88 ppm.

4.3. SEASONAL VARIATION

For considering the effect of seasonal variation one may assume; May as summer; February as later part of winter and June to October as monsoon season.

4.3.1. PHYSICAL PARAMETERS

The temperature of springs measured in various seasons are summarised in Table 4.3. The values of flow rates of various springs are summarised in Table 2.1. From these data it is apparent that the temperature as well as the flow rate exhibit considerable seasonal variation. The general trend being the lower value of these parameters in winter and a sharp increase after rains.

4.3.2. CHEMICAL COMPOSITION

The investigation of the variation of chemical composition as a function of seasonal variation is restricted because of the very low content of chemical species. The observations could vary well within the range of analytical accuracy.

In the Rajgir group of springs the pH values are slightly acidic which are not affected by season and by

the consequent change in the temperature. The concentration of chemical species viz., Na^+, K^+, Ca^{++}, Mg^{++}, Cl^- and $SO_4^=$ as well as the specific conductivity are relatively higher (Table 4.3) in the winter and decrease remarkably after rains. The silica concentration is low in winter and increases by about 20% after rains. The HCO_3^- alkalinity fluctuates in an erratic manner. In these Rajgir group of springs the concentration of total dissolved solids is usually higher compared to the values at other springs. The possible hydrological factor in the spring circulation system governing such observed variation is unresolved.

In Bhimbandh group of springs the pH values are relatively lower compared to Rajgir group of springs. The silica content, on the other hand, is relatively high which can be correlated with high vent temperature in these springs. The variation of major elements composition is observed to vary within 10 percent across the three seasons.

In Sitakund hot spring the temperature variation is much pronounced compared to Rajgir and Bhimbandh group of springs. The pH values vary from 7.0 at 47°C in May to 6.5 at 65°C in October 1977. This shows the variation of pH values as fluctuation of temperature rise due to variation in season. HCO_3^-, pH, Na^+, K^+, Cl^- and T.D.S. concentrations are higher in winter compared to other two

seasons. The other species Ca^{++} and Mg^{++} have intermediate value in summer and after rainy seasons in February. The Sitakund hot spring is located close to Monghyr town therefore contamination in concentrations particularly of Na^{+} and Cl^{-} is possible due to domestic sewage.

The observed variation in temperature and chemical compositions clearly points to strong influence of rainfall in the month of May and June. It is suggested that the springs represent recycled ground-water which descend through fractured and jointed quartzite to a hot-zone at depth. The water after equilibrating at this zone rapidly rises under thermo-artesian condition to emerge as a hot spring at the surface. After rainfall, the depth of ground-water circulation increases and hence, the temperature of spring shows an upward trend. The increased discharge lowers the chemical concentration by dilution. However, silica which reflects equilibrium with quartz at depth shows a reverse trend, because the temperature of equilibrium is higher at a greater depth of circulation. This suggested model is further developed on the basis of geochemical indicators in the next chapter.

Chapter 5

GEOCHEMICAL INDICATORS OF SUBSURFACE CONDITIONS

5.1. SUBSURFACE TEMPERATURE

Estimation of subsurface temperature based upon water chemistry is a convenient and useful method for exploration of geothermal resources. Several chemical constituents of thermal springs are derived from the country rock when ground water reacts with rock forming minerals at high temperature and pressure during deep circulation. Many such rock-water reactions have now been studied in field and laboratory. One of the most significant contributions of modern geochemistry has been to establish that natural water systems can be treated as systems at thermodynamic equilibrium (Garrels and Christ, 1965; Krauskopf, 1967). Equilibrium reactions between rock and water follow the 'Law of Mass Action' and an expression for equilibrium constant (K) can be written out. The fundamental relationships are:

$$\Delta G_r^o = - RT \ln K = - 2.303 RT \log K \qquad (5.1)$$

Where ΔG_r^o is the change in free energy during reaction under standard conditions, R is Universal Gas Constant and T is the temperature on absolute scale.

The change in free energy of reaction can also be expressed as:

$$\Delta G^{o}_{r} = \Delta H^{o}_{r} - T\Delta S^{o}_{r} \qquad (5.2)$$

Where ΔH^{o}_{r} and ΔS^{o}_{r} are the standard heat of reaction (enthalpy) and entropy of reaction respectively. For small temperature ranges ΔH^{o}_{r} and ΔS^{o}_{r} can be assumed to be independent of temperature (van't Hoff assumption). Thus for two temperatures T_1 and T_2,

$$\Delta G^{o}_{rT_1} = -2.303\, RT_1 \log K_{T_1}$$

$$= \Delta H^{o}_{r} - T_1 \Delta S^{o}_{r} \qquad (5.3)$$

and

$$\Delta G^{o}_{rT_2} = -2.303\, RT_2 \log K_{T_2}$$

$$= \Delta H^{o}_{r} - T_2 \Delta S^{o}_{r} \qquad (5.4)$$

So,

$$\log K_{T_1} = \frac{-\Delta H^{o}_{r}}{2.303\, R}\left(\frac{1}{T_1}\right) + \frac{\Delta S^{o}_{r}}{2.303\, R} \qquad (5.5)$$

and

$$\log K_{T_2} = \frac{-\Delta H^{o}_{r}}{2.303\, R}\left(\frac{1}{T_2}\right) + \frac{\Delta S^{o}_{r}}{2.303\, R} \qquad (5.6)$$

Therefore,

$$\log K_{T_2} - \log K_{T_1} = \frac{-\Delta H^{o}_{r}}{2.303\, R}\left(\frac{1}{T_2} - \frac{1}{T_1}\right) \qquad (5.7)$$

or, in a general way,

$$\log K_T = \frac{-\Delta H^o_r}{2.303\,R}\left(\frac{1}{T}\right) + \frac{\Delta S^o_r}{2.303\,R} \qquad (5.8)$$

which represents a straight line relationship between log K and 1/T. The log K increases with temperature, where ΔH^o_r is a positive quantity. This relationship can also be expressed in the differential form,

$$\frac{d \ln K}{dT} = \frac{\Delta H^o_r}{RT^2} \qquad (5.9)$$

The linear plot between log K and 1/T is commonly used to estimate underground temperature at known concentrations of dissolved chemicals representing the equilibrium constant of a given reaction. Although many such qualitative temperature indicators have been suggested, three rock-water equilibrium reactions have been widely used. These are:

(1) the silica geothermometer,

(2) sodium-potassium geothermometer,

(3) sodium-potassium-calcium geothermometer.

The temperature thus estimated is known as the base temperature of the geothermal reservoir. This is a useful parameter during exploration stages. In general, reservoir base temperatures below 150°C have little importance for future power production (White, 1970).

5.1.1. SILICA GEOTHERMOMETER

It has been well established that the silica content of thermal springs commonly fall above quartz saturation and

below amorphous silica saturation at the spring temperatures (Raymahashay, 1968 and Figure 5.1). Such observations have led to the suggestion that the waters reflect saturation with quartz at depth at temperatures higher than the vent temperatures. The solubility of quartz in water can be represented by the equilibrium reaction:

$$\text{Silica (quartz)} + 2H_2O = H_4SiO_4 \text{ (aqueous)}$$

Where H_4SiO_4 (aq) is the monomeric species representing dissolved silica. The equilibrium constant of the reaction is therefore, simply:

$$K = a\,H_4SiO_4 \qquad (5.10)$$

Where $a\,H_4SiO_4$ is the activity of H_4SiO_4 species being approximately equal to moles per liter dissolved silica. Activities of pure quartz and water are assumed to be unity. Quartz solubility increases with temperature along a logarithmic curve (Fournier, 1973).

Knowing the variation of quartz solubility with temperature one can, therefore, estimate the temperature at which the given concentration level in the spring is achieved at depth. Two important assumptions are that (1) the concentration represents equilibrium composition and (2) there was no change in concentration by precipitation, dissolution, dilution, steam loss etc. during the rapid rise of the spring water to the surface. Fournier

and Rowe (1966) and Fournier (1973) have presented empirical curves which include the effect of steam loss on the base temperature estimated from silica content in the springs, (Figure 5.2). The correction is negligible at temperatures lower than 120°C. On the other hand, excellent agreement between silica base temperatures and actual borehole measurements has been recorded by Mahon (1966) and Fournier and Rowe (1966). For best results, temperature is estimated from total (colloidal plus dissolved) silica which is practically equal to dissolved silica at low concentration levels.

Some workers have pointed out that other forms of silica like cristobalite and chalcedony might control the silica level in hot springs (Fournier, 1973; Arnorsson, 1975). However, quartz is the stable form of silica and has the lowest solubility. Therefore, equilibrium between water and other silica phases can only be metastable. Moreover, the difference in solubility between various silica phases becomes negligible at relatively lower temperature. Similarly, effect of pressure and dissolved salts on quartz solubility is significant only near the critical temperature of water and can be neglected for low base temperatures (Ellis and Mahon, 1977). Quartz solubility is also unaffected by pH particularly when buffered below 7.5 by rock-water reaction (Fournier, 1973). It turns out that at the present time the silica method

based on quartz solubility is the most reliable and most widely used geothermometer for estimation of base temperatures.

Truesdell (1975) has suggested the following empirical relationship between base temperature and silica concentration in parts per million:

$$t°C = \frac{1533.5}{5.768 - \log SiO_2} - 273.15 \qquad (5.11)$$

It is clear, however, that an appropriate correction has to be made for springs which result from mixing of shallow and deep-waters. This is elaborated in a later section.

5.1.2. SODIUM-POTASSIUM GEOTHERMOMETER

This geothermometer is based on the exchange of sodium and potassium ions between alkali feldspars. The relevant equilibrium is given by the equation:

$$\text{Na-feldspar} + K^+ = \text{K-feldspar} + Na^+ \qquad (5.12)$$

The equilibrium constant given by

$$K = \frac{aNa^+}{aK^+} \qquad (5.13)$$

has been found to decrease with increasing temperature and $\log \frac{aNa^+}{aK^+}$ has a positive linearity with 1/T according to the van't Hoff relationship (Orville, 1963; Ellis, 1970). Truesdell (1975) suggests the following empirical relationship between sodium-potassium ratio expressed in parts per million and base temperature:

$$t°C = \frac{855.6}{\log Na/K + 0.8573} - 273.15 \qquad (5.14)$$

Inspite of these theoretical and experimental relationships, the Na-K geothermometer has limited application in geothermal areas. Very commonly the base-temperature obtained by this method is anomolously high (Table 5.2). This is, probably, because the above simple cation exchange between sodium ions and potassium ions is usually not the dominant reaction in natural systems. This method is particularly unsuitable in carbonate depositing springs where the effect of dissolved calcium is significant. Fournier and Truesdell (1973) have recommended a modified sodium-potassium-calcium geothermometer as discussed below.

5.1.3. SODIUM-POTASSIUM-CALCIUM GEOTHERMOMETER

This geothermometer is based on ion exchange among plagioclase feldspars. A typical equilibrium reaction is given by the equation:

$$Ca_{1/6}\ Na_{2/3}\text{-feldspar} + K^+ = K\text{-feldspar} + \frac{2}{3}\ Na^+ + \frac{1}{6}\ Ca^{++} \qquad (5.15)$$

Therefore,

$$K = \frac{aNa^{+2/3} \times aCa^{++1/6}}{aK^+} \qquad (5.16)$$

$$= \left(\frac{aNa^+}{aK^+}\right)\left(\frac{\sqrt{aCa^{++}}}{aNa^+}\right)^{1/3} \qquad (5.17)$$

so,

$$\log K = \log \frac{aNa^+}{aK^+} + \frac{1}{3} \log \frac{\sqrt{aCa^{++}}}{aNa^+} \qquad (5.18)$$

or in general,

$$\log K = \log \frac{aNa^+}{aK^+} + \beta \log \frac{\sqrt{aCa^{++}}}{aNa^+} \qquad (5.19)$$

where β varies from 1/3 to 4/3.

Fournier and Truesdell (1973) observed a linear relationship between log K and 1/T and recommended these geothermometers for waters where $\frac{\sqrt{mCa^{++}}}{mNa^+} > 1$, where the concentration of Ca and Na are expressed in moles per liter.

Truesdell (1975) has suggested the following empirical relationship between sodium-potassium-calcium concentrations in moles per litre and base temperature:

$$t°C = \frac{1647}{\log (\frac{Na}{K}) + \beta \log (\frac{Ca^{\frac{1}{2}}}{Na}) + 2.24} - 273.15 \qquad (5.20)$$

Where $\beta = 4/3$ for $Ca^{1/2}/Na > 1$ and $t_{1/3} < 100°C$

$\beta = 1/3$ for $Ca^{1/2}/Na < 1$ or, if $t_{4/3} > 100°C$.

The following steps are suggested:

Using molal concentrations, $(Ca^{1/2}/Na)$ is calculated. If this is less than 1, a value 1/3 is used for β and the temperature is estimated. If the $(Ca^{1/2}/Na)$ is greater than 1, a value of 4/3 is used for β. If the temperature

estimated in the latter way is greater than 100°C, one should revert to a value of 1/3 for β and use the temperature obtained; otherwise the temperature for $\beta = 4/3$ is taken as correct.

Paces (1975) suggested a correction for the Na-K-Ca geothermometer incorporating the effect of carbon dioxide pressure in the following way,

$$\log K = \log Q - I \qquad (5.21)$$

$$\text{Where, } I = -1.36 - 0.253 \log P_{CO_2} \qquad (5.22)$$

P_{CO_2} being partial pressure of carbon dioxide, calculated from alkalinity and pH at the spring temperature and $Q = \log \frac{aNa^+}{aK^+} + \frac{4}{3} \log \frac{\sqrt{aCa^{++}}}{aNa^+}$. The K value thus obtained is used to estimate the base temperature from the Na-K-Ca geothermometer. This correction was found to be applicable for low temperature spring water below 75°C and P_{CO_2} above 10^{-4} atmosphere, where the aquifer base temperature is approximately equal to the spring temperature. Fournier and Potter (1979) also suggested a correction to the Na-K-Ca geothermometer for magnesium rich waters at temperatures above 70°C and $R^* = Mg/(Mg + Ca + K)$ ratio in equivalents below 50 percent. The amount of temperature correction is a function of Na-K-Ca base temperature and R^*.

It is to be pointed out that the Na-K and Na-K-Ca geothermometers are affected by mixing of shallow and deep waters and hence give anomalous base temperatures under such hydrologic conditions.

5.2. SUBSURFACE TEMPERATURE INDICATORS IN RAJGIR-BHIMBANDH-MONGHYR AREA

The three major geothermometers namely silica, sodium-potassium and sodium-potassium-calcium were used to estimate the base temperature from water analysis (Table 4.4) of the Rajgir-Monghyr-Bhimbandh springs, assuming at the first instance that the chemical constituents represent undiluted equilibrium levels.

For the silica geothermometer, temperature was estimated from the empirical curve of Fournier (1973) (Figure 5.2) and this value was compared with the empirical equation of Truesdell (1975). A sample calculation for two springs of the Monghyr area is summarised below.

Spring	Silica	Temperature °C from graph	Temperature °C from equation
Sitakund Hot February 1978	49	102°C	102.91°C
Rishikund South October 1977	35	88°C	89.90°C

As is obvious from this calculation, the agreement between the estimates from the graphical and calculation method is quite satisfactory, hence, the Truesdell (1975) equation was fitted into a computer programme* and base temperatures were estimated for all the springs in the Rajgir-Monghyr and Bhimbandh area. The results are given in the Table 5.1. In a similar manner, the Truesdell (1975)

* Please see the Appendix for the computer programme.

TABLE 5.1. ESTIMATION OF SUBSURFACE TEMPERATURES FROM THE SILICA CONTENT OF WATERS DISCHARGED FROM THE RAJGIR-MONGHYR HOT SPRINGS. AFTER TRUESDELL (1975).

Spring	Date	Silica (ppm)	Estimated Subsurface Temperature (°C)
Sitakund Hot	25.2.78	49.0	102.90°
Rishikund South	24.10.77	35.0	89.90°
Rishikund North	24.10.77	37.0	91.90°
Bhimbandh (Road Side)	26.2.78	51.0	104.52°
Bhimbandh (Pool)	24.5.78	39.0	93.90°
Chormara	23.5.78	88.0	127.90°
Rameshwarkund	25.10.77	41.5	96.40°
Singhirishi	28.10.77	20.5	70.97°
Agnikund	30.10.77	41.5	96.37°
Surajkund	31.10.77	27.0	80.47°
Brahamkund	29.5.78	25.0	77.76°
Makhdumkund	31.10.77	28.0	81.75°

equations for Na-K and Na-K-Ca geothermometers were also run through a computer and the results obtained have been summarised in Tables 5.2 and 5.3.

It is clear that there is considerable discrepancy among the three geothermometers and because these are relatively low temperature springs, the possibility of dilution by mixing of shallow ground water cannot be ruled out.

Under these circumstances, the finer corrections to the Na-K-Ca geothermometer suggested by Paces (1975); Fournier and Potter (1979) also are not warranted. On the other hand, it is worthwhile to utilize existing chemical models to estimate the mixing ratio and the physicochemical parameters of the hot water component which would more clearly reflect the subsurface conditions. The details are discussed in the next section.

5.3. MIXING AND CIRCULATION MODELS

Fournier and Truesdell (1974) suggested the following criteria for recognition of mixing of cold meteoric water with deeper higher temperature water in a geothermal area containing several springs: (i) variation in spring temperatures, (ii) variation in the content of relatively non-reactive constituents like chloride, (iii) a difference between estimated subsurface estimated temperature and the spring temperature by more than 25°C. The relevant

TABLE 5.2. ESTIMATION OF SUBSURFACE TEMPERATURE BASED UPON SODIUM-POTASSIUM RATIO USING EMPIRICAL RELATIONSHIP SUGGESTED BY TRUESDELL (1975)

Spring	Date	Na^+ (ppm)	K^+ (ppm)	Estimated Sub-Surface Temperature
Sitakund Hot	25.2.78	26.00	4.10	242.43°C
Rishikund South	24.10.77	3.50	1.20	373.95°C
Rishikund North	24.10.77	3.10	1.10	381.34°C
Bhimbandh (Road Side)	26.2.78	4.80	1.60	368.02°C
Bhimbandh (Pool)	24.5.78	4.80	1.96	413.37°C
Chormara	23.5.78	5.06	0.50	186.23°C
Rameshwarkund	25.10.77	2.00	0.21	192.83°C
Singhirishi	28.10.77	4.01	0.40	187.24°C
Agnikund	30.10.77	7.00	0.84	208.03°C
Surajkund	31.10.77	2.80	1.20	425.14°C
Brahamkund	29.5.78	3.60	1.50	418.23°C
Makhdumkund	31.10.77	2.90	1.10	396.17°C

TABLE 5.3. ESTIMATION OF SUBSURFACE TEMPERATURE BASED UPON SODIUM-POTASSIUM-CALCIUM CONTENT OF WATERS DISCHARGE FROM THE RAJGIR-MONGHYR HOT SPRINGS, USING EMPIRICAL RELATIONSHIP SUGGESTED BY TRUESDELL (1975).

Spring	Date	Concentration in millimoles per liter Na^{+}	K^{+}	Ca^{++}	Estimated Subsurface Temperature
Sitakund Hot	25.2.78	1.13	0.100	0.878	78.13°C
Rishikund South	24.10.77	0.15	0.030	0.078	76.76°C
Rishikund North	24.10.77	0.13	0.030	0.070	76.74°C
Bhimbandh (Road Side)	26.2.78	0.21	0.040	0.060	93.21°C
Bhimbandh (pool)	24.5.78	0.21	0.050	0.050	102.50°C
Chormara	23.5.78	0.22	0.010	0.090	50.04°C
Rameshwarkund	25.10.77	0.09	0.005	0.040	35.30°C
Singhirishi	28.10.77	0.17	0.010	0.050	53.83°C
Agnikund	30.10.77	0.30	0.020	0.120	59.23°C
Surajkund	31.10.78	0.12	0.030	0.110	71.90°C
Brahamkund	29.5.78	0.16	0.040	0.150	74.07°C
Makhdumkund	31.10.77	0.13	0.030	0.100	70.02°C

TABLE 5.4. TEST FOR MIXED WATER
(Fournier and Truesdell, 1974).

Spring	Date	Cl (ppm).	SiO_2 (ppm)	Base Temperature by Silica Geothermometer (t_H °C)	Vent Temperature t_{sp} °C	$t_H - t_{sp}$
Rishikund South	22.5.78	5.49	32.0	86.60°	39°	47.60
Rishikund North	22.5.78	5.49	38.0	92.00°	44°	48.00
Rishikund South	24.10.77	4.97	35.0	89.90°	42°	47.90
Rishikund North	24.10.77	5.68	37.0	91.99°	45°	46.99
Rishikund South	26.2.78	5.00	37.0	91.99°	40°	51.00
Rishikund North	26.2.78	5.50	38.0	92.00°	41°	51.00
Rameshwarkund	25.10.77	3.35	41.5	96.37°	45°	51.37
Bhimbandh Pool	24.10.77	7.81	45.0	99.50°	63°	36.50
Bhimbandh Road Side	24.10.77	4.02	57.0	109.00°	60°	49.00
Bhimbandh Pool	26.2.78	7.50	45.0	99.50°	65°	34.50
Bhimbandh Road Side	26.2.78	7.40	51.0	104.52°	65°	39.52
Bhimbandh Pool	24.5.78	7.38	39.0	93.99°	60°	33.99
Bhimbandh Road Side	24.5.78	7.38	54.0	106.80°	59°	47.80
Chormara	23.5.78	4.99	88.0	127.92°	65°	62.90

Contd...

TABLE 5.4 (continued)

Spring	Date	Cl (ppm)	SiO_2 (ppm)	Base Temperature by Silica Geothermometer t_H °C	Vent Temperature t_{sp} °C	$t_H - t_{sp}$
Near Agnikund	20.10.77	2.90	34.0	88.82°	35°	53.83
Agnikund	30.10.77	3.57	41.5	96.37°	49°	47.37
Surajkund	31.10.77	5.96	27.0	80.46°	41°	39.46
Brahamkund	31.10.77	5.96	26.0	79.13°	41°	38.13
Makhdumkund	31.10.77	5.68	28.0	81.76°	35°	46.76
Agnikund	30.5.78	4.49	60.0	111.20°	41°	70.26
Surajkund	29.5.78	5.68	28.0	81.76°	41°	40.76
Brahamkund	29.5.78	5.82	25.0	77.76°	45°	32.76
Makhdumkund	29.5.78	5.68	28.0	81.76°	32°	49.76

(i) Temperature of cold water before mixing

(ii) Silica content of cold water

(iii) Temperature of warm spring

(iv) Silica content of warm spring

In this calculation, the following assumptions are made; (i) the initial silica content of deep hot water is controlled by the solubility of quartz, (ii) that no further solution or deposition of silica occur before or after mixing, (iii) the enthalpy of hot water that heat up the cold water is the same as the initial enthalpy of the deep hot water.

Two equations can be written to solve the two unknowns i.e., the temperature of the hot water and the proportion of the hot and cold water, because the silica content and temperature of the warm springs are different functions of the original temperature of the hot water component.

The first equation relates the heat content or enthalpies of hot water, cold water and spring water. The fractions of cold water and hot water are represented as X and (1 - X) respectively. Therefore,

$$(H_{Cold})(X) + (H_{Hot})(1 - X) = H_{Spring} \qquad (5.23)$$

The relation of temperature and enthalpy of saturated water can be obtained from the steam tables quoted by Fournier and Truesdell (1974) and reproduced in Table 5.5. In a similar manner, the second equation relates the silica contents of the hot water in parts per million.

TABLE 5.5. THE VALUES OF SILICA SOLUBILITY IN PARTS PER MILLION AND CORRESPONDING ENTHALPY CHANGE AS A FUNCTION OF TEMPERATURE (Fournier and Truesdell, 1974).

Temperature °C	Enthalpy cal/g	Silica (ppm)
50°	50.0	13.5
75°	75.0	26.6
100°	100.1	48.0
125°	125.4	80.0
150°	151.0	125.0
175°	177.0	185.0
200°	203.6	265.0
225°	230.9	365.0
250°	259.2	486.0
275°	289.0	614.0
300°	321.0	692.0

$$(Si_{Cold})(X) + (Si_{Hot})(1 - X) = Si_{Spring} \quad (5.24)$$

Equations 5.23 and 5.24 can be solved by graphical method as given below:

(i) assume a series of values of enthalpies of hot water for the temperature listed in Table 5.5 and calculate X_t for each as follows:

$$X_t = \frac{(\text{Enthalpy of hot water}) - (\text{Temperature of warm spring})}{(\text{Enthalpy of hot water}) - (\text{Temperature of cold spring})} \quad (5.25)$$

Below 100°C, the enthalpy of water coexisting with steam (saturated water) in cal/g is essentially equivalent in magnitude to the temperature of the water in degree Celsius.

(ii) plot the calculated values of X_t with respect to the temperature from which the assumed hot water enthalpy values were derived.

(iii) assume a series of points of silica content of hot water appropriate for the temperature listed in Table 5.5 and evaluate X_{Si} for each silica content, as follows:

$$X_{Si} = \frac{(\text{Silica in hot component}) - (\text{Silica in warm spring})}{(\text{Silica in hot component}) - (\text{Silica in cold water})} \quad (5.26)$$

(iv) on the graph, previously used, plot the calculated values of X_{Si} in relation to temperatures for which the silica content were obtained.

(v) the point of intersection gives the estimated temperature of hot water component and the fraction of cold water X, 1-X will be the fraction of hot water. For example Bhimbandh (road side) spring's data are plotted and calculated by this method (Figure 5.4 and Table 5.5).

Name of the spring: Bhimbandh (road side)
Sampled on February 26, 1978

Observations

Cold Water Sample (Bhimbandh tubewell)

Temperature	27°C
Silica content	18 ppm

Bhimbandh spring (road side)

Spring temperature	65°C
Silica content	51 ppm

Supposing, temperatures of the hot component are 50°C, 75°C, 100°C, 125°C and so on, then, by solving the following equations:

$$X_t = \frac{H_{hot} - H_{spring}}{H_{hot} - H_{cold}}, \qquad X_{Si} = \frac{Si_{hot} - Si_{spring}}{Si_{hot} - Si_{cold}}$$

Where X_t and X_{Si} are fraction of cold water in warm spring; H_{hot}, H_{spring} and H_{cold} represent enthalpy of hot component warm spring and cold water respectively. Similarly, Si_{hot}, Si_{spring} and Si_{cold} represent silica content in hot component, spring water and cold water respectively.

The values obtained for X_t and X_{Si} at different enthalpies are summarised in Table 5.6. These values of

Table 5.6. THE EVALUATION OF SUBSURFACE TEMPERATURE USING SILICA GEOTHERMOMETER BY GRAPHICAL METHOD (Fournier and Truesdell, 1974)*

Spring -	Bhimbandh (Road Side)	Cold Water -	Bhimbandh Tube Well
Temp.	65°C		27°C
Silica Content	51 ppm		18 ppm

Temperature (t) °C	X_t at t	X_{Si} at t
75°	0.208	-2.837
100°	0.480	-0.033
125°	0.614	0.468
150°	0.694	0.692
175°	0.747	0.802
200°	0.785	0.866
225°	0.814	0.905
250°	0.836	0.930
275°	0.855	0.945
300°	0.871	0.951

* These data are represented in graphical form in Figure 5.4.

X_t and X_{Si} and corresponding temperatures were plotted on graph sheet. The curves X_t and X_{Si} obtained intersect at point I (Figure 5.4) which gives a base temperature 150°C and fraction of cold water 0.693 or 69.3 percent, so fraction of hot water in warm spring is 1-X = 0.307 or 30.7 percent.

Truesdell and Fournier (1977) have given an easier and quicker graphical method for estimating the fraction and temperature of hot water component. A line joining SiO_2 and temperature values of the cold water and the spring is extended upto the modified quartz solubility curve. The point of intersection represents the hot water component. In Figure 5.5 points A and B represent silica content and temperature values of cold water and warm spring water. Point C is the intersection point represents hot component. Fraction of hot component in spring water is equal to the length ratio: AB/AC.

This method was also tried for Bhimbandh (road side) spring (February 26, 1978) and results are given below:

Method	Hot component	
	Temperature	Fraction
Fournier and Truesdell (1974)	150°C	30.7%
Truesdell and Fournier (1977)	155°C	29.2%

Results obtained by both the methods are almost similar, hence the Truesdell and Fournier (1977) method was adopted for all the springs. The Bhimbandh tubewell water which has the lowest silica level was taken to represent the cold water component for the entire hot spring belt. The final results are summarised in Table 5.7.

Very recently, Fritz et al. (1980) have proposed a graphical method for estimating base temperature from molar mNa^+/mK^+ ratio in mixed waters. In the Plombieres region of France, Na/K ratio in low-temperature thermal waters do not show a decrease with increasing temperature, as demanded by alkali feldspar Na-K exchange. On the other hand, a hyperbolic trend line given by the equation $\frac{mNa^+}{mK^+} = (0.090884\ t - 2.717)/(0.001981\ t - 0.009)$ intersects the feldspar equilibrium curve of Ellis (1970) around 115°C (Figure 5.6) which could be a probable temperature of the hot component. The Rajgir-Monghyr waters do not show a clear trend but fall very close to the Fritz curve (Figure 5.6). It is interesting to note that the temperature of intersection is of the same order of magnitude as estimated by the Silica Method discussed above.

5.4. ISOTOPE DATA

It is clear from the preceding discussion that the source and circulation pattern of water in a geothermal area (including the Rajgir-Monghyr area) are critical

TABLE 5.7. ESTIMATION OF SUBSURFACE TEMPERATURE, FRACTION OF HOT WATER MIXED IN WARM SPRING AND SILICA CONTENT IN HOT FRACTION, BASED UPON SILICA CONTENT OF WATERS DISCHARGED FROM RAJGIR-MONGHYR THERMAL SPRINGS

Spring	Sitakund Hot	Rishikund South	Rishikund North
Date	25.2.78	24.10.77	24.10.77
SiO_2 (ppm)	49.0	35.0	37.0
Temperature, °C	45°	42°	45°
Silica Content in Hot Fraction, ppm	250	215	215
Temperature of Hot Fraction	200°C	188°C	188°C
Percentage of Hot Fraction	11.4%	9.3%	10.6%
Depth of Hot Zone Assuming 38°/km Thermal Gradient	4.08 km	3.84 km	3.76 km

Spring	Bhimbandh Road Side	Bhimbandh Pool	Chormara
Date	26.2.78	25.5.78	23.5.78
SiO_2 (ppm)	51.0	39.0	88.0
Temperature, °C	65°	60°	65°
Silica Content in Hot Fraction, ppm	135	80	425
Temperature of Hot Fraction	155°C	125°C	240°C
Percentage of Hot Fraction	29.2%	34.1%	17.6%
Depth of Hot Zone Assuming 38°/km Thermal Gradient	2.36 km	1.71 km	4.60 km

Contd...

TABLE 5.7 (Continued)

Spring	Rameshwarkund	Singhirishi	Agnikund
Date	25.10.77	28.10.77	30.10.77
SiO_2 (ppm)	41.5	20.5	41.5
Temperature, °C	45°	32°	49°
Silica Content in Hot Fraction, ppm	300	56	165
Temperature of Hot Fraction	215°C	105°C	160°C
Percentage of Hot Fraction	9.6%	6.2%	16.3%
Depth of Hot Zone Assuming 38°/km Thermal Gradient	4.47 km	1.92 km	2.92 km

Spring	Surajkund	Brahamkund	Makhdumkund
Date	31.10.78	29.5.78	31.10.77
SiO_2 (ppm)	27.0	25.0	28.0
Temperature, °C	41°	45°	35°
Silica Content in Hot Fraction, ppm	85	45	230
Temperature of Hot Fraction	125°C	95°C	192°C
Percentage of Hot Fraction	13.4%	25%	3.8%
Depth of Hot Zone Assuming 38°/km Thermal Gradient	2.21 km	1.31 km	4.13 km

Note: Cold water sample used as reference for the purpose of all the calculations is given below:

Bhimbandh Tube Well, Dated 25.5.78, SiO_2 = 18.00 ppm, Temperature = 27°C.

information in the context of interpretation of water quality. It has long been recognised that certain environmental isotopes present in the geothermal waters act as "identification tags" for this purpose (White, 1957). The most commonly used are the stable isotopes of oxygen and hydrogen i.e. O^{18} and H^2 or Deutrium (D).

The isotopic composition of waters is expressed by the delta convention represented by

$$\delta\ {}^{o}/_{oo}\ (\text{per mil}) = \left(\frac{R_{sample}}{R_{standard}} - 1\right) \times 1000$$

Where R = isotopic ratio e.g. O^{18}/O^{16}, D/H etc. The water standard most commonly used is standard mean ocean water (SMOW) in which $H_2^{16}O : H_2^{17}O : HDO = 10^6 : 2000 : 420 : 316$. A world-wide survey of isotopic composition of fresh water samples has shown that the δD and δO^{18} variations can be grouped along a statistical line given by the equation

$$\delta D = 8 \cdot \delta O^{18} + 10 \qquad (5.27)$$

This is known as the 'Meteoric Water Line' for oxygen and hydrogen isotopes. A comparison of the same isotopic composition of waters from major geothermal areas of the world (Craig, 1963) brought out the interesting pattern that the δD values are approximately equal to that of the local meteoric waters whereas the δO^{18} values show an enrichment in O^{18} content expressed as the "oxygen shift"

(Figure 5.7). The following explanation was offered for this distribution pattern.

Meteoric waters normally have negative δO^{18} and δD values i.e., they are depleted in O^{18} and D with respect to SMOW through evaporation process in the hydrologic cycle. On the other hand, rocks particularly silicates, have highly positive δO^{18} values. This results in pronounced O^{18}-exchange between rock and water during circulation of subsurface water enriching the water in O^{18}. The δD value remains unchanged, presumably because of the lower abundance of hydrogen in rocks. Some "hydrogen shift" is obviously possible where hydrated minerals like mica or chlorite are present. A large "oxygen shift", on the other hand, would indicate a relatively young hydrothermal system with abundant fresh rocks (Ellis and Mahon, 1977).

Craig (1963) also attempted to evaluate the δO^{18} and δD distribution in geothermal areas in terms of mixing with a deep magmatic or juvenile component. His argument was that juvenile water in equilibrium with silicates at high temperature will have largely positive δO^{18} values (Figure 5.7). Variable mixing with local meteoric water would produce thermal waters whose composition would fall on trend lines connecting the two points. In fact, isotope contours for various mixing ratios can also be drawn. Although no isotope analysis was carried out

during the course of the present investigation, the limited data available on the Rajgir-Monghyr area have been evaluated in the light of the above discussion. Sharma and Pillai (1970) reported that monsoon rain water at Patna in August-September, 1963 had δO^{18} values between $-9.4^{o}/_{oo}$ and $-10.2^{o}/_{oo}$. These can be projected upto the meteoric water line giving δD values around $-70^{o}/_{oo}$.

Sharma, Pillai and Pandey (1970 and personal communication) also carried out O^{18} analysis of the Rajgir-springs and reported δO^{18} values ranging from $-6.42^{o}/_{oo}$ to $-6.82^{o}/_{oo}$ with respect to SMOW. As seen in Figure 5.7, if we assume no change in δD from the meteoric water value, the above O^{18} concentration would imply mixing of 20 to 30 percent juvenile water in the hot springs. This is in excellent agreement with the mixing ratios estimated from silica content in section 5.3.

A discussion of isotopes in geothermal areas would not be complete without mentioning the use of radio isotopes for determination of age and residence time. The heavier isotope of hydrogen, H^3 or tritium (T) is the most commonly used tracer. Tritium has a half life of 12.5 years and its concentration in water is expressed in tritium units, 1 T.U. being equal to 1 atom of H^3 per 10^{18} H^1. It is generated in the atmosphere by nuclear reactions induced by cosmic ray bombardment. A comparison of tritium in thermal waters with the local mateoric water

value, therefore, allows an estimate of the time elapsed in the aquifer (Begemann and Libby, 1957).

Scattered information on the tritium content of Bhimbandh hot springs in the Rajgir-Monghyr belt is available from Gupta and Sukhija (1974). The Bhimbandh hot spring values range from 7 to 12 T.U. which are higher, for example, than the Puga springs in the Himalayas and is comparatively closer to the rain water values. This led the authorsto conclude that Bhimbandh waters, compared with Puga, show shallower circulation, smaller turnover time or predominant mixing with recently recharged water. These conclusions are quite tenable in the context of the mixing models established in the previous sections.

5.5. SUMMARY

Water chemistry in the Rajgir-Monghyr Belt has been utilised to estimate subsurface temperature and condition of mixing of a deep seated hot water component with cold meteoric water descending from the surface. Considerable variation in spring temperature and in the concentration of a non-reactive constituent like chloride are indicators of a Mixed Water in this hot spring belt (Table 5.4). Moreover, subsurface temperatures estimated from standard geochemical indicators differ from the spring temperatures by much more than 25°C. This also indicates non-equilibrium i.e. mixing of hot and cold waters (Fournier and Truesdell, 1974).

It is, therefore, not surprising that a direct application of the SiO_2, Na-K and Na-K-Ca geothermometers without considering dilution by mixing gives variable estimates of the Base Temperature (Table 5.8). A more realistic estimate of the temperature at depth comes from the temperature of the hot component in the mixed water (Table 5.8). From these temperatures and an average geothermal gradient of 38°C/km reported for this area (NCST, 1975), the depth to the hot zone is estimated in Table 5.7. It is interesting to note that the hot zone is deeper around Bhimbandh and Monghyr compared to Rajgir.

An indirect support to the mixing model has also come from isotope data. The δD and δO^{18} values of Rajgir meteoric water and hot spring water are such that mixing of around 20% of a 'juvenile' component will be reasonable. This is close to the estimate of 25% hot component in the Brahmakund, Rajgir water.

With this background model of mixing of hot and cold water, it is also easy to explain the variation of chloride in the spring water. Assuming dilution of cold meteoric water of known chloride content by the estimated fraction of chloride-free hot water, the chloride in spring water can be predicted. This is remarkably close to the actual chloride analysis in the springs (Table 5.9) and explains the apparent paradox of lower chloride content in hot spring water compared to cold meteoric water.

TABLE 5.8. COMPARISON OF SUBSURFACE TEMPERATURES AS ESTIMATED ACCORDING TO DIFFERENT GEOCHEMICAL THERMOMETERS ON THE BASIS OF MODELS INVOLVING (a) NO MIXING AND (b) MIXING.

Spging	Date	Estimated Temperature Assuming No Mixing, °C			Estimated Temperature Considering Mixing Model, °C	
		T_{SiO_2}	T_{Na-K}	$T_{Na-K-Ca}$	Percentage of Hot Component from Silica Method	Maximum Subsurface Temperature
Sitakund Hot	25.2.78	102.90°	242.43°	78.13°	11.4%	200°
Rishikund South	24.10.77	89.90°	373.95°	76.76°	9.3%	188°
Rishikund North	24.10.77	91.90°	381.34°	76.74°	10.6%	188°
Bhimbandh (Road Side)	26.2.78	104.50°	368.02°	93.21°	29.2%	155°
Bhimbandh (Pool)	24.5.78	93.90°	413.37°	102.50°	34.1%	125°
Chormara	23.5.78	127.90°	186.23°	50.04°	17.6%	240°
Rameshwar-kund	25.10.77	96.40°	192.83°	35.30°	9.6%	215°
Singhi-rishi	28.10.77	70.97°	187.24°	53.83°	6.3%	105°
Agnikund	30.10.77	96.37°	208.03°	59.23°	16.3%	160°
Surajkund	31.10.77	80.47°	425.14°	71.90°	13.4%	125°
Brahamkund	29.5.78	77.70°	418.23°	74.07°	25.0%	95°
Makhdum-kund	31.10.77	81.75°	396.17°	70.02°	3.8%	192°

TABLE 5.9. CALCULATED CHLORIDE CONCENTRATION FROM MIXING OF NON-THERMAL WATER WITH CHLORIDE-FREE HOT WATER COMPONENT.

Spring	Date	Cl (ppm)	Hot Water % by Silica Method	Calculated Cl (ppm)
Rishikund South	24.10.77	4.97	9.3%	5.65
	26.2.78	5.00	6.7%	5.82
	22.5.78	5.49	7.3%	5.78
Rishikund North	24.10.77	5.68	10.6%	5.57
	26.2.78	5.50	7.3%	5.78
	22.5.78	5.49	9.9%	5.62
Bhimbandh Road Side	24.10.77	4.02	21.2%	4.92
Chormara	23.5.78	4.99	17.6%	5.14
Rameshwarkund	25.10.77	3.35	9.6%	5.64
Singhirishi	28.10.77	3.79	6.3%	5.85
Agnikund	30.10.77	3.57	16.3%	5.22
	30.5.78	4.49	19.3%	5.03
Surajkund	31.10.77	5.96	13.4%	5.40
	29.5.78	5.68	13.4%	5.40
Brahamkund	31.10.77	5.96	12.0%	5.49
	29.5.78	5.82	25.4%	4.65
Makhdumkund	31.10.77	5.68	3.8%	6.00
	29.5.78	5.68	2.0%	6.11

DESCRIPTION OF FIGURES

Figure 5.1. Silica Solubility Versus Temperature Plot.

Figure 5.2. Standard Curves for Silica Geothermometer. From Fournier (1973)

Figure 5.3. Circulation Model for Mixed Water Hot Spring. After Fournier and Truesdell (1974)

Figure 5.4. Estimation of Fraction of Hot Water in Mixed Water Hot Spring. From Fournier and Truesdell (1974)

Figure 5.5. Estimation of Hot Water Fraction in Mixed Water Hot Spring. From Fournier (1977)

Figure 5.6. Estimation of Base Temperature from Na/K Molar Ratio. From Fritz et.al. (1980)

Figure 5.7. Oxygen^{18} and Deuterium Isotope Variation in Thermal Waters. From Craig (1963)

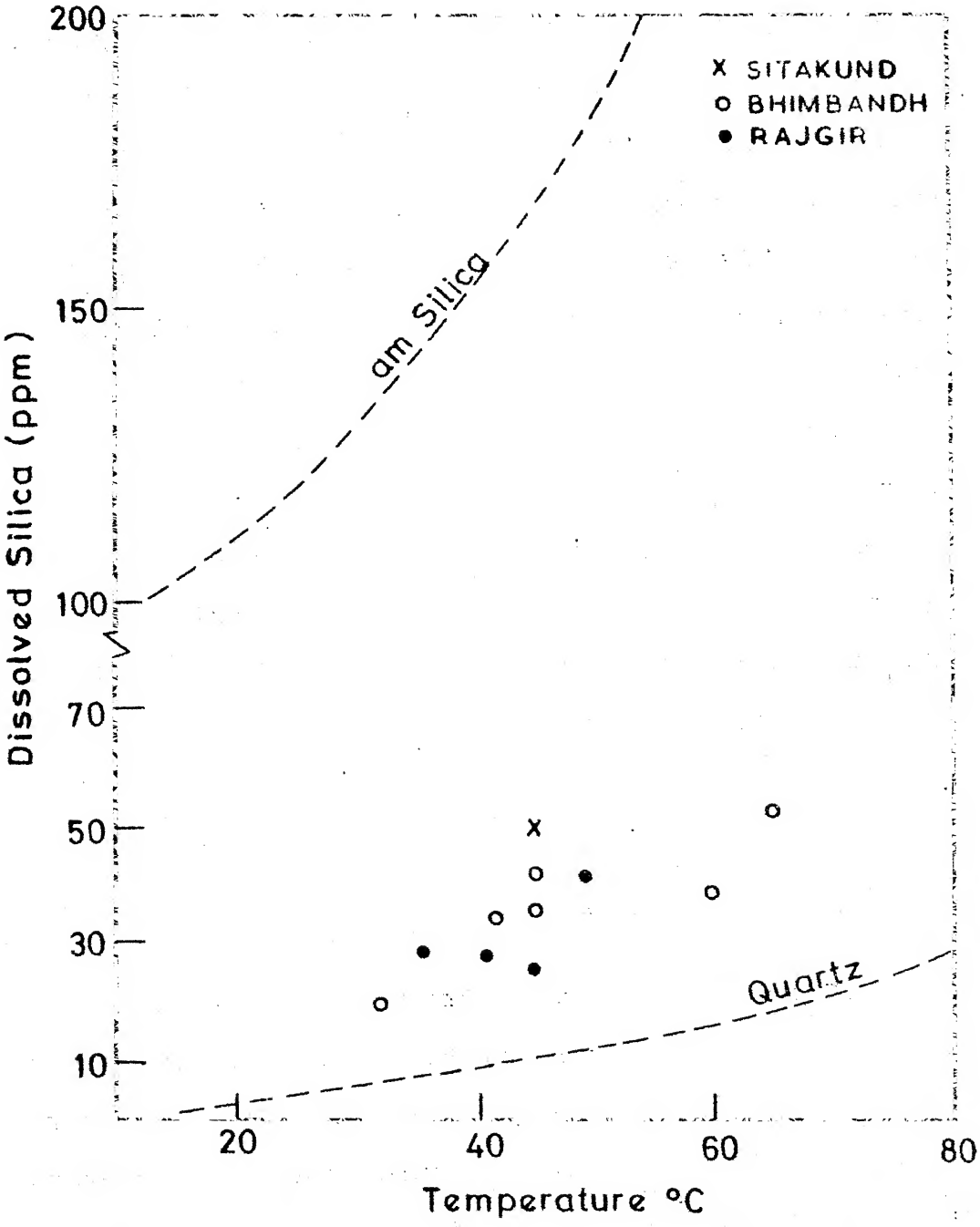
200
150
100
70
50
30
10
Dissolved Silica (ppm)
X SITAKUND
O BHIMBANDH
● RAJGIR
am Silica
Quartz
20
40
60
80
Temperature °C

Fig. 5.1

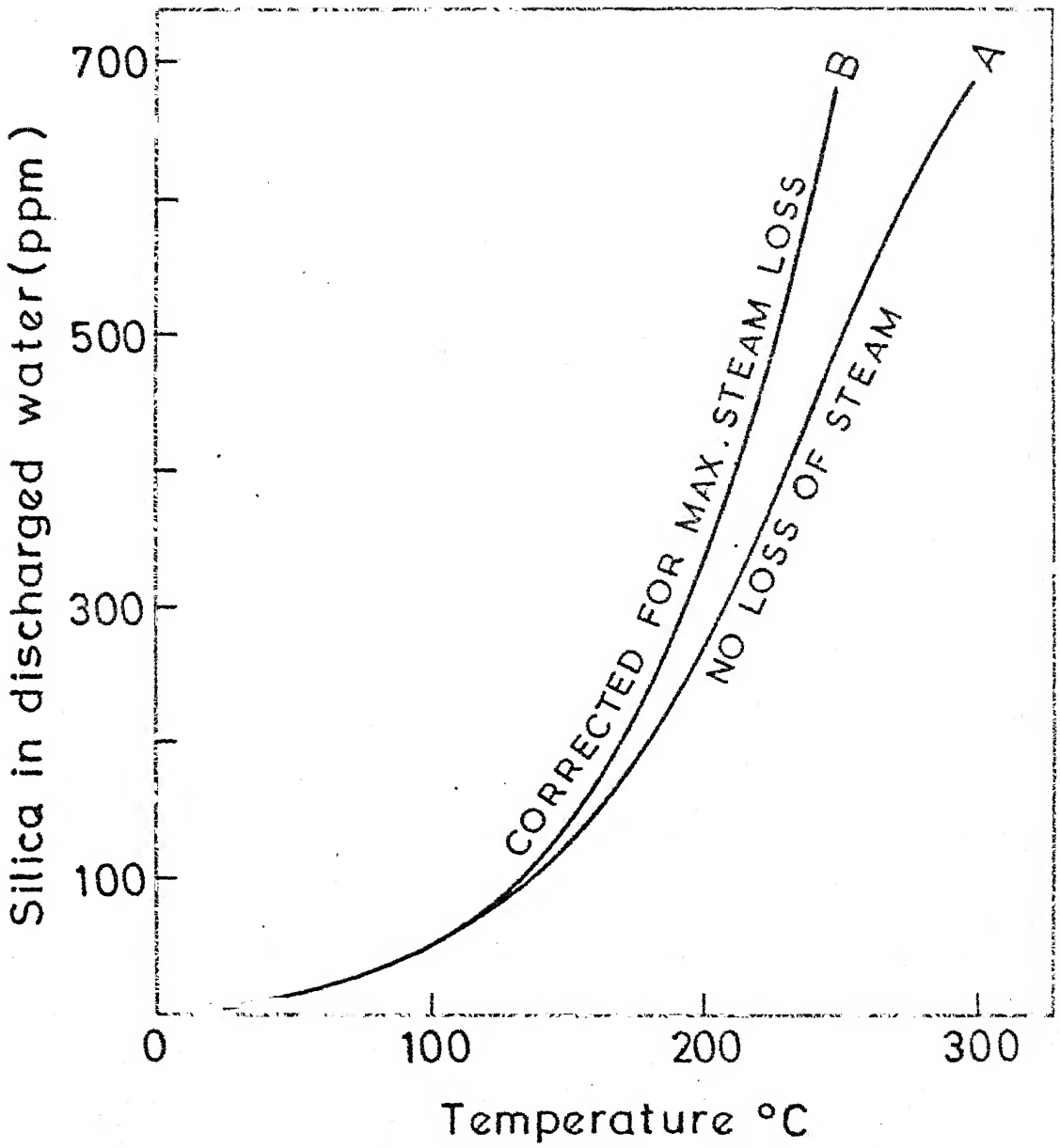
Silica in discharged water (ppm)
700
500
300
100
0
100
200
300
Temperature °C
B
A
CORRECTED FOR MAX. STEAM LOSS
NO LOSS OF STEAM

F.g. 5.2

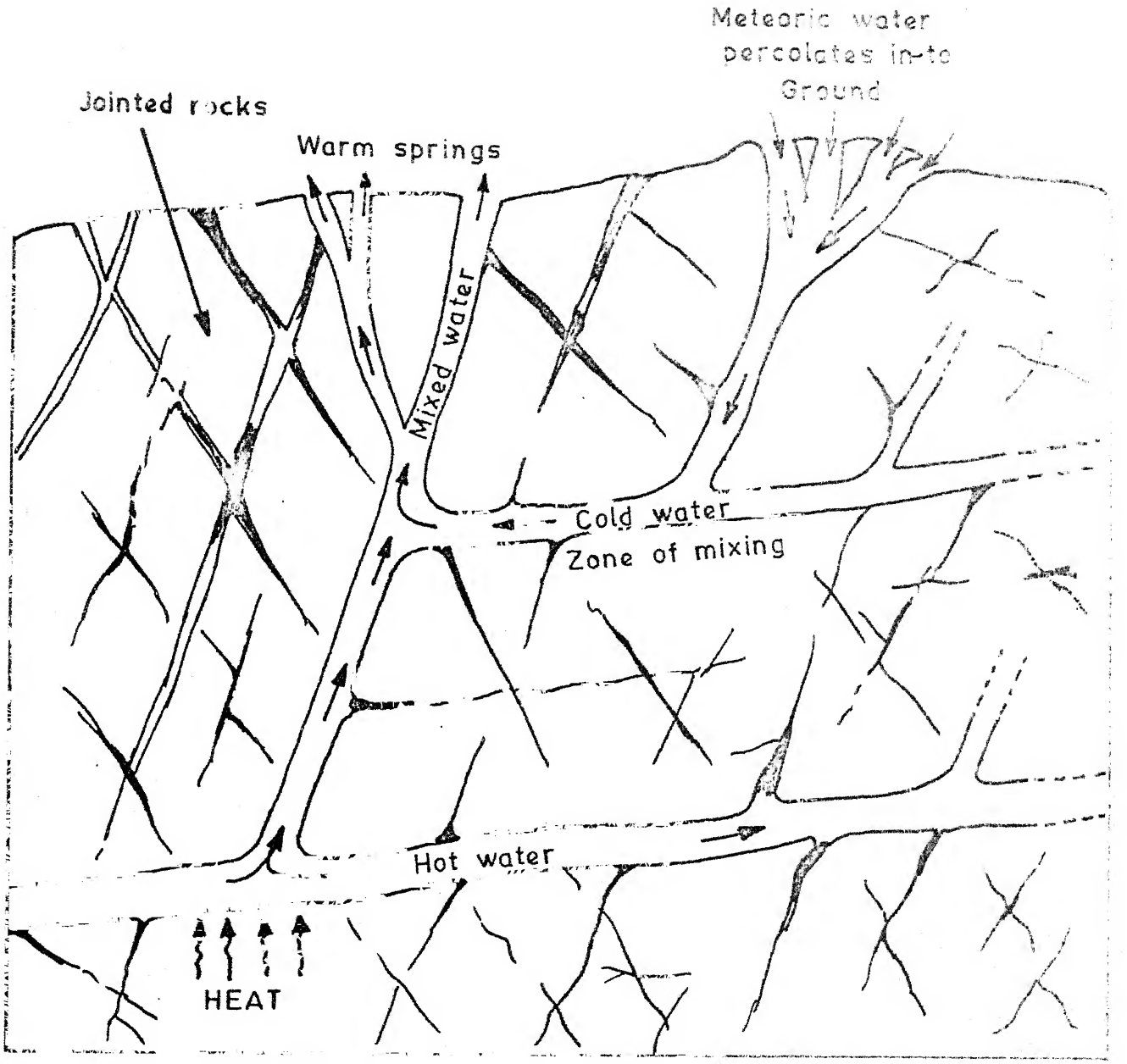
Meteoric water
percolates in-to
Ground
Jointed rocks
Warm springs
Mixed water
Cold water
Zone of mixing
Hot water
HEAT

Fig. 5.3

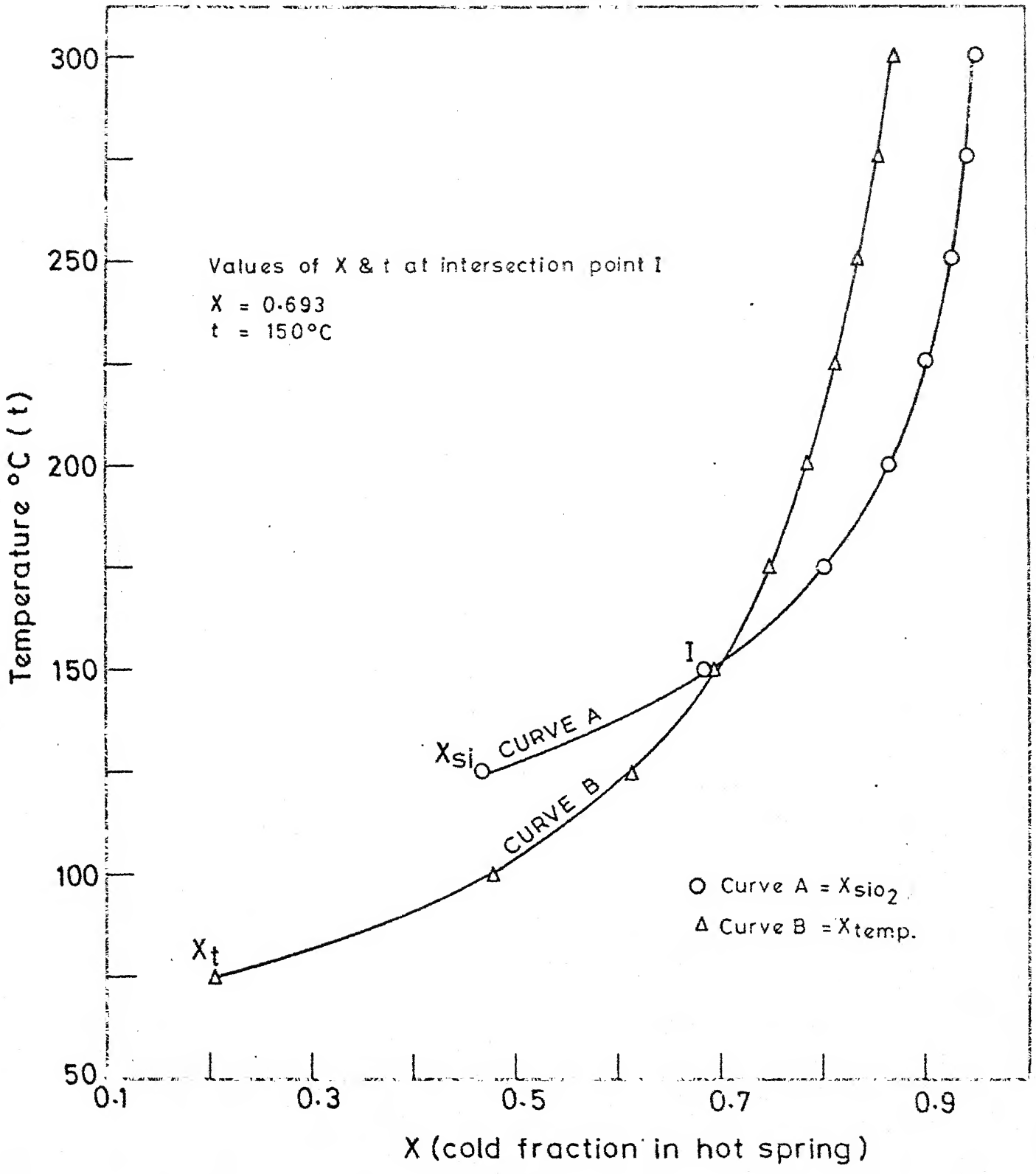
Values of X & t at intersection point I
X = 0·693
t = 150°C
Temperature °C (t)
300
250
200
150
100
50
0·1
0·3
0·5
0·7
0·9
X (cold fraction in hot spring)
I
X_{si_O} CURVE A
CURVE B
X_t
O Curve A = X_{sio_2}
Δ Curve B = $X_{temp.}$

Fig. 5.4

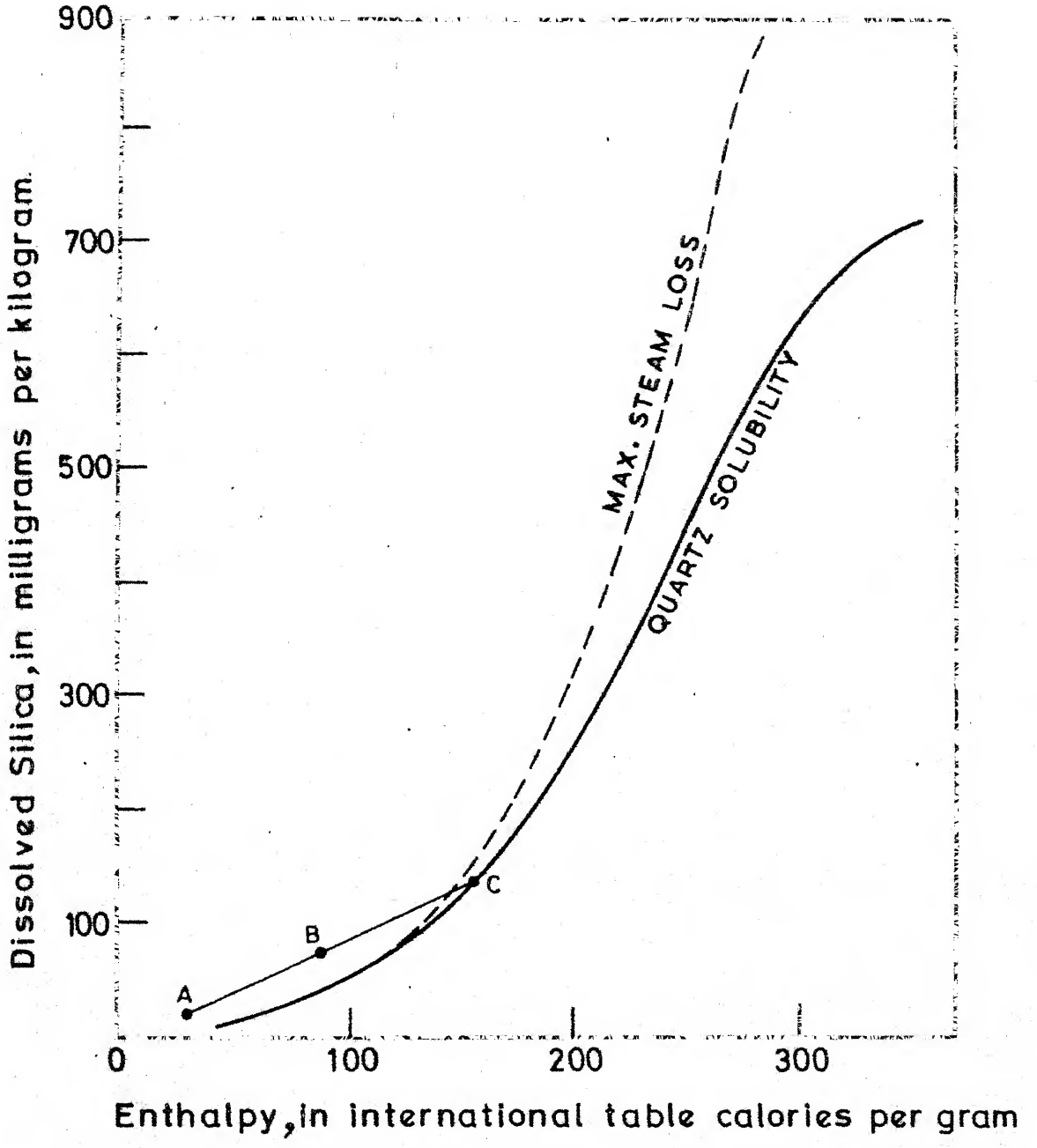
900
700
500
300
100
0
100
200
300
Dissolved Silica, in milligrams per kilogram
Enthalpy, in international table calories per gram
MAX. STEAM LOSS
QUARTZ SOLUBILITY
A
B
C

Fig. 5.5

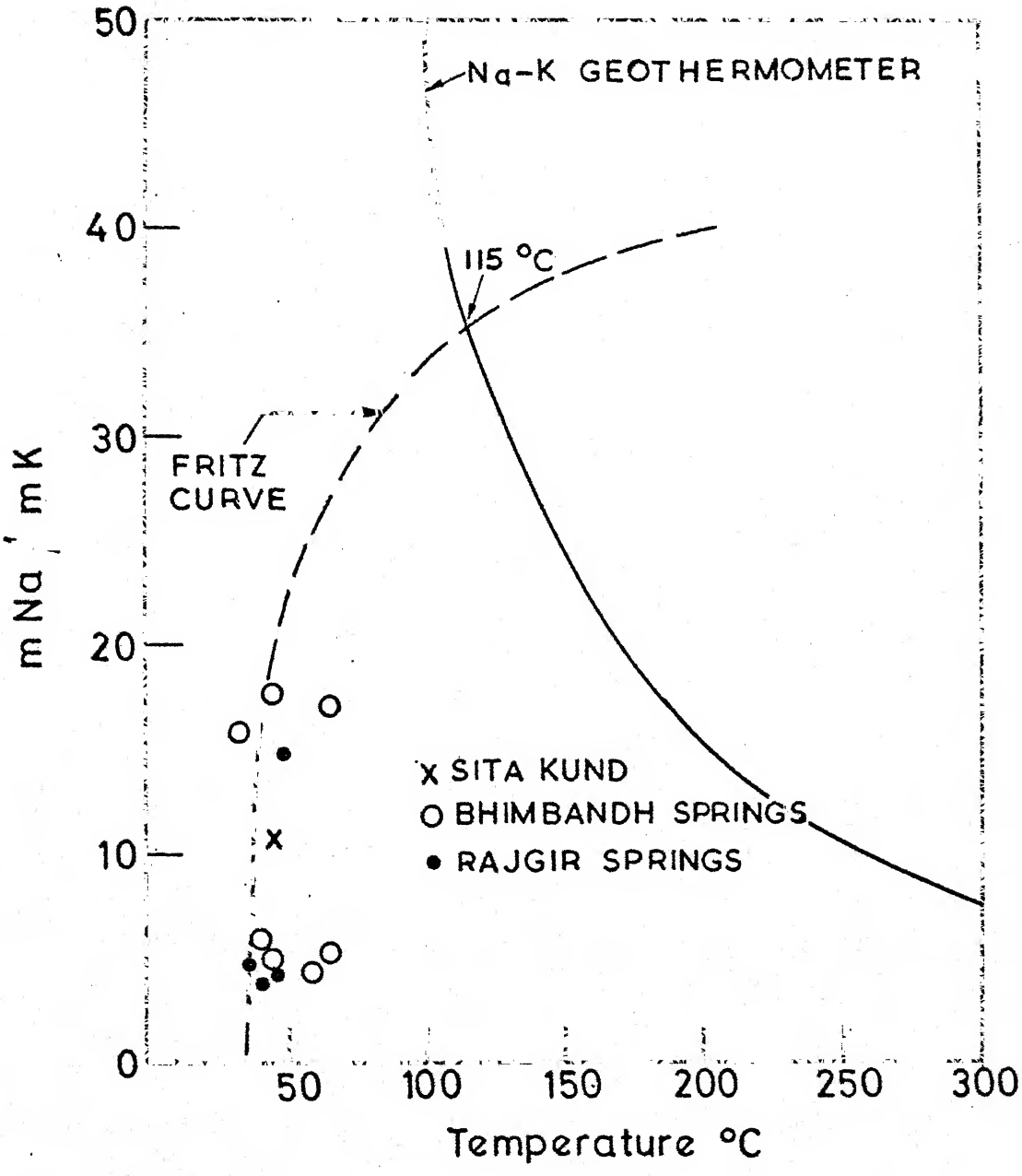
Na-K GEOTHERMOMETER
115 °C
FRITZ CURVE
X SITA KUND
O BHIMBANDH SPRINGS
• RAJGIR SPRINGS
mNa ' mK
Temperature °C
0
10
20
30
40
50
50
100
150
200
250
300

Fig. 5.6

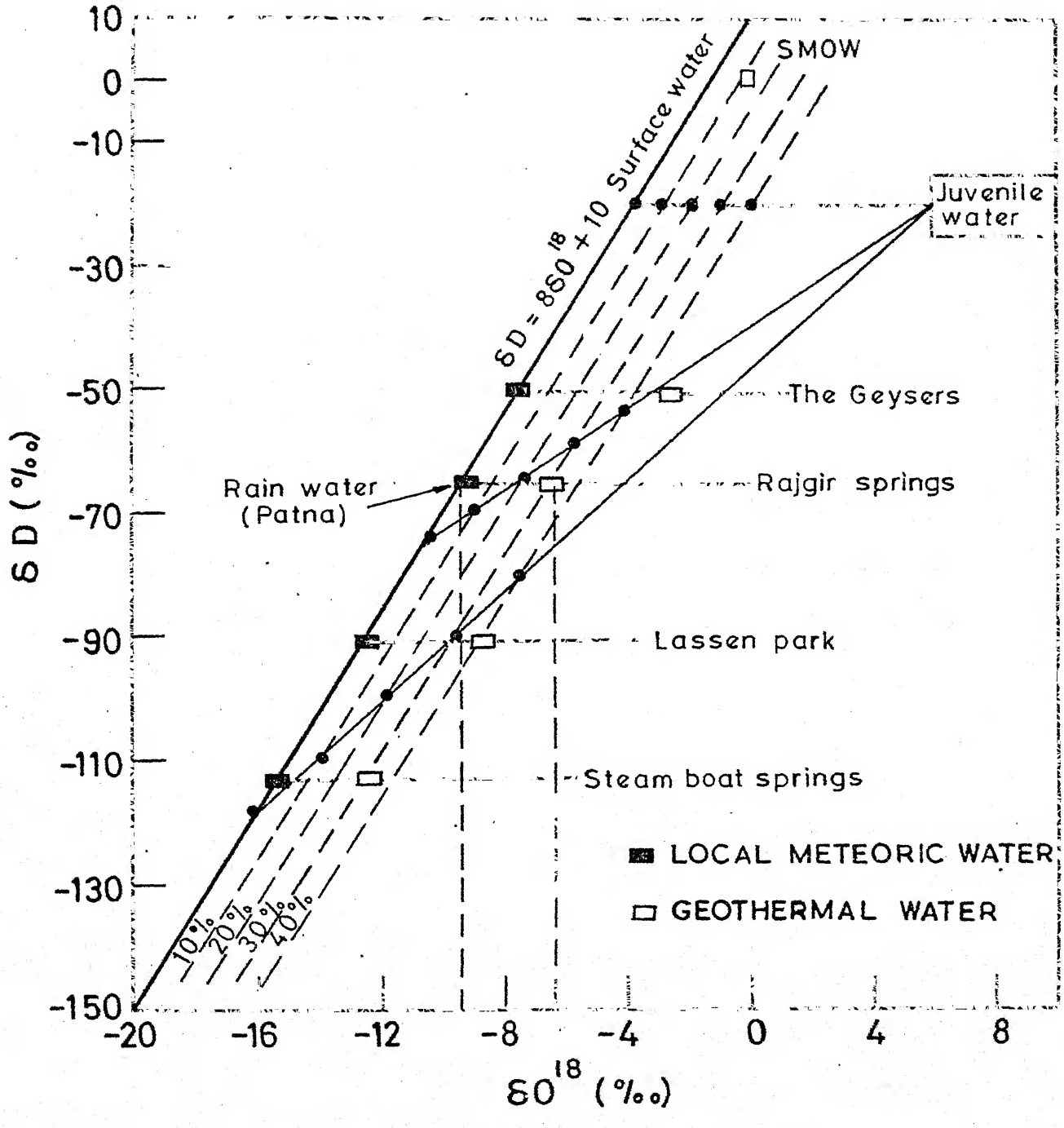
10
0
-10
-30
-50
-70
-90
-110
-130
-150
δ D (‰)
-20
-16
-12
-8
-4
0
4
8
δO18 (‰)
δD = 8δO18 + 10 Surface water
SMOW
Juvenile water
The Geysers
Rajgir springs
Lassen park
Steam boat springs
Rain water (Patna)
10%
20%
30%
40%
LOCAL METEORIC WATER
GEOTHERMAL WATER

Fig. 5.7

Chapter 6

ROCK-WATER INTERACTION

6.1. INTRODUCTION

Investigations in major hot spring areas throughout the world have established that rock-water interaction is important in two different contexts. One of the most controversial topics of long standing is the origin of chemicals in natural hot waters. The common rock forming constituents such as SiO_2, Al^{+3}, Na^+, K^+, Ca^{++}, Mg^{++} are available in abundance in country rocks for release into the hot waters under appropriate conditions of mineral-water equilibrium. The major control in this case is obviously the composition of the rocks, permeability of the geothermal reservoir, depth of circulation, rock to water ratio etc. The concentration of these chemicals is determined by temperature dependent mineral-water equilibria. On the other hand, there is a group of constituents like chloride, bromide, boric acid, arsenic and cesium which do not participate in silicate-water equilibria and are commonly believed to be indicators of a magmatic source. However, most of the explored geothermal systems have a limited magmatic component, if any. This is based on two important observations in recent times (i) the experiments of Ellis and Mahon

(1964, 1967) showed that rocks typical of thermal areas can liberate large quantities of so-called magmatic constituents at high temperatures and large water to rock ratio, (ii) the stable isotope analysis of thermal waters shows that the δD and δO^{18} values are practically same as those of the local meteroic waters (Craig, 1963). It thus turns out that rock-water interactions within a geothermal field at relatively shallow depths can greatly influence the composition of water flowing out from hot springs.

The second major application of rock-water interaction has been the utilisation of the temperature dependence of the equilibrium constants of silicate-water reactions in estimating underground temperatures. This is the basis of several useful geothermometers like the silica, Na-K, Na-K-Ca methods discussed in detail in Chapter 5.

A major product of rock-water interaction in geothermal areas is the well known hydrothermal rock alteration which is represented by a complex series of hydrolysis, devitrification, recrystallisation, solution and deposition reactions. The major factors are once again temperature and pressure of reaction, water composition, original rock composition, porosity, permeability, and residence time. It is, therefore, natural that significant rock alteration features have been observed

in geothermal fields located in volcanic rocks containing high-temperature geothermal waters or steam fields (Ellis and Mahon, 1977; Raymahashay, 1968). The common products of alteration by acidic hot waters are kaolinite, alunite, sulphur and gypsum. Alkaline geothermal waters, on the other hand, convert the country rocks to zeolites and montmorillonite type clays.

The Rajgir-Monghyr hot spring belt is rather peculiar in the sense that the country rocks are Precambrian quartzites containing very little reactive minerals. At the same time, the spring waters are extremely low in T.D.S. (less than 40 mg/l) and have relatively low temperatures at the point of emergence. These features tend to suggest that rock-water interaction in this field is minimal and is consistent with a geohydrological model in which ground water descends to a shallow hot-zone and is flushed out after a relatively short residence time as discussed in Chapter 5.

6.2. WEATHERING AND ROCK ALTERATION IN RAJGIR-MONGHYR AREA

Representative samples of fresh rock, rock in contact with hot spring water as well as soil and sediment samples in thermal areas were studied in detail. Summary of observations is given in Table 6.1. Further details are supplied below.

TABLE 6.1. SUMMARY OF PETROGRAPHIC EXAMINATION OF SAMPLES FROM RAJGIR-MONGHYR HOT SPRING BELT.

XRD = X-ray Diffraction
DTA = Differential Thermal Analysis
EM = Electron Microscopy

Sample No.	Ag-1	Ag-2	Ag-3
Location	Exposure near Agnikund, Rajgir	Lateritic soil from quarry, 2 km west of Agnikund, Rajgir	Near Agnikund, Rajgir
Description of sample	Banded ferruginous quartzite (fresh rock)	Typical red-coloured iron-rich soil	Fresh rock sample of orthoquartzite
Minerals	Quartz, microcline, magnetite, muscovite	Quartz, kaolinite, illite, goethite	Quartz, opaque iron-oxide
Identification methods	Thin section study under petrological microscope	XRD, DTA, EM	Thin section study

Sample No.	Ag-4	Ag-5	RM-1
Location	Agnikund, Rajgir	Near Agnikund, Rajgir	Rishikund pond, Munghyr
Description of sample	Kund mud, brown to black in colour	Quartzite coated with iron-oxide	Fine grained, Quick-sand
Minerals	Quartz, kaolinite, illite, feldspar, halloysite, goethite	Quartz, kaolinite, illite, magnetite, goethite	White coloured quartz grains well rounded, spheroidal in shape
Identification methods	XRD, DTA, EM	XRD clay fraction and bulk	Under binocular microscope, XRD bulk

Contd...

TABLE 6.1 (continued)

Sample No.	RM-2	RM-3	RM-4
Location	Rishikund, Monghyr	Rishikund, Monghyr	Rishikund, Monghyr
Description of sample	Black-brown mud from pond	Quartzite, white to grey, in contact with thermal water	Quartzite in contact of hot water
Minerals	Quartz, kaolinite, illite	Quartz, kaolinite, illite, halloysite	Quartz, kaolinite, illite, chlorite, calcite
Identification methods	XRD of clay fraction and bulk	XRD of slide and bulk	Thin section, XRD clay fraction and bulk

Sample No.	RM-5	RM-6	RM-7
Location	Rishikund, Monghyr	Rishikund, Monghyr	Rishikund, Monghyr
Description of sample	Quartzite from hot water pool	Quartzite coated with iron-oxide	Bed-load material
Minerals	Quartz, kaolinite, illite	Quartz, kaolinite, illite	Quartz, kaolinite, illite
Identification methods	XRD of clay fraction	XRD of clay fraction and bulk	XRD of bulk

Contd...

TABLE 6.1 (continued)

Sample No.	RM-8	RM-9	RM-11
Location	Bhimbandh (pool)	Bhimbandh Road Side	Rameshwarkund, Monghyr
Description of sample	Scrapped thin white coating	Weathered portion of quartzite in contact with hot water	Bottom sand from pond
Minerals	Amorphous silicate of Mg and Ca	Quartz, kaolinite, illite, halloysite	Quartz, illite
Identification methods	XRD, spectroscopic examination	XRD of clay fraction	XRD of bulk

Sample No.	RM-12	RM-15	RR-16
Location	Near bridge over Man river, Bhimbandh	Singhirishi, Monghyr	Agnikund, Rajgir
Description of sample	Weathered phyllite	Weathered quartzite in contact with hot water	Leached ferruginous material
Minerals	Quartz, kaolinite, illite, chlorite	Quartz, kaolinite, illite, halloysite, chloride	Quartz, kaolinite, illite, goethite, hematite, muscovite
Identification methods	XRD, EM	XRD, DTA, EM	XRD, megascopic study

Contd...

TABLE 6.1 (continued)

Sample No.	RR-17	RR-18	RR-19
Location	Agnikund, Rajgir	Near Roapway, Rajgir	Agnikund, Rajgir
Description of sample	Quick-sand, white in colour	Shale, pink in colour (weathered rock)	Weathered phyllite
Minerals	Quartz, illite	Quartz, halloysite, kaolinite, illite	Quartz, kaolinite, illite, halloysite
Identification methods	XRD of bulk	XRD of clay fraction	XRD of bulk and clay fraction, EM

6.2.1. FRESH ROCKS

6.2.1.1. White and Grey Quartzites

These quartzites are, in general, medium to fine grained, hard, compact, massive in nature and light grey, dull white to pure white in colour. The rocks are highly jointed and fractured. Some details about orientation of joint planes are given later. At places excellent cross-bedding (Photo 6.1), parallel bedding and ripple marks (Photo 6.2) are also noticed which indicate their derivation by metamorphism of original siliceous sediments.

Thin section studies reveal that these quartzites are composed of fine grains of quartz as major constituent. The quartz grains are not equidimensional but are elongated with longer axes roughly parallel to each other (Figure 6.1). These grains are subrounded to angular in shape, having sutured boundaries. Quartz grains show undulose extinction indicating their deformed nature. The preferred orientation of quartz grains shows the effect of directional stress during metamorphism. Potash feldspar (microcline) is also present in trace quantities. Other accessory constituent minerals are sphene and magnetite. Small flakes of mica, colourless to pale yellow in colour, are also present on the bedding planes.

6.2.1.2. Joints in Quartzite

The Monghyr springs follow the strike of the quartzite ridge of Kharagpur hills trending from NNE-SSW to NE-SW. Similarly the ENE-WSW trend of the Rajgir springs is parallel to the strike of the quartzite ridge. These quartzites are highly fractured and jointed (Photo 6.3). It has been observed in the field that the water is emerging from almost vertical joints trending N 50° E at Rishikund, from NE-SW joints at Bhimbandh, and from joints trending N-S at Singhirishi. The most prominent joints from which water comes out in Rajgir area have strike N-S and NE-SW. The rose-diagram plotted in Figure 6.2 also indicates the most prominent joints have N-S, E-W and NE-SW strike directions parallel to bedding. Most of these joints have steep dip angle (70°-87°) or are vertical. It can be concluded, therefore, that hot water from depth is channelised by the set of bedding joints.

6.2.1.3. Ferruginous Quartzite

These quartzites are very similar to the grey and white quartzites but have alternate bands of red and brown jasper. The colour banding is due to the presence of ferruginous cementing material. The major constituent is quartz with sphene and iron-oxide as accessories.

6.2.1.4. Phyllites

These are foliated rocks composed of fine grained minerals with slaty cleavage. These rocks show cross-folding and colour banding or alternate laminations of iron-rich material. The X-ray diffraction studies reveal that these phyllites are composed of quartz, kaolinite and mica. Kaolinite is possibly secondary in origin.

6.2.2. WEATHERED ROCKS

6.2.2.1. Weathered Quartzite

These quartzites are brown, red, grey to greenish white in colour. This colour variation is due to presence of ferruginous, micaceous, and chloritic material. Thin-section examination reveals that the material pale green to yellowish green in colour, found along the cracks and fissures, is chlorite (Figure 6.3). Irregular patches of opaque iron-oxide are also noticed. The minerals detected by X-ray diffraction studies are quartz, kaolinite, illite and possibly halloysite (Figure 6.4). In a few samples chlorite, goethite and magnetite are also present (Figure 6.5). Electron micrographs of selected samples show the presence of kaolinite and halloysite, which confirms the X-ray diffraction data (Figure 6.6).

6.2.2.2. Weathered Phyllite

These phyllites are brown to red in colour. X-ray diffraction studies show the presence of quartz, kaolinite, illite, chlorite and possibly halloysite (Figures 6.7 and 6.8). Halloysite is confirmed in the Electron micrograph (Figures 6.9 and 6.10).

6.2.2.3. Leached Ferruginous Material

The joint surface is frequently highly weathered and coated with leached iron and micaceous materials. Megascopic study of this material under binocular microscope confirms the presence of iron-coated quartz grains, flakes of muscovite mica, limonitic material and perfect crystals of hematite. The minerals detected by X-ray diffraction are quartz, kaolinite, muscovite, illite, hematite and goethite.

6.2.2.4. Quick-Sand

From the bottom of the Rishikund pool white coloured quick-sand is flowing out (Photo 6.4). These quartz grains are well rounded, spheroidal in shape and have average diameter 0.5 mm. This roundness is due to continuous attrition among sand grains themselves while circulating with ascending water.

with thermal water. This thin coating, scratched from the rocks, was found amorphous in X-ray diffraction examination. Proton Induced X-ray Emission and spectroscopic analysis reveal the presence of Mg, Ca as major constituents and Fe, Zn, Ti, Cu, As, Sr, Zr in traces. Silica is estimated to be 66 percent by weight according to chemical analysis. Therefore, this substance could be an amorphous silicate of magnesium and calcium.

6.3. THERMODYNAMICS OF SILICATE-WATER EQUILIBRIA

The equilibrium based concepts of rock-water reactions as discussed above (Section 6.1) leads to the logical conclusion that there will be semi-quantitative correlation between the chemistry of hot waters and the occurrence of particular mineral assemblages in the country rocks and their weathered equivalents. An important test of the approach to equilibrium in proposed mineral-water reactions would be to confirm whether the hot-water environment is suitable for thermodynamic stability of the minerals present. For this purpose, the technique of construction of mineral stability diagrams was introduced by Garrels and Christ (1965) and extended by several workers. Sufficient thermodynamic data are now available for dissolved ions and mineral phases for the three systems K_2O-Al_2O_3-SiO_2-H_2O, Na_2O-Al_2O_3-SiO_2-H_2O and CaO-Al_2O_3-SiO_2-H_2O. As illustrated below, the

equilibrium constants of relevant reactions are simple functions of cation to H^+ ion activity ratio like aK^+/aH^+, aNa^+/aH^+, $aCa^{++}/(aH^+)^2$ and dissolved silica (H_4SiO_4) concentration. Table 6.2 summarises the thermodynamic data utilized to compute the equilibrium constants of the following reactions:

K-SYSTEM

Gibbsite (gibb) $Al_2(OH)_6$

Kaolinite (kaol) $Al_2Si_2O_5(OH)_4$

Muscovite (musco) $KAl_3Si_3O_{10}(OH)_2$

K-Feldspar (K-feld) $KAlSi_3O_8$

Halloysite (halloy) $Al_2Si_2O_5(OH)_4$

(1) $\quad kaol + 5H_2O = gibb + 2H_4SiO_4\ aq$

$\quad\quad \log a_{H_4SiO_4} = -4.62$

(2) $\quad 2\ musco + 2H^+_{aq} + 3H_2O = 3kaol + 2K^+_{aq}$

$\quad\quad \log(aK^+/aH^+) = 5.98$

It is to be noted that this equilibrium constant is particularly sensitive to small variations in the thermodynamic data. For example, Tardy (1971) gives a value of $\log aK^+/aH^+ = 4.52$ for the muscovite-kaolinite equilibrium which corresponds to an energy of reaction only $\sim$4 kcal more than that calculated from the data in Table 6.2. Similarly, Garrels and Christ (1965) list $\log aK^+/aH^+ = 6.5$ for this boundary based on an older set of thermodynamic data (Refer insert in Figure 6.14).

TABLE 6.2. STANDARD-STATE THERMODYNAMIC DATA FOR MINERALS AND RELATED SUBSTANCES AT 25°C.

Composition	ΔG_f^o (kcal/mole)	S^o (cal/deg-mole)	Reference
H_2O	-56.70	16.70	1
H_4SiO_4 aq	-312.80	43.40	1
H^+_{aq}	00.00	00.00	1
K^+_{aq}	-67.70	24.50	1
Na^+_{aq}	-62.60	14.10	1
Ca^{++}_{aq}	-132.35	-13.20	2
$Al_2(OH)_6$ Gibbsite	-548.30	33.50	1
$Al_2Si_2O_5(OH)_4$ Kaolinite	-903.00	48.50	1
$KAl_3Si_3O_{10}(OH)_2$ Muscovite	-1329.00	69.00	1
$KALSi_3O_8$ K-feldspar	-891.00	52.50	1
$Na_{0.33}Al_{2.33}Si_{3.67}O_{10}(OH)_2$ Na-montmorillonite	-1277.40	63.70	1
$Ca_{0.17}Al_{2.34}Si_{3.66}O_{10}(OH)_2$ Ca-montmorillonite	-1278.84	59.60	4
$CaAl_2Si_2O_8$ Anorthite	-955.625	48.45	3
$Al_2Si_2O_5(OH)_4$ Halloysite	-898.40	48.60	3

ΔG_f^o and S^o represent standard-state Gibbs free energy of formation and entropy respectively.

Reference: 1. Raymahashay (1968); 2. Berner (1971); 3. Robie and Waldbaum (1968); 4. Calculated from $\log K = -15.7$ for kaolinite-montmorillonite equilibrium, Tardy (1971).

aq. refers to substances in solution.

(3) $2\ musco + 2H^+_{aq} + 18H_2O = 3gibb + 2K^+_{aq} + 6H_4SiO_4\ aq$

Slope of the boundary = - 3:1

(4) $3K\text{-felds} + 2H^+_{aq} + 12H_2O = musco + 6H_4SiO_4\ aq + 2K^+_{aq}$

$3 \log aH_4SiO_4 + \log (aK^+/aH^+) = - 4.5$

(5) $2K\text{-felds} + 2H^+_{aq} + 9H_2O = kaol + 2K^+_{aq} + 4H_4SiO_4\ aq$

$\log(aK^+/aH^+) + 2\log aH_4SiO_4 = - 0.99$

Slope of the boundary = - 2:1

(6) $halloy + 5H_2O = gibb + 2H_4SiO_4\ aq$

$\log aH_4SiO_4 = - 2.97$

(7) $2K\text{-felds} + 2H^+_{aq} + 9H_2O = halloy + 4H_4SiO_4\ aq + 2K^+_{aq}$

$\log(aK^+/aH^+) + 2\log H_4SiO_4 = - 2.676$

(8) $2musco + 3H_2O + 2H^+_{aq} = 3halloy + 2K^+_{aq}$

$\log(aK^+/aH^+) = 0.915$

(9) Solubility of quartz (6 ppm SiO_2)

$\log a\ H_4SiO_4 = - 4$

(10) Solubility of amorphous silica (120 ppm SiO_2)

$\log a\ H_4SiO_4 = - 2.7$

Na-SYSTEM

Gibbsite

Kaolinite

Na-montmorillonite (Na-mont) $Na_{0.33}Al_{2.33}Si_{3.67}O_{10}(OH)_2$

(1) $6\text{Na-mont} + 2H^+_{aq} + 23H_2O = 7\text{kaol} + 8H_4SiO_{4\ aq} + 2Na^+_{aq}$

$\log(aNa^+/aH^+) + 4\log aH_4SiO_4 = -7.3$

(2) $6\text{Na-mont} + 2H^+_{aq} + 58H_2O = 7\text{gibb} + 22H_4SiO_{4\ aq}$

Slope of the boundary = - 11:1

Ca-SYSTEM

Gibbsite

Kaolinite

Ca-montmorillonite (Ca-mont) $Ca_{0.17}Al_{2.34}Si_{3.66}O_{10}(OH)_2$

Anorthite (anor) $CaAl_2Si_2O_8$

(1) $\text{anor} + 2H^+_{aq} + H_2O = \text{kaol} + Ca^{++}_{aq}$

$\log(aCa^{++}/ aH^{+\ 2}) = 16.88$

(2) $\text{anor} + 2H^+_{aq} + 6H_2O = \text{gibb} + 2H_4SiO_{4\ aq} + Ca^{++}_{aq}$

Slope of the boundary = - 2:1

(3) $6\text{Ca-mont} + 2H^+_{aq} + 23H_2O = 7\text{kaol} + 8H_4SiO_{4\ aq} + Ca^{++}_{aq}$

$\log(aCa^{++}/ aH^{+\ 2}) + 8\log H_4SiO_4 = -15.7$

(4) $7\text{anor} + 12H^+_{aq} + 8H_4SiO_4 = 6\text{Ca-mont} + 16H_2O + 6Ca^{++}$

Slope of the boundary = + 4:3

As indicated in Table 6.2 the thermodynamic data for Ca-montmorillonite were calculated by the following procedure. Tardy (1971) gives the equilibrium constant for Ca-mont-kaolinite reaction as:

$8\log H_4SiO_4 + \log(aCa^{++}/ aH^{+\ 2}) = -15.7$ at 25°C.

The change in the free-energy of reaction ΔG_r^o therefore, - 1.364 x (- 15.7) or 21.41 kcal. Using the free-energy of formation of all other species, the value for Ca-montmorillonite is estimated to be -1278.84 kcal/mole. The entropy value was estimated by considering the difference in entropy between Na_2O and CaO and Na^+ and Ca^{++} and suitably correcting the S^o of Na-mont given by Raymahashay (1968). This procedure gives an average entropy of Ca-mont equal to 59.6 cal/mole. It should be pointed out that these calculated values shown in Table 6.2 are very close to ΔG_f^o = - 1279.24 kcal/mole, S^o = 61.2 cal/mole listed by Helgeson (1969).

After the phase boundaries at 25°C were constructed by using standard free-energy values as indicated above, the stability fields at an elevated temperature of 65°C were superimposed by means of the relationship:

$$\Delta G^o_{r \text{ at } 65°C} - \Delta G^o_{r \text{ at } 25°C} = - \Delta S^o_r \times (65 - 25)$$

and $$\log K \text{ at } 65°C = - \Delta G^o_{r \text{ at } 65°C} \div 1.547$$

where ΔS^o_r representing the entropy of the reaction at 25°C, is assumed to be constant at this small temperature interval (van't Hoff assumption). This temperature range of 25°C to 65°C covers the measured spring temperatures in the Rajgir-Monghyr hot spring belt. Table 6.3 lists the log K values at 65°C and the relevant stability diagrams are shown in Figures 6.14, 6.15 and 6.16. The

TABLE 6.3. CALCULATED log K VALUES AT 65°C.

A. K-SYSTEM

Muscovite-Kaolinite Boundary

$$\log \frac{aK^+}{aH^+} = 5.35$$

K-Feldspar-Kaolinite Boundary

$$\log(aK^+/aH^+) + 2\log aH_4SiO_4 = -0.67$$

K-Feldspar-Muscovite Boundary

$$\log(aK^+/aH^+) + 3\log aH_4SiO_4 = -3.7$$

Kaolinite-Gibbsite Boundary

$$\log aH_4SiO_4 = -3.92$$

Muscovite-Halloysite Boundary

$$\log(aK^+/aH^+) = 0.8945$$

K-Feldspar-Halloysite Boundary

$$\log(aK^+/aH^+) + 2\log aH_4SiO_4 = -2.15$$

Halloysite-Gibbsite Boundary

$$\log aH_4SiO_4 = -2.77$$

B. Na-SYSTEM

Na-Montmorillonite-Kaolinite Boundary

$$\log(aNa^+/aH^+) + 4\log aH_4SiO_4 = -5.76$$

Contd...

TABLE 6.3 (continued)

C. Ca-SYSTEM

Ca-Montmorillonite-Kaolinite Boundary

$$\log aCa^{++}/(aH^{+})^{2} + 8\log aH_4SiO_4 = -15.6$$

Anorthite-Kaolinite Boundary

$$\log aCa^{++}/(aH^{+})^{2} = +14.11$$

calculated activities of major ions in Rajgir-Monghyr thermal-waters at their respective vent temperatures are given in Table 6.4.

The chemistry of the hot water environment was then compared with the mineral stability field by plotting the relevant activity ratios (Table 6.5) on the three stability diagrams.

It is important to note at this stage that the Sitakund water stands out as a distinct type because of its relatively high activity of cation and pH values. On the other hand, all other waters have a chemical composition such that a kaolinite-type clay mineral would be stable in this environment. As pointed out in the previous section, the weathered rocks of Rajgir-Monghyr area contain halloysite together with kaolinite. Interestingly enough, the free energy of formation of these two structurally related clay minerals differ by such an extent that the halloysite stability field is much smaller than that of kaolinite (Figure 6.14). Looking at it from another point of view, the aK^+/aH^+ ratio is much lower for K^+-mica-halloysite equilibrium than K^+-mica-kaolinite equilibrium, and the dissolved silica value for gibbsite-halloysite equilibrium is much higher than the gibbsite-kaolinite equilibrium (Figure 6.14). It is apparent from Figure 6.14 that the presence of halloysite as a secondary mineral

TABLE 6.4. CALCULATED ACTIVITIES OF MAJOR IONS IN RAJGIR-MONGHYR THERMAL WATERS AT THEIR RESPECTIVE VENT TEMPERATURE AND 1 atm. PRESSURE.

Spring	Sitakund Hot	Rishikund South	Rishikund North
Date	25.2.78	24.10.77	24.10.77
Vent Temp. °C	45°	42°	45°
$aNa^{+} \times 10^{3}$	1.046	0.148	0.131
$aK^{+} \times 10^{3}$	0.097	0.030	0.027
$aCa^{++} \times 10^{3}$	0.813	0.076	0.066
$aHCO_3^{-} \times 10^{3}$	2.303	0.205	0.185
$aH_4SiO_4 \times 10^{3}$	0.804	0.574	0.607
$aH^{+} \times 10^{5}$	0.0295	1.3800	0.1550
Calculated $aCO_3^{=}$	4.99×10^{-7}	9.18×10^{-10}	7.62×10^{-9}
Calculated log P_{CO_2}	-1.108	-0.587	-1.528
Calculated Ionic Strength $\times 10^{3}$	4.930	0.499	0.451

Spring	Bhimbandh Road Side	Bhimbandh Pool	Chormara
Date	26.2.78	24.5.78	23.5.78
Vent Temp. °C	65°	60°	65°
$aNa^{+} \times 10^{3}$	0.173	0.203	0.213
$aK^{+} \times 10^{3}$	0.040	0.049	0.013
$aCa^{++} \times 10^{3}$	0.053	0.048	0.085
$aHCO_3^{-} \times 10^{3}$	0.226	0.215	0.408
$aH_4SiO_4 \times 10^{3}$	0.836	0.639	1.442
$aH^{+} \times 10^{5}$	0.0972	0.3080	0.3060
Calculated $aCO_3^{=}$	1.76×10^{-8}	5.06×10^{-9}	1.06×10^{-8}
Calculated log P_{CO_2}	-1.458	-1.022	-0.696
Calculated Ionic Strength $\times 10^{3}$	0.562	0.539	0.733

Contd...

TABLE 6.4 (continued)

Spring	Rameshwarkund	Singhirishi	Agnikund
Date	25.10.77	28.10.77	30.10.77
Vent Temp. °C	45°	32°	49°
$aNa^{+} \times 10^{3}$	0.085	0.170	0.294
$aK^{+} \times 10^{3}$	0.005	0.011	0.021
$aCa^{++} \times 10^{3}$	0.039	0.046	0.116
$aHCO_3^{-} \times 10^{3}$	0.205	0.123	0.387
$aH_4SiO_4 \times 10^{3}$	0.681	0.336	0.681
$aH^{+} \times 10^{5}$	0.3090	0.3090	0.0968
Calculated $aCO_3^{=}$	4.23×10^{-9}	2.11×10^{-9}	2.67×10^{-8}
Calculated log P_{CO_2}	-1.180	-1.550	-1.359
Calculated Ionic Strength $\times 10^{3}$	0.383	0.453	0.829

Spring	Surajkund	Brahamkund	Makhdumkund
Date	31.10.78	29.5.78	31.10.77
Vent Temp. °C	41°	45°	35°
$aNa^{+} \times 10^{3}$	0.118	0.151	0.123
$aK^{+} \times 10^{3}$	0.030	0.037	0.027
$aCa^{++} \times 10^{3}$	0.109	0.143	0.101
$aHCO_3^{-} \times 10^{3}$	0.286	0.376	0.245
$aH_4SiO_4 \times 10^{3}$	0.442	0.410	0.459
$aH^{+} \times 10^{5}$	0.0972	0.0770	0.0973
Calculated $aCO_3^{=}$	1.79×10^{-8}	3.12×10^{-8}	1.40×10^{-8}
Calculated log P_{CO_2}	-1.597	-1.569	-1.697
Calculated Ionic Strength $\times 10^{3}$	0.662	0.804	0.606

Contd...

TABLE 6.4 (continued)

Note: The activity is defined as:

$$a_i = \gamma_i \cdot m_i \quad \text{and}$$

$$\log \gamma_i = \frac{-A Z^2 (I)^{1/2}}{1 + a^o B (I)^{1/2}} \quad \ldots \text{Debye-Hukel equation}$$

and, $$I = \frac{1}{2} \sum m_i z_i^2$$

where
- a_i = activity
- γ_i = individual ion-activity-coefficient
- m_i = refers to each and every ion in solution
- log = base 10 logarithm
- Z = valency charge of the ion
- I = ionic strength
- A, B = constants, depending on temperature and nature of the solvent
- a^o = radius of the hydrated ion.

TABLE 6.5. CATIONS TO H^+ ION ACTIVITY RATIOS.

Spring	$\log \frac{aK^+}{aH^+}$	$\log \frac{aNa^+}{aH^+}$	$\log \frac{aCa^{++}}{(aH^+)^2}$	$\log aH_4SiO_4$
Sitakund Hot	2.517	3.550	9.971	-3.095
Rishikund South	0.339	1.032	5.602	-3.241
Rishikund North	1.249	1.929	7.439	-3.217
Bhimbandh Road Side	1.611	2.251	7.751	-3.172
Bhimbandh Pool	1.199	1.819	6.701	-3.194
Chormara	0.623	1.842	6.957	-2.8408
Rameshwarkund	0.230	1.439	6.611	-3.1673
Sringhirishi	0.531	1.740	6.690	-3.4736
Agnikund	1.331	2.483	8.092	-3.1673
Surajkund	1.486	2.085	8.062	-3.3540
Brahamkund	1.683	2.294	8.381	-3.3874
Makhdumkund	1.449	2.100	8.028	-3.3382

possibly exerts a strong control on the water-chemistry of Rajgir-Monghyr hot springs, because most of the water compositions lie close to the boundaries of halloysite stability field.

6.4. MINERAL SATURATION

Field measurements of temperature, pH and alkalinity allow estimates of (i) apparent CO_2 partial pressure in the spring water and (ii) state of saturation with respect to the mineral calcite.

6.4.1. APPARENT P_{CO_2}

As noted earlier, none of the spring waters show reaction with phenolpthalein indicating that $CO_3^{=}$ - alkalinity is relatively negligible. As a first approximation, the total alkalinity is assumed to be equal to HCO_3^- concentration and field alkalinity values were expressed as $mHCO_3^-$ (Table 4.4). Then at the prevailing ionic strength of each spring $aHCO_3^- = \gamma HCO_3 \times mHCO_3^-$ can be calculated from the Debye-Hückel relationship. Now, from the solubility of CO_2 gas in water at any temperature and the first dissociation constant of dissolved H_2CO_3:

$$K_{CO_2} = aH_2CO_3 / P_{CO_2}$$

or, $aH^+ \cdot aHCO_3^- = K_1 \cdot K_{CO_2} \cdot P_{CO_2}$ (Garrels and Christ, 1965)

Using K_{CO_2} and K_1 values at the spring temperature (Garrels and Christ, 1965; Helgeson, 1969) and $aHCO_3^-$, P_{CO_2} values were calculated as shown in Table 6.4. The range of values ($10^{-1.697}$ to $10^{-0.697}$) is much higher than the atmospheric $P_{CO_2} = 10^{-3.5}$ atm. This is obviously responsible for the copious bubbling of CO_2 gas at the springs.

6.4.2. CALCITE SATURATION

For a more exact calculation of $CO_3^=$ ion activity, the pH, HCO_3^- ion activity and the second dissociation constant of H_2CO_3 at the spring temperature can be utilised in the following relationship:

$$K_2 = \frac{aCO_3^= \cdot aH^+}{aHCO_3^-}$$

The $CO_3^=$ ion activity thus calculated can be combined with Ca^{++} ion activity calculated from dissolved Ca^{++} concentration to estimate the ion activity product $aCa^{++} \times aCO_3^=$ (Table 6.6). This product when compared with the known solubility product of calcite at the spring temperature (see Figure 6.17) indicates that each of the spring remains undersaturated with respect to calcite. This explains the absence of calcite deposition at the spring vents. In other words, the prevailing temperature, pH and alkalinity conditions are such that there is no possibility of incrustation or sealing of pore spaces by calcite.

TABLE 6.6. CARBONATE EQUILIBRIA.

Spring	Temp. °C	aCa^{++}	aCO_3^{--}	Product $aCa^{++} \times aCO_3^{=}$	$K_{calcite}$
Sitakund hot	45°	0.813×10^{-3}	4.99×10^{-7}	$10^{-9.39}$	$10^{-8.57}$
Rishikund South	42°	0.076×10^{-3}	9.18×10^{-10}	$10^{-13.16}$	$10^{-8.52}$
Rishikund North	45°	0.066×10^{-3}	7.62×10^{-9}	$10^{-12.30}$	$10^{-8.57}$
Bhimbandh Road Side	65°	0.053×10^{-3}	1.76×10^{-8}	$10^{-12.03}$	$10^{-8.72}$
Bhimbandh Pool	60°	0.048×10^{-3}	5.06×10^{-9}	$10^{-12.62}$	$10^{-8.70}$
Chormara	65°	0.085×10^{-3}	1.06×10^{-8}	$10^{-12.05}$	$10^{-8.72}$
Rameshwarkund	45°	0.039×10^{-3}	4.23×10^{-9}	$10^{-12.78}$	$10^{-8.57}$
Sringhirishi	32°	0.046×10^{-3}	2.11×10^{-9}	$10^{-13.00}$	$10^{-8.40}$
Agnikund	49°	0.0116×10^{-3}	2.669×10^{-8}	$10^{-11.51}$	$10^{-8.63}$
Surajkund	41°	0.0109×10^{-3}	1.79×10^{-8}	$10^{-11.71}$	$10^{-8.52}$
Brahamkund	45°	0.143×10^{-3}	3.12×10^{-8}	$10^{-11.35}$	$10^{-8.57}$
Makhdumkund	35°	0.101×10^{-3}	1.40×10^{-8}	$10^{-11.85}$	$10^{-8.46}$

$K_{calcite}$ values are solubility products of calcite at spring temperatures calculated from Garrels and Christ (1965).

DESCRIPTION OF FIELD PHOTOGRAPHS

Photo 6.1. Cross-bedding in Quartzite Ridge Between Makhdumkund and Surajkund, Rajgir.
19 February, 1977
Photo: B.C. Raymahashay

Photo 6.2. Ripple Mark in Quartzite Ridge Between Makhdumkund and Surajkund, Rajgir.
19 February, 1977
Photo: B.C. Raymahashay

Photo 6.3. Jointed and Fractured Ferruginous Quartzite, Chormara, Bhimbandh.
23 May, 1978
Photo: G.S. Shukla

Photo 6.4. Quick-Sand Upwelling at Rishikund (South).
24 October, 1977
Photo: G.S. Shukla

← PHOTO 6·1

PHOTO 6·2 →

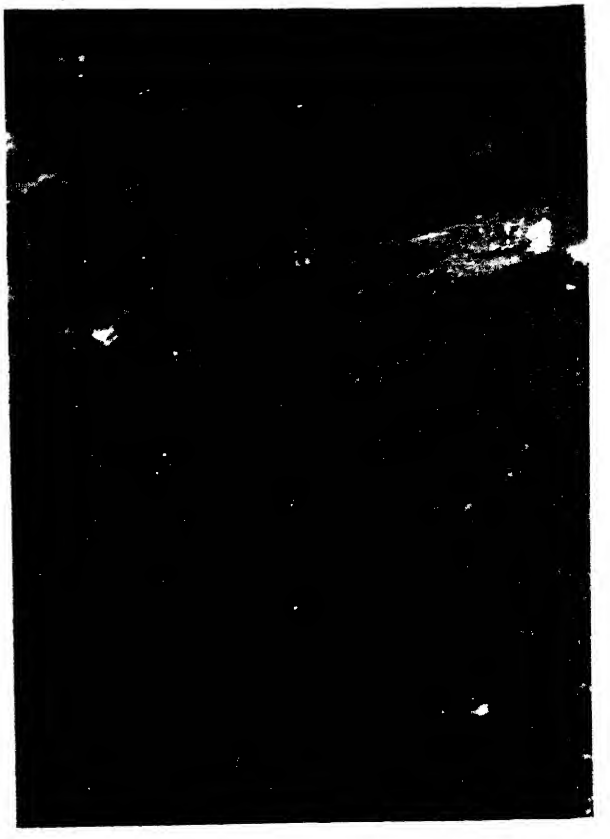

PHOTO 6·3

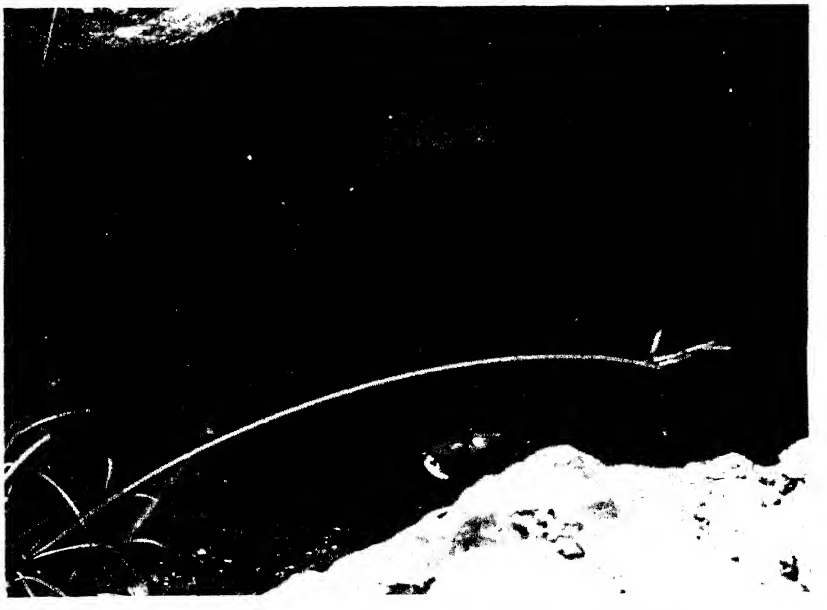

PHOTO 6·4

DESCRIPTION OF FIGURES

Figure 6.1. Sketch of Thin Section View of Fresh Quartzite (Ag-1), Rajgir, Mag. 100X

Figure 6.2. Rose Diagram of Strike of Joint Planes in Quartzite Exposures in the Rajgir-Monghyr Belt

Figure 6.3. Sketch of Thin Section View of Weathered Quartzite in Contact with Hot Water (RM-4), Rishikund, Monghyr, Mag 100X

Figure 6.4. Sketch of X-ray Diffractogram of Weathered Quartzite (RM-4), Same Sample as in Figure 6.3

Figure 6.5. Sketch of X-ray Diffractogram of Weathered Ferruginour Quartzite (Ag-5), Agnikund, Rajgir

Figure 6.6. Transmission Electron Micrograph of Weathered Quartzite (RM-15), Singhirishi Spring, Monghyr, Mag. 37,596X

Figure 6.7. Sketch of X-ray Diffractogram of Weathered Phyllite (RM-12), Man River Bridge, Bhimbandh

Figure 6.8. Sketch of X-ray Diffractogram of Weathered Phyllite (RR-19), Agnikund, Rajgir

Figure 6.9. Transmission Electron Micrograph of Weathered Phyllite (RM-12), Same Sample as in Figure 6.7, Mag.8,194X

Figure 6.10. Transmission Electron Micrograph of Weathered Phyllite (RR-19), Near Ropeway, Rajgir, Mag. 18,798X

Figure 6.11. DTA Pattern of Red Soil (Ag-2), Agnikund Road, Rajgir

Figure 6.12. Transmission Electron Micrograph of 'Kund' Mud (Ag-4), Agnikund, Rajgir, Mag. 1,06,040X

Figure 6.13. Transmission Electron Micrograph of 'Kund' Mud (Ag-4), Agnikund, Rajgir, Mag. 1,06,040X

Figure 6.14. Mineral Stability Diagram for K-system at 25°C and 65°C with Hot Spring Composition. Lines G & C and T Represent Musco-kaol Boundary Given by Garrels and Christ (1965) and Tardy (1971)

Figure 6.15. Mineral Stability Diagram for Na-system at 25°C and 65°C with Hot Spring Composition

Figure 6.16. Mineral Stability Diagram for Ca-system at 25°C and 65°C with Hot Spring Composition

Figure 6.17. Calcite Solubility Product Compared with Ca x CO_3 Activity Product at Spring Temperature

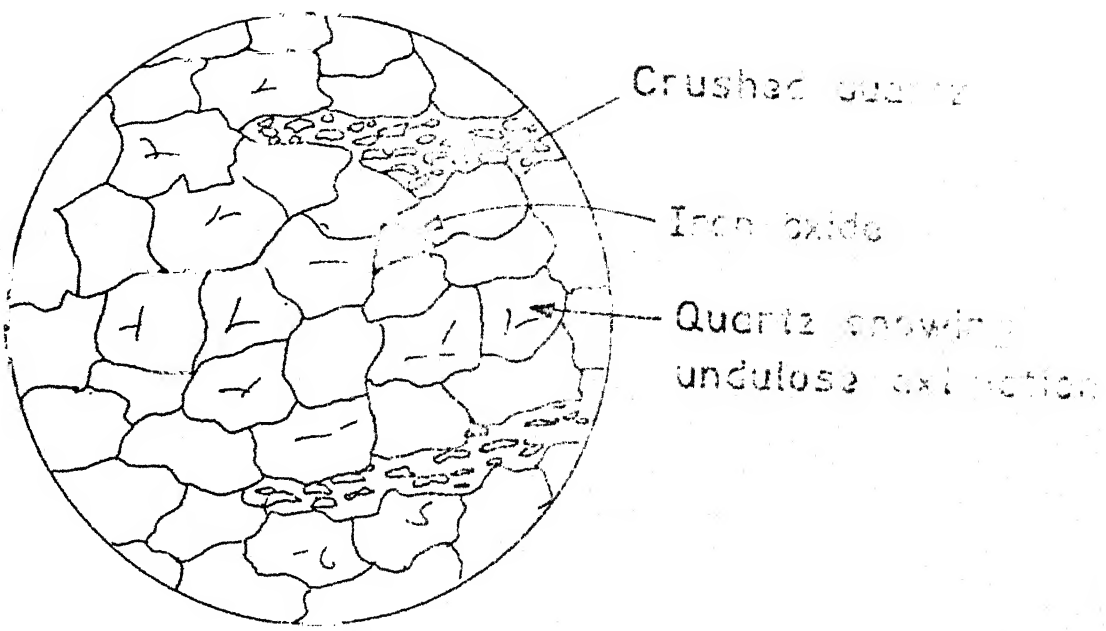
Crushed quartz
Iron oxide
Quartz showing
undulose extinction

Fig. 6.1

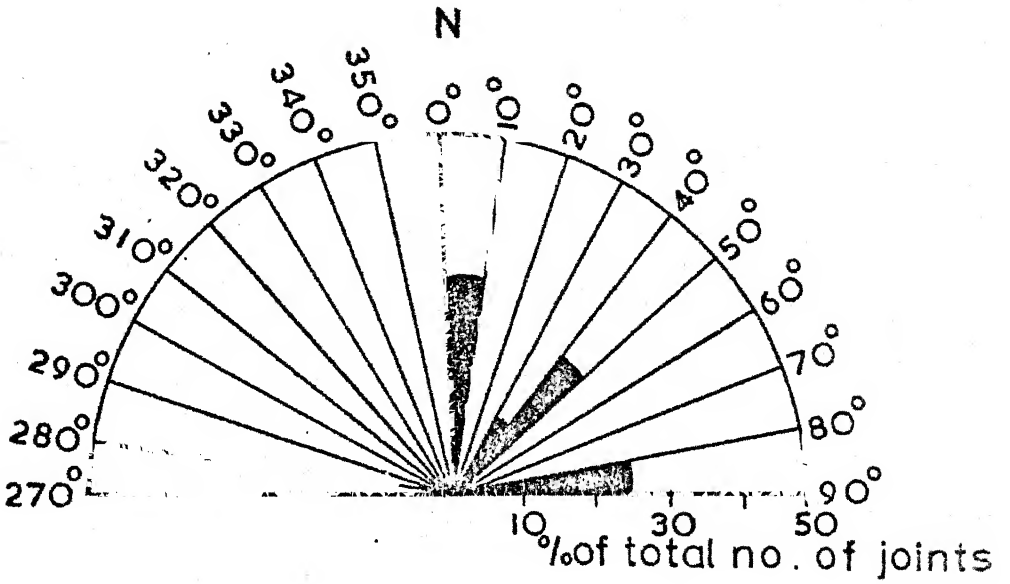

TOTAL No. OF READING = 288

Fig. 6.2

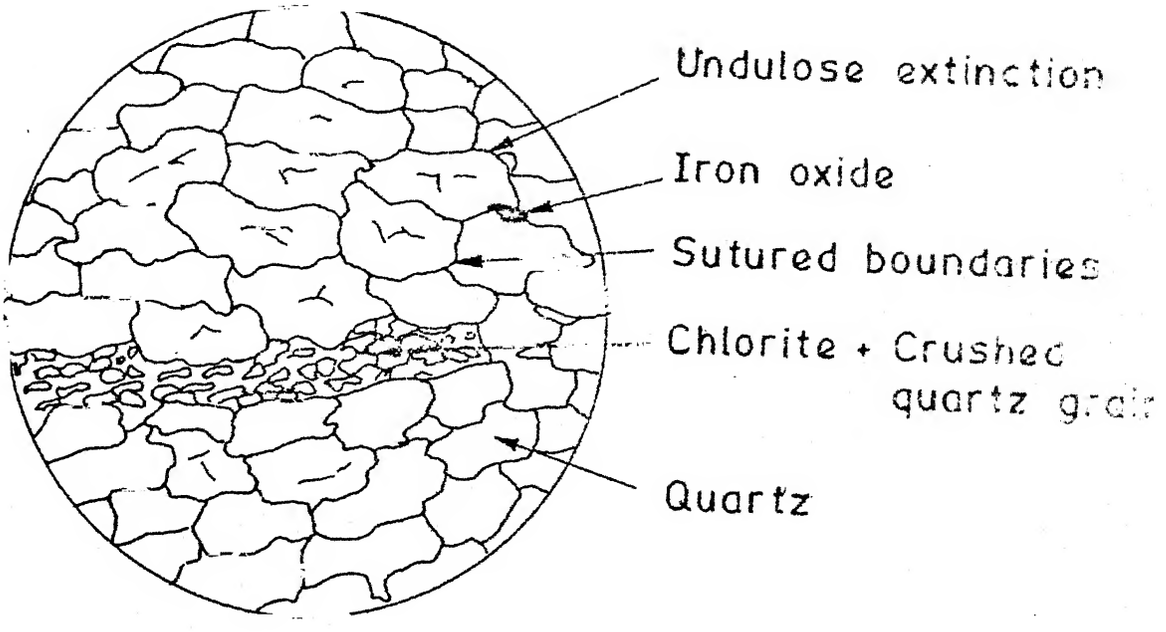
Undulose extinction
Iron oxide
Sutured boundaries
Chlorite + Crushed
quartz grai
Quartz

Fig. 6.2

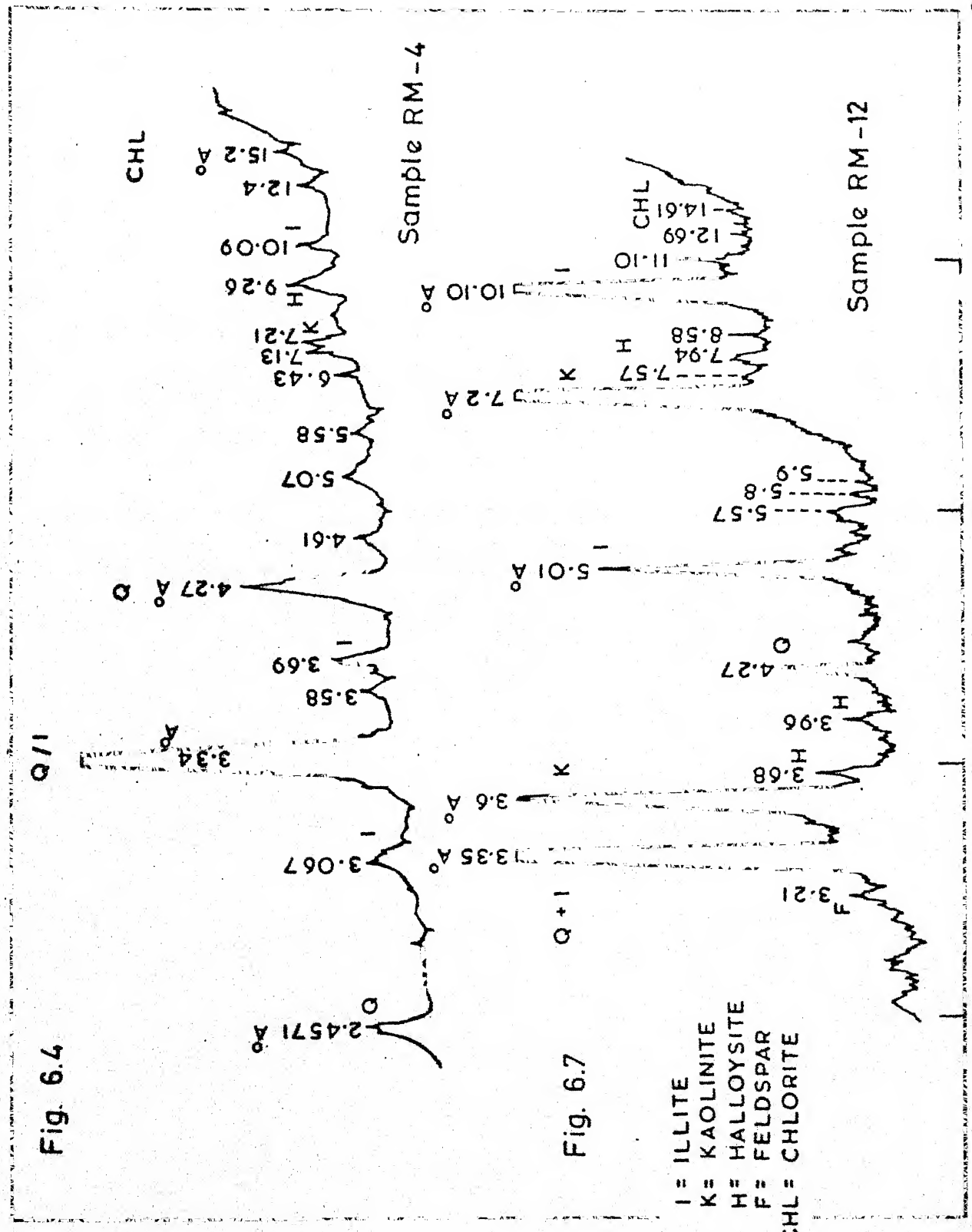
Fig. 6.4
Q / I
2.4571 Å°
3.067
3.34 Å°
3.58
3.69
4.27 Å°
4.61
5.07
5.58
6.43
7.13
7.21
9.26
10.09
12.4
15.2 Å°
CHL
Sample RM-4
Fig. 6.7
Q + I
13.35 Å°
3.6 Å°
3.21
3.68
3.96
4.27
5.01 Å°
5.57
5.8
5.9
7.2 Å°
7.57
7.94
8.58
10.10 Å°
11.10
12.69
14.61
CHL
Sample RM-12
I = ILLITE
K = KAOLINITE
H = HALLOYSITE
F = FELDSPAR
CHL = CHLORITE
0
10
20
30
40
2θ (FeKα)

Fig. 6.6

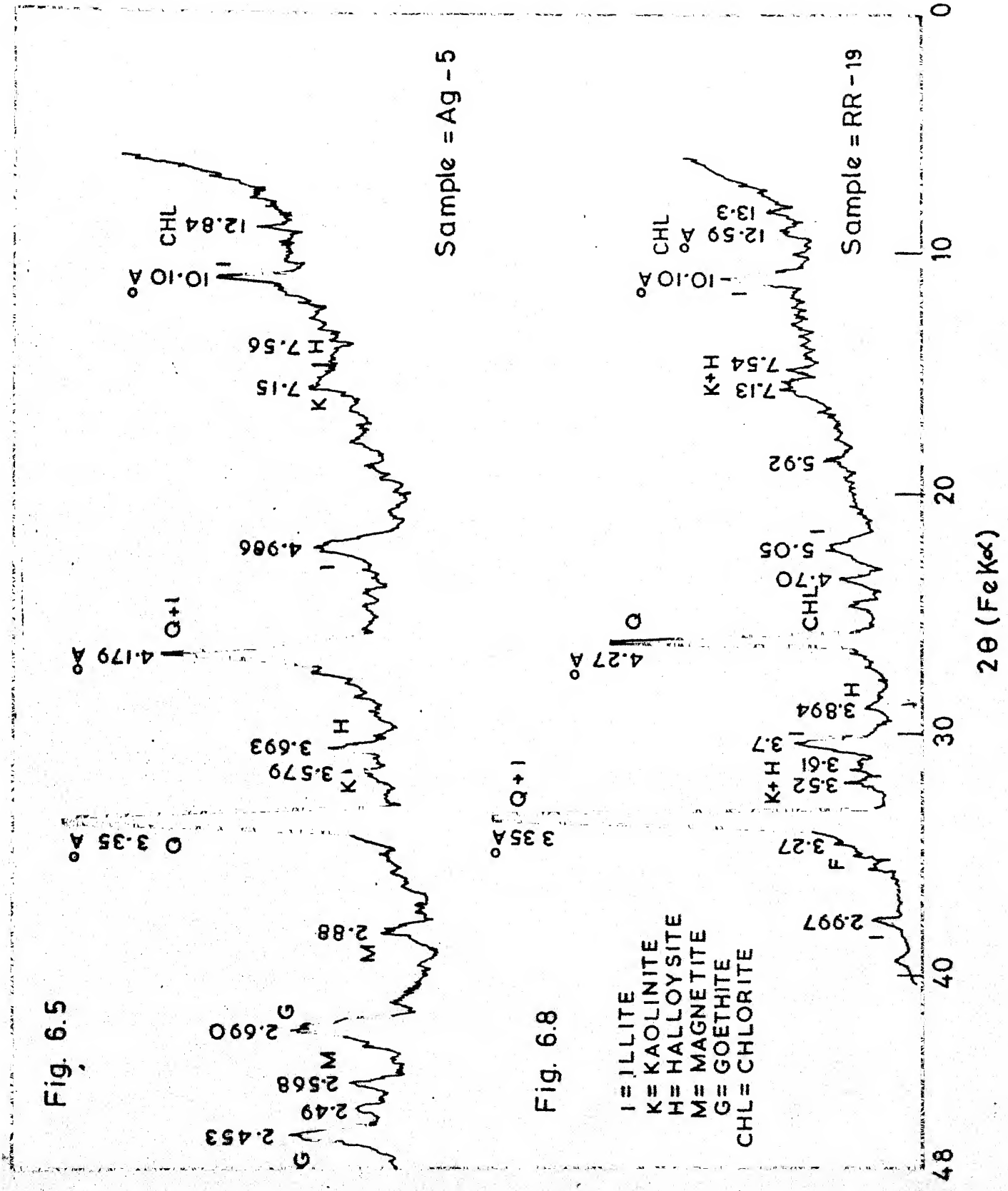
Sample = Ag - 5
Sample = RR - 19
I = ILLITE
K = KAOLINITE
H = HALLOYSITE
M = MAGNETITE
G = GOETHITE
CHL = CHLORITE
2θ (FeKα)
0
10
20
30
40
48
Q 3.35 Å°
Q+I
4.179 Å°
10.10 Å°
12.84
CHL
7.56
7.15
4.986
3.693
3.579
2.690
2.568
2.49
2.453
4.27 Å°
12.59 Å°
13.3
7.54
7.13
5.92
5.05
4.70
3.894
3.7
3.61
3.52
3.27
2.997

Fig. 6.5

Fig. 6.8

Fig. 6·9

Fig. 6·10

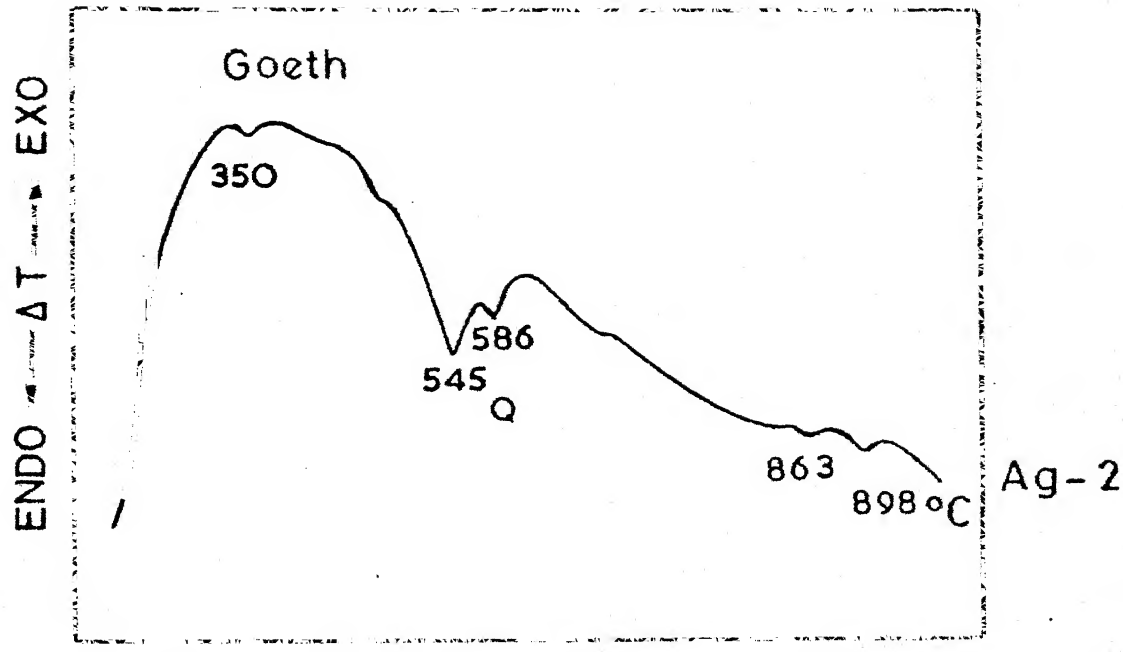

Fig. 6.11

Fig. 6·12

Fig. 6·13

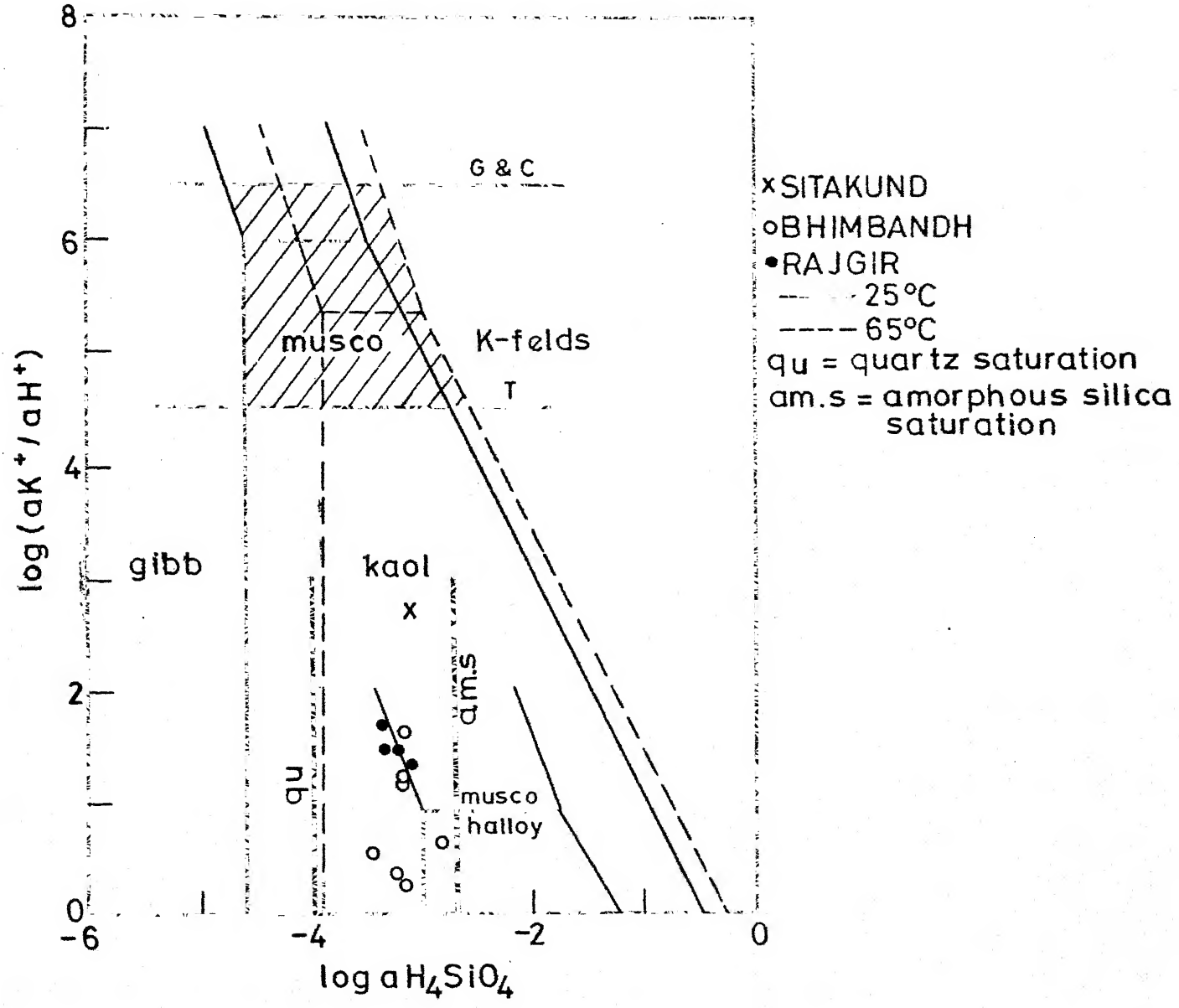
8
6
4
2
0
-6
-4
-2
0
log (aK⁺/aH⁺)
log a H4SiO4
G & C
musco
K-felds
T
gibb
kaol
x
qu
am.s
musco
halloy
x SITAKUND
o BHIMBANDH
• RAJGIR
25°C
65°C
qu = quartz saturation
am.s = amorphous silica saturation

Fig. 6.14

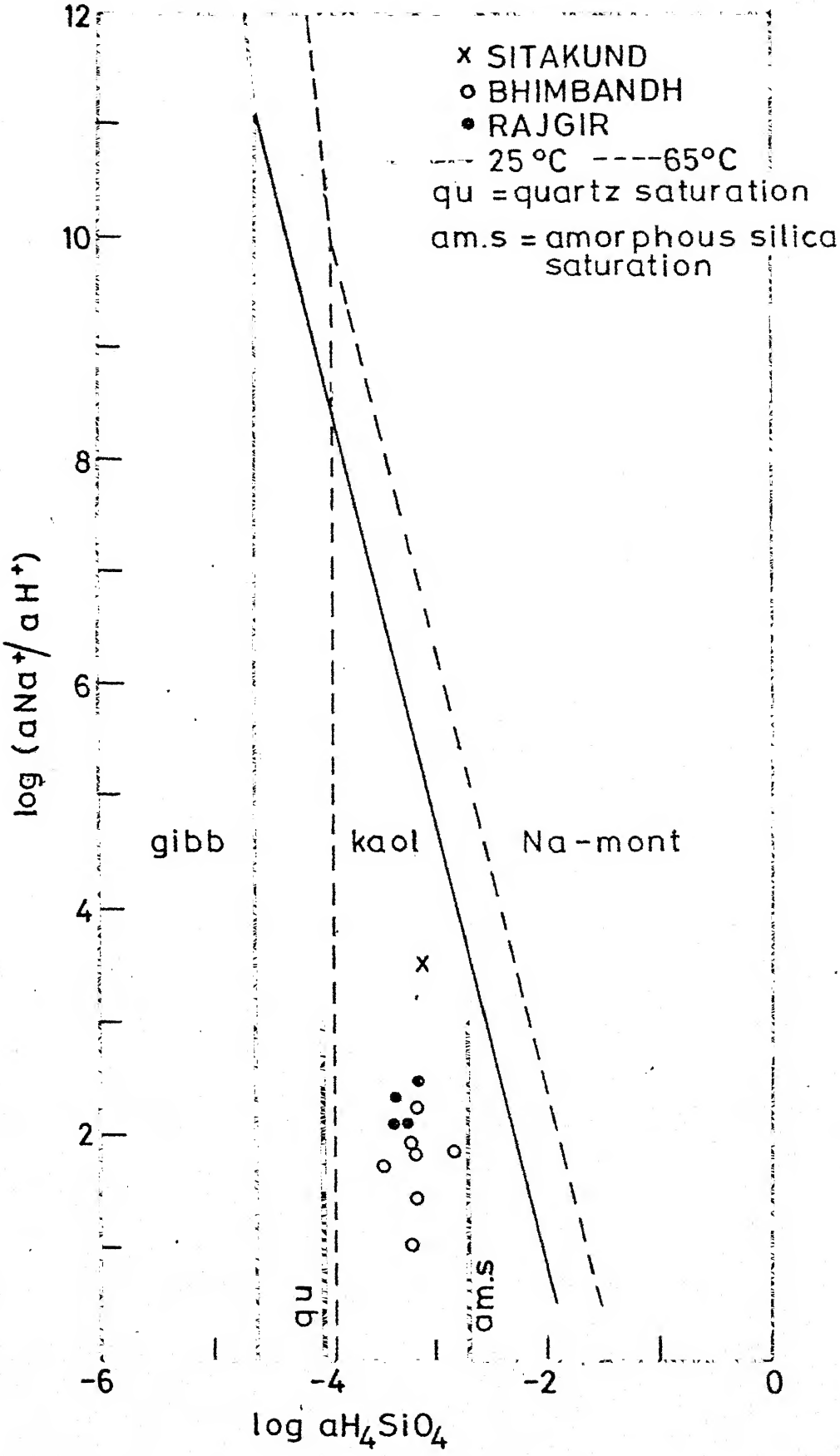
x SITAKUND
o BHIMBANDH
• RAJGIR
25 °C ----65°C
qu = quartz saturation
am.s = amorphous silica saturation
gibb
kaol
Na-mont
qu
am.s
log (aNa+/aH+)
log aH4SiO4
12
10
8
6
4
2
-6
-4
-2
0

Fig. 6.15

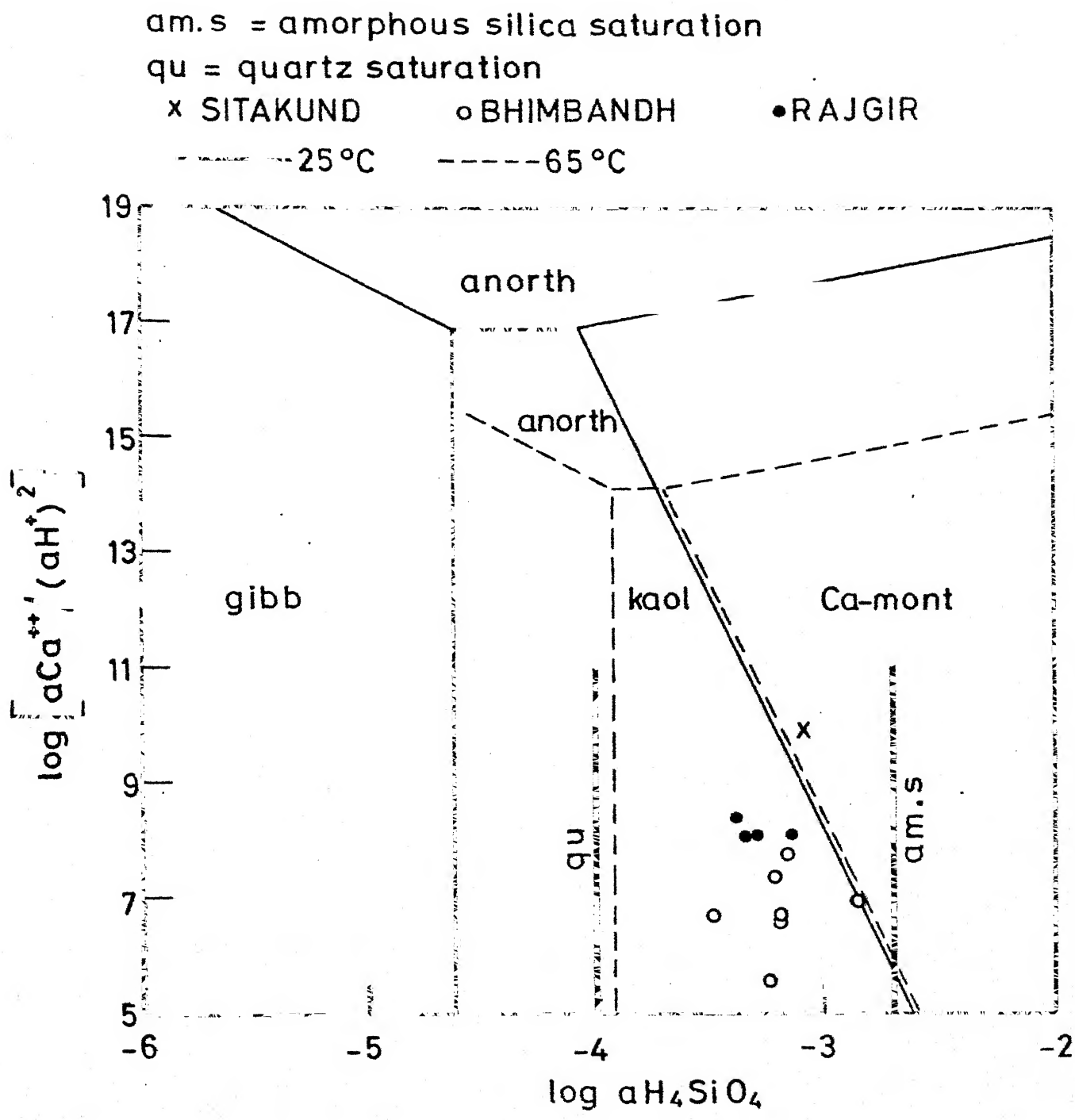
am.s = amorphous silica saturation
qu = quartz saturation
x SITAKUND
o BHIMBANDH
• RAJGIR
25 °C
65 °C
anorth
anorth
gibb
kaol
Ca-mont
qu
am.s
x
19
17
15
13
11
9
7
5
-6
-5
-4
-3
-2
log aCa++ / (aH+)2
log aH4SiO4

Fig. 6.16

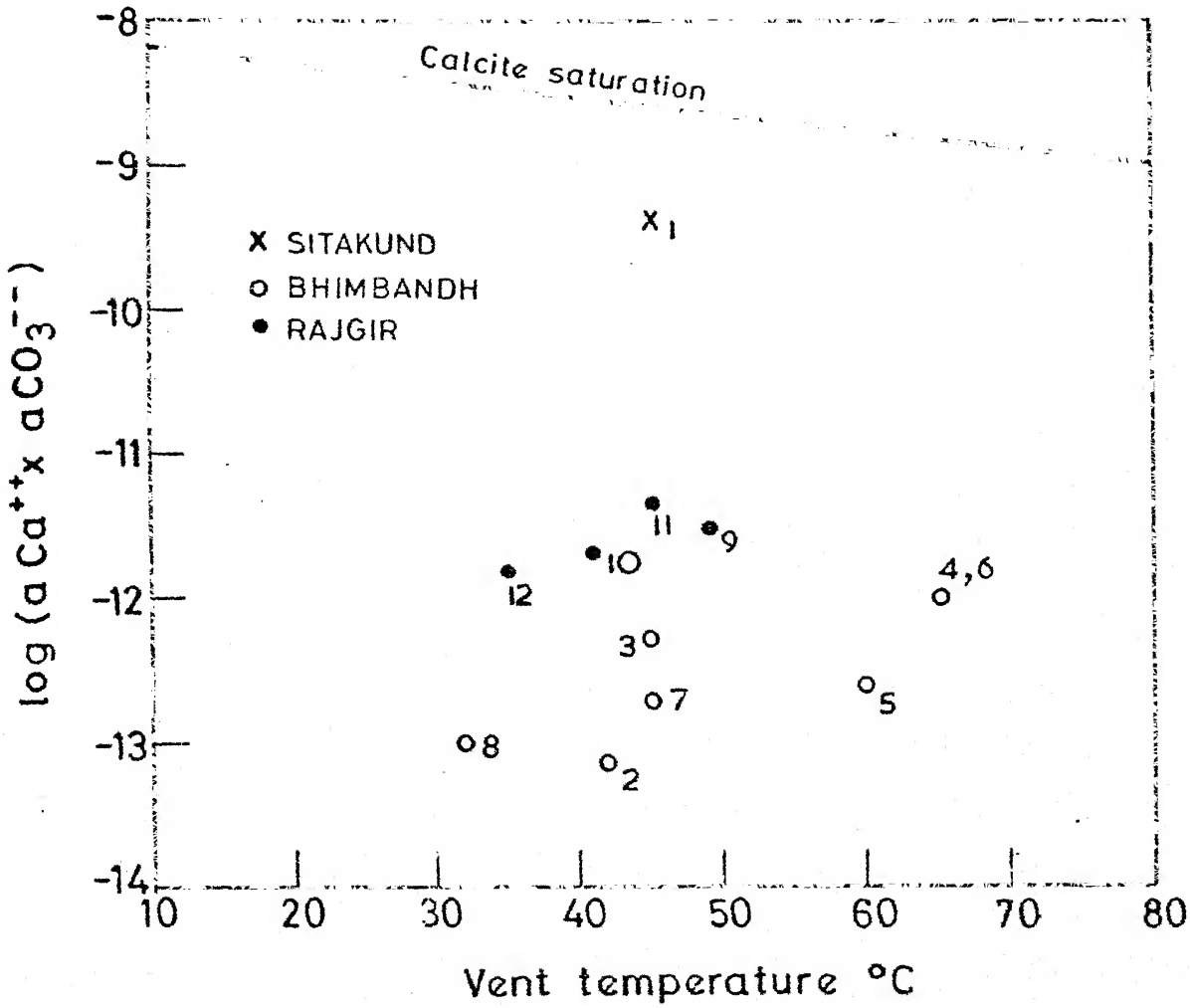
Calcite saturation
X SITAKUND
o BHIMBANDH
• RAJGIR
log (a Ca++ x aCO3--)
-8
-9
-10
-11
-12
-13
-14
10
20
30
40
50
60
70
80
Vent temperature °C
X1
•11
•9
•10
12
4,6
3
7
5
8
2

Fig. 6.17

Chapter 7

CONCLUSIONS AND RECOMMENDATIONS

7.1. SUMMARY

The Rajgir-Monghyr hot spring belt is a typical Low Temperature ("Semi-Thermal" according to Armstead, 1978) geothermal field. Hot water in the temperature range 30°C to 65°C emerges through fracture and joint planes of massive Precambrian quartzites interbedded with argillites.

In the regional tectonic set-up, this is a shield area with tertiary shear zones and complex cross-folds. The springs are located within a NE-SW trending tectonic zone stretching from Ambikapur, Madhya Pradesh to Monghyr, Bihar.

A remarkable aspect of the thermal waters is their relatively low (around 40 mg/l) dissolved chemical content. The composition does not show any significant seasonal variation. The pH values remain near-neutral at the spring temperature. It is concluded that 65.9 to 96.2 percent of the spring water is recycled ground (meteoric) water which descends to a shallow hot zone at temperatures between 95°C and 240°C, mixes with a deeper hot component and is quickly flushed out after rains under thermo-artesian pressure. This research did not involve investigation of the reported curative properties and radio-activity of the thermal waters of Rajgir and Monghyr.

Because of the hydrological condition summarised above, rock-water interaction is minimum. No sub-surface rock sample was studied. However, rocks in contact with hot water at the surface contain secondary silicate minerals like kaolinite and halloysite. Using thermo-chemical data, it is concluded that these kaolinite type of clay minerals are stable in the hot water environment and possibly exert a chemical control on the water quality. The Bhimbandh springs show an incrustation over the country rocks which has been tentatively identified as a silicate of magnesium and calcium in an X-ray amorphous state. The lack of extensive hydrothermal rock alteration is thus consistent with the low chemical content of the waters.

7.2. UTILISATION OF THERMAL WATER

The most glamorous use of thermal waters is for electrical power generation. However, for economic and technical feasibility, commercial geothermal plants are located in dry steam fields or boiling water dominated "hyper thermal" fields. At the present time, "semi thermal" fields like the Rajgir-Monghyr Belt hold little promise for geothermal power. This does not, however, rule out technology transfer from on-going research projects which utilise low temperature hot water along with a low boiling point fluid e.g., isobutane or freon to generate power. In some countries e.g., U.S.A. and Britain, pumping of hot

water into artificially fractured subsurface rocks and reuse of the water for power production is being seriously contemplated.

It is, therefore, logical to recommend the Rajgir-Monghyr waters for applications other than power generation. Armstead (1978) lists the following modes of utilisation of low temperature hot water fields: (i) evaporation and concentration of salt solutions, (ii) drying and curing of light aggregate cement slabs, (iii) drying of farm products like wool, vegetable, fish, (iv) space heating and green house construction with water at temperature around 80°C, (v) refrigeration with a lower limit of utilization at 70°C, (vi) swimming pool, soil warming, deicing etc.

In India, pilot scale utilization of thermal waters for space heating, green house and refrigeration has already been considered (U.N., 1975). In the Puga Valley, bore hole discharge of 60 lpm steam at 125°C, 2.5 kg/cm^2 was utilised to erect an experimental space heating hut in 1973-74. During the same period, a green house was designed utilizing 120 lpm steam and hot water at 90°C. At Manikaran in Parbati Valley, a 100 ton ammonia-water absorption refrigeration plant for fruit preservation has been proposed. It has been estimated that for a storage temperature of -5°C, about 400 lpm of cold river water (10°C) along with 140 lpm thermal water (90°C) can be utilised.

In the Rajgir-Monghyr belt, the Bhimbandh springs are particularly suitable for such applications because of the moderately high temperature (65°C) and large discharge (about 70,000 liters per hour at Bhimbandh and Chormara combined). The Forest Rest House at Bhimbandh already has a swimming pool using hot spring water (Photo 7.1). Other industrial applications using forest products and hot water e.g., paper and pulp industry (Kraft process) appear quite feasible at Bhimbandh.

As Rajgir-Monghyr and Bhimbandh are tourist spots, development of spa and related recreational facilities is worth consideration.

The Rajgir-Monghyr spring waters are 'potable' because of the low total dissolved solids. Mineral water bottling plants are definitely viable in these areas.

As pointed out earlier, further investigation of trace element content and radioactivity of these waters is necessary to establish utilisation for agricultural and therapeutic needs.

REFERENCES

Armstead, H.C. (1978). Geothermal Energy, E & F.N. Spon Ltd., London (John Wiley).

Arnorsson, S. (1975). Application of the silica geothermometer in low-temperature hydrothermal areas in Iceland, Amer. Jour. Sci., Vol. 275, pp. 763-784.

Begemann, F. and Libby, W. (1957). Continental water balance, ground water inventory and storage time, surface ocean mixing rates, and world-wide circulation patterns from cosmic ray and bomb tritium, Geochim. Cosmochim. Acta, Vol. 12, pp. 277-296.

Berner, R.A. (1971). Principles of Chemical Sedimentology, Mc-Graw Hill, New York.

Chaterji, G.C. and Guha, S.K. (1968). The problem of the origin of high temperature springs of India, Proc. 23rd Int. Geol. Cong., Prague, p. 141.

Council of Scientific and Industrial Research (CSIR), Govt. of India (1962). Wealth of India, Mineral Springs, Vol. 6, p. 385.

Craig, H. (1963). The isotopic geochemistry of water and carbon in geothermal areas. In Nuclear Geology in Geothermal Areas (editor: E. Tongiorgi), pp. 17-53, Consiglio Naziorelle delle Ricerche, Rome.

Das, Bhagwan (1967). On the lithologic sequence and overall structure of the rocks around Rajgir, Bihar, Bull. Geol. Soc. India, Vol. 4, pp. 46-49.

Ellis, A.J. (1970). Quantitative interpretation of chemical characteristics of hydrothermal systems. Proc. U.N. Sympo. Geothermal Resources, Pisa, Geothermics, Sp. Issue 2, Vol. 2, p. 516.

Ellis, A.J. and Mahon, W.A.J. (1964). Natural hydrothermal systems and experimental hot water/rock interaction, Geochim. Cosmochim. Acta, Vol. 25, pp. 1323-1357.

Ellis, A.J. and Mahon, W.A.J. (1967). Natural hydrothermal systems and experimental hot water/rock interactions (Part II), Geochim. Cosmochim. Acta, Vol. 31, pp. 519-538.

Ellis, A.J. and Mahon, W.A.J. (1977). Chemistry and Geothermal Systems, Academic Press, New York.

Fournier, R.O. (1973). Silica in Thermal Waters: Laboratory and Field Investigations. In Hydrogeochemistry, Proc. Sympo. Hydrogeochem. and Biogeochem., Tokyo, Vol. 1, pp. 122-139. The Clarke Co., Washington, D.C.

Fournier, R.O. and Potter, R.W. II (1979). Magnesium correction to the Na-K-Ca chemical geothermometer. Geochim. Cosmochim. Acta, Vol. 43, pp. 1543-1550.

Fournier, R.O. and Rowe, J.J. (1966). Estimation of underground temperature from silica content of water from hot spring and wet-steam wells, Amer. Jour. Sci., Vol. 264, pp. 685-697.

Fournier, R.O. and Truesdell, A.H. (1973). An empirical Na-K-Ca geothermometer for natural waters. Geochim. Cosmochim. Acta, Vol. 37, pp. 1255-1275.

Fournier, R.O. and Truesdell, A.H. (1974). Geochemical indicators of subsurface temperature, Part 2. Estimation of temperature and fraction of hot water mixed with cold water, Jour. Res. U.S. Geol. Survey, Vol. 2, pp. 263-270.

Fritz, B., Bittencourt, A. and Tardy, Y. (1980). Geochemistry of thermal waters of Plombiers, France. Proc. 3rd International Sympo. Water-Rock Interaction, Edmonton, Canada, pp. 127-128.

Garrels, R.M. and Christ, C.L. (1965). Solutions, Minerals and Equilibria, Harper & Row, New York.

Ghosh, P.K. (1954). Mineral springs of India, Rec. Geol. Survey Ind.,,Vol. 80, pp. 541-558.

Guha, S.K. (1970). Some aspects of studies on the thermal springs of Rajgir area, Bihar, Rec. Papers on Ground Water Potential in Hard Rock Area, Geol. Survey Ind./ Ind. Statistical Inst.

Gupta, M.L. and Sukhija, B.S. (1974). Preliminary studies of some geothermal areas in India, Geothermics, Vol. 3, pp. 105-112.

Gupta, M.L., Narain, Hari and Saxena, V.K. (1975). Geochemistry of thermal waters from various geothermal province of India, Publ. No. 119, IAHS, Proc. Grenoble Sympo., pp. 47-58.

Helgeson, H.C. (1969). Thermodynamics of hydrothermal systems at elevated temperatures and pressures, Amer. Jour. Sci., Vol. 267, pp. 729-804.

Krauskopf, K.B. (1967). An Introduction to Geochemistry, McGraw-Hill, New York.

Krishnaswamy, V.S. (1975). A review of Indian geothermal provinces and their potential for energy utilization. Proc. 2nd U.N. Sympo. on Geothermal Resources, San Francisco, Vol. 1, pp. 143-156.

Mahon, W.A.J. (1966). Silica in hot-water discharges from drill holes at Wairakai, Newzealand, N.Z. Jour. Sci., Vol. 9, pp. 135-144.

National Committee on Science and Technology (NCST), Govt. of India, (1975). Final Report, Expert Panel on Geothermal Energy Utilisation.

Orville, P.M. (1963). Alkali ion exchange between vapor and feldspar phases, Amer. Jour. Sci., Vol. 261, pp. 201-237.

Paces, T. (1975). A systematic deviation from Na-K-Ca geothermometer below 75°C and above 10^{-4} atm P_{CO_2}, Geochim. Cosmochim. Acta, Vol. 39, pp.541-544.

Raymahashay, B.C. (1968). A geochemical study of rock alteration by hot springs in the Paint Pot Hill area, Yellowstone Park, Geochim. Cosmochim. Acta, Vol. 32, pp. 499-522.

Robie, R.A. and Waldbaum, D.R. (1968). Thermodynamic properties of minerals and related substances at 298.15°K (25°C) and one atmosphere (1.013 bars) pressure and higher temperatures, U.S. Geol. Survey, Bull. 1259, p. 256.

Sharma, T. and Pillai, NV. (1970). Oxygen isotope variations in rain water at Patna (abs.), Sympo. Applications of Geochemistry in Earth Sciences, Patna, p. 35.

Sharma, T., Pillai, N.V. and Pandey, G.C. (1970). O^{18}/O^{16} determination in thermal springs of Rajgir, Bihar (abs.), Sympo. Applications of Geochemistry in Earth Sciences, Patna, p. 36.

Srivastava, G.S. and Sengupta, D.K. (1968). Significance of non-diastrophic structure around Rajgir, Patna district, Bihar, Jour. Ind. Geosci. Assoc., Vol. 8, pp. 93-101.

Standard Methods for Examination of Water and Waste Water (1975). 12th Ed., Am. Pub. Health Assoc., New York.

Tardy, Y. (1971). Characterization of the principal weathering types by the geochemistry of waters from some European and African crystalline massifs, Chem. Geol., Vol. 7, pp. 253-271.

Truesdell, A.H. (1975). Summary of Section III. Geochemical Techniques in Exploration, Proc. 2nd U.N. Symp. Geothermal Resources, San Francisco, Vol. 2, pp. liii-lxxx.

Truesdell, A.H. and Fournier, R.O. (1977). Procedure for estimating the temperature of a hot-water component in a mixed water by using a plot of dissolved silica versus enthalpy, Jour. Res. U.S. Geol. Survey, Vol. 5, pp. 49-52.

United Nations (U.N.)(1975). Proc. 2nd Sympo. on Geothermal Resources, San Francisco, California.

Uzumasa, Y. (1965). Chemical Investigations of Hot Springs in Japan, Tsukiji Shoken Co. Ltd., Tokyo.

Wadia, D.N. (1975). Geology of India, 4th Ed., Tata-McGraw-Hill, New Delhi.

Water Well Hand Book (1967). 2nd Ed. (Editor: Keith E. Anderson), Missouri Water Well Drillers Association, Rolla, Mo, U.S.A.

White, D.E. (1957). Thermal waters of volcanic origin, Bull. Geol. Soc. Amer., Vol. 68, pp. 1637-1658.

White, D.E. (1970). Geochemistry applied to the discovery, evaluation and exploitation of geothermal energy resources. Rapporteur's Report, Proc. U.N. Sympo. Development and Utilization of Geothermal Resources, Pisa.

****
APPENDIX
****

PROGRAM FOR THE CALCULATIONS FOR STABILITY DIAGRAMS

```
      DIMENSION PH(12),SOD(12),CAL(12),STL(12),KMU(12),POT(12),XA(12),
     1XB(12),HCO(12),CL(12),SO(12),MG(12),XH(12),XSOD(12),XPOT(12),XC
     2AL(12),XSTL(12),XMG(12),XHCO(12),XCL(12),XSO(12),XGPOT(12),XGSO
     3D(12),XGHCO(12),XGCL(12),XGCAL(12),XGMG(12),XGSO(12),XAPOT(12),
     4XASOD(12),XACAL(12),XAMG(12),XAHCO(12),XASO(12),XACL(12),XASIL(
     512),XAH(12),XBHAH(12),XPKH(12),XPCAH(12),XRMGH(12),XGH(12),XLSI
     6L(12),
      REAL PH,SOD,CL,STL,KMU,POT,HCO,CAL,MG,SO
C     NOTE : CONCENTRATION VALUES ARE IN PPM
      N=12
      READ*,(PH(I), I=1,N)
      READ*,(SOD(I),I=1,N)
      READ*,(POT(I),I=1,N)
      READ*,(CAL(I),I=1,N)
      READ*,(MG(I), I=1,N)
      READ*,(HCO(I),I=1,N)
      READ*,(CL(I), I=1,N)
      READ*,(SO(I), I=1,N)
      READ*,(STL(I),I=1,N)
      READ*,(XA(I), I=1,N)
      READ*,(XB(I), I=1,N)
      PRINT*,(I,PH(I),SOD(I),POT(I),CAL(I),MG(I),HCO(I),CL(I),SO(I),ST
     1L(I),XA(I),XB(I),I=1,N)
      DO 100 I=1,N
C     NOTE : CALCULATION OF MOLAR CONCENTRATIONS
      XH(I)=(10**(-PH(I)))
      XSOD(I)=SOD(I)/22997.0
      XPOT(I)=POT(I)/39098.0
      XCAL(I)=CAL(I)/40080.0
      XMG(I)=MG(I)*0.00004112
      XHCO(I)=HCO(I)/61000.0
      XCL(I)=CL(I)/35457.0
      XSO(I)=SO(I)*0.00001041
      XSTL(I)=STL(I)/61000.0
      XLSIL(I)=ALOG10(XSIL(I))
      CONTINUE
      PRINT*,(I,XH(I),XSOD(I),XPOT(I),XCAL(I),XMG(I),XHCO(I),XCL(I),XS
     1O(I),XSTL(I),XLSIL(I),I=1,N)
      DO 222 I=1,N
C     NOTE : CALCULATION OF IONIC STRENGTH
      KMU(I)=(0.5*(XSOD(I)+XPOT(I)+XHCO(I)+XCL(I)+(2.0*(XCAL(I)+XMG(
     1I)+XSO(I)))
      CONTINUE
      PRINT*,(I,KMU(I),I=1,N)
      DO 323 I=1,N
C     NOTE : CALCULATION OF ACTIVITY COEFFICIENT
      XGH(I)=10**((-XA(I)*(SQRT(KMU(I))))/(1.0+(XB(I)*9.0*(SQRT(KMU(I)
     1))))))
      XGSOD(I)=10**((-XA(I)*(SQRT(KMU(I))))/(1.0+(XB(I)*4.0*(SQRT(KMU(
     1I))))))
      XGPOT(I)=10**((-XA(I)*(SQRT(KMU(I))))/(1.0+(XB(I)*3.0*(SQRT(KMU
     1(I))))))
      XGHCO(I)=10**((-XA(I)*(SQRT(KMU(I))))/(1.0+(XB(I)*4.0*(SQRT(KMU
     1(I))))))
      XGCAL(I)=10**((-XA(I)*(SQRT(KMU(I))))/(1.0+(XB(I)*6.0*(SQRT(KMU
     1(I))))))
      XGMG(I)=10**((-XA(I)*(SQRT(KMU(I))))/1.0+(XB(I)*8.0*(SQRT(KMU(I
     1))))))
      XGSO(I)=10**((-XA(I)*(SQRT(KMU(I))))/1.0+(XB(I)*4.0*(SQRT(KMU(I
     1))))))
      XGCL(I)=10**((-XA(I)*(SQRT(KMU(I))))/1.0+(XB(I)*4.0*(SQRT(KMU(I
     1))))))
      CONTINUE
```

```
                                                  ****************
                                                  *  CONTINUED   *
                                                  ****************

      WRITE(6,454)(I,XGH(I),XGSOD(I),XGPOT(I),XGCAL(I),XGMG(I),XGHCO(I),XGSO(
     1I),XGSIL(I),I=1,N)
      DO 454 I=1,N

C     THIS : CALCULATION OF ACTIVITY COEFFICIENT

      XASOD(I)=XSOD(I)*XGSOD(I)
      XAPOT(I)=XPOT(I)*XGPOT(I)
      XACAL(I)=XCAL(I)*XGCAL(I)
      XAMG(I) =XMG(I)*XGMG(I)
      XAHCO(I)=XHCO(I)*XGHCO(I)
      XACL(I) =XCL(I)*XGCL(I)
      XASO(I) =XSO(I)*XGSO(I)
      XASIL(I)=XSIL(I)
454   WRITE(6,
      WRITE(6,*)(I,XAH(I),XASOD(I),XAPOT(I),XACAL(I),XAMG(I),XAHCO(I),XAC
     1L(I),XASO(I),XASIL(I),I=1,N)
      DO 555 I=1,N

C     THIS : CALCULATION OF ACTIVITY RATIOS

      XRNAH(I)=ALOG10(XASOD(I)/XAH(I))
      XRKH(I) =ALOG10(XAPOT(I)/XAH(I))
      XRCAH(I)=ALOG10(XACAL(I)/(XAH(I)**2))
      XRMGH(I)=ALOG10(XAMG(I)/(XAH(I)**2))
555   WRITE(6,
      WRITE(6,*)(I,XRNAH(I),XRKH(I),XRCAH(I),XRMGH(I),I=1,N)
      STOP
      END
```

```
*****************************************************************
                        AID FOR DECODING
*****************************************************************
PH = -LOG(HYDROGEN ION), SOD = SODIUM , POT = POTASSIUM,

CAL = CALCIUM , MG = MAGNESIUM , HCO = BICARBONATE ION ,

CL = CHLORIDE , SO = SULFATE , SIL = SILICA,KMU = IONIC

STRENGTH , XA & XB =THE CONSTANTS A&B IN DEBYE HUCKELL EQ.

X( REPRESENTS MOLAR CONCENTRATION OF #

XG# REPRESENTS ACTIVITY COEFFICIENT OF #

XA# REPRESENTS ACTIVITY OF ION #

XRNAH = ACTIVITY OF SODIUM ION / ACTIVITY OF HYDROGEN ION

XRKH  = ACTIVITY OF POTASSIUM ION /ACTIVITY OF HYDROGEN ION

XRCAH = ACTIVITY OF CALCIUM ION / SQUARE OF HYDROGENION ACTIVITY

XRMGH = ACTIVITY OF MAGNESIUM ION/SQUARE OF HYDROGENION ACTIVITY
*****************************************************************
```

```
C*****************************************************************
C       PROGRAM FOR SILICA,SODIUM-POTASSIUM,SODIUM-POTASSIUM-CALCIUM
C                          GEOTHERMOMETER
C*****************************************************************


      DIMENSION SIL(38),TSIL(38),SOD(38),POT(38),CAL(38),XRNK(38),TNK
     1(38),XRCN(38),XMSOD(38),XMPOT(38),XMCAL(38),TCNK(38)
      READ *, SIL,TSIL,SOD,POT,CAL,TNK,TCNK
      N=38
      R=4/3
      READ*,(SIL(I),I=1,N)
      READ*,(SOD(I),I=1,N)
      READ*,(POT(I),I=1,N)
      READ*,(CAL(I),I=1,N)

C     NOTE : SILICA GEOTHERMOMETER

      DO 1000 I=1,N
      TSIL(I)=(1533.5/(5.768-ALOG10(SIL(I))))-273.15

C     NOTE : SODIUM-POTASSIUM GEOTHERMOMETER

      TNK(I)=(855.6/(ALOG10(SOD(I)/POT(I))+0.8573))-273.15

C     NOTE : SODIUM-POTASSIUM-CALCIUM GEOTHERMOMETER

      XMSOD(I)=SOD(I)/22997.0
      XMPOT(I)=POT(I)/39096.0
      XMCAL(I)=CAL(I)/40080.0
      XRNK(I)=XMSOD(I)/XMPOT(I)
      XRCN(I)=(SQRT(XMCAL(I)))/XMSOD(I)
      TCNK(I)=(1647/(ALOG10(XRNK(I))+(B*(ALOG10(XRCN(I))))+2.24))-273.
     115
1000  CONTINUE
      PRINT*,I,TSIL(I),TNK(I),TCNK(I)
      STOP
      END

C*****************************************************************
C                    AID FOR DECODING
C*****************************************************************
SIL=SILICA,SOD=SODIUM,POT=POTASSIUM,CAL=CALCIUM CONCENTRATIONS IN PPM

XMM=MOLAR CONCENTRATION OF THE SPECIES M

XRNK=MOLAR RATIO OF SODIUM TO POTASSIUM

XRCN=MOLAR RATIO OF SQRT.OF CALCIUM TO SODIUM

TSIL=TEMPERETURE ESTIMATED BY SILICA GEOTHERMOMETER

TNK =TEMPERETURE ESTIMATED BY SODIUM-POTASSIUM GEOTHERMOMETER

TCNK=TEMPERETURE ESTIMATED BY SODIUM-POTASSIUM-CALCIUM GEOTHERMOMETER

*****************************************************************
```